Alma Mater Studiorum – Università di Bologna

DOTTORATO DI RICERCA IN

SCIENZA E CULTURA DEL BENESSERE E DEGLI STILI DI VITA

Ciclo XXXIII

Settore Concorsuale: 05/G1 - FARMACOLOGIA, FARMACOLOGIA CLINICA E FARMACOGNOSIA

Settore Scientifico Disciplinare: BIO/14 - FARMACOLOGIA

IN VITRO STUDY OF NATURAL COMPOUNDS AND THEIR SEMI-SYNTHETIC DERIVATIVES AS INDUCERS OF NON-CANONICAL CELL DEATH

Presentata da: Dott.ssa Giulia Greco

Coordinatore Dottorato

Chiar.ma Prof.ssa
Carmela Fimognari

Supervisore

Chiar.ma Prof.ssa
Carmela Fimognari

Esame finale anno 2021

INDEX

Abstract

Introduction: Cancer burden continues to raise globally, causing a great deal of pressure on people, families, societies, and health systems, mentally, socially, and financially. Despite the increasing efficacy of current cancer therapies, several drugs display their anticancer activity by inducing apoptosis in cancer cells. However, it is now widely known that tumor cells could develop the ability to evade apoptosis, thus leading to tumor growth and resistance to anticancer treatments. In recent years, accumulating evidence increasingly pointed out that various non-apoptotic, also called non-canonical, forms of programmed cell death, such as ferroptosis and necroptosis, can be triggered independently of apoptosis or when the apoptotic process appears to be altered or inhibited, thus becoming a potential strategy to improve anticancer therapies.

Nature is a never-ending source of preventive and curative agents, and still represents an exhaustible source of pharmacologically active compounds, especially in the field of anticancer therapy. The enormous potential of natural products relies on their great biodiversity. As natural products are composed of innumerable molecules, they could interact with various molecular targets and regulate different biological pathways. Therefore, it is not surprisingly that many different natural compounds were discovered to be effective anticancer agents by promoting non-canonical cell death mechanisms.

***Objective*:** The aim of the research during my PhD was to analyse the anticancer potential of the natural isothiocyanate sulforaphane (SFN) and two semisynthetic isothiocyanate derivatives, named MG28 and MG46, together with an indole semisynthetic derivative, named AD05, with the main purpose of investigating their ability to induce non-canonical cell death in different leukemia cancer cells models.

Materials and Methods: MG28, MG46, SFN and AD05 were tested on different human acute myeloid leukemia (AML) cell lines (U-937, OCI-AML3, MOLM-13, MV4-11) and human acute lymphoblastic leukemia (ALL) cell line (Jurkat). The mechanism of cell death was investigated through an experimental integrated approach that includes several assays and several techniques including fluorescence microscopy, Western blotting, flow cytometry, ELISA. The genotoxic potential of MG28, MG46, and AD05 was assessed by analysing micronuclei formation (on TK6 human normal B lymphoblastoid cells) and H2AX phosphorylation, respectively.

Results: In all tested cell lines, MG28 and MG46 exhibited a much more marked cytotoxic activity than SFN, particularly in MV4-11 cells. However, in U-937 and MV4-11 cells, MG28 and MG46 induced exclusively caspase-dependent apoptosis, as showed by the observed increase in apoptotic cells, the cleavage of caspase-3 and PARP-1, and the abrogation of all these effects by Z-VAD-FMK pre-treatment. On the contrary, SFN triggered different cell death modalities in a dose-dependent manner: at relatively low dose (25μM), it induced apoptotic cell death, as confirmed also by pre-treating cell with

Z-VAD-FMK; at higher concentration (50μM), instead, SFN induced different non-canonical cell death pathways. In particular, ferroptosis, necroptosis, parthanatos, and MPT-driven necrosis were triggered by SFN, even if with a more remarkably effect in U-937 cells. However, by further investigating necroptosis occurrence through the analysis of MLKL and p-MLKL, we did not observe its phosphorylation, hence instilling some doubts about the ability of SFN to fully activate the necroptotic process. Lastly, MG28 and MG46, but not SFN, increased the protein expression of GRP78; on the contrary, SFN, but not the isothiocyanate derivatives, leads to the extracellular release of high-mobility group box 1 (HMGB1), which could be primordially correlated to its ability to induce non-canonical cell death.

Regarding AD05, it exhibited a strong cytotoxic activity on Jurkat cells. Its cytotoxic potential was closely associated with its ability to block cancer cells proliferation in the G2/M phase of cell cycle, without modulating cyclin B1 nor CDK1 expression but downregulating the expression of cyclin A. Additionally, as a consequence of its cytostatic activity, AD05 triggered apoptosis in Jurkat cells through the modulation of both the intrinsic and extrinsic pathway, as shown by the increased activity of caspase-3/-8 and the increased percentage of cells with reduced mitochondrial potential. However, apoptosis was the unique mechanism of cell death involved in its anticancer activity. Indeed, AD05 did not induce ferroptosis, necroptosis or parthanatos, as pharmacological inhibitors of these specific non-canonical cell deaths were not able to restore AD05-treated cells viability.

Finally, MG28 and MG46 increased the frequency of micronuclei formation, thus being classified as mutagens. On the contrary, AD05 lacked any genotoxic effect, as it did not promote H2A.X. phosphorylation.

Conclusions: On the whole, our results indicate that only SFN triggers non-canonical cell death in AML cells, while the two isothiocyanate derivates MG28 and MG46 and the indole derivative AD05 induce caspase-dependent apoptotic cell death in AML and ALL cells, respectively. Anyway, even if they were not able to trigger non-canonical cell death, they exhibited a strong anticancer effect.

In particular, MG28 and MG46 showed a great cytotoxic activity, correlated to their pro-apoptotic activity, in MV4-11 cells, which are characterized by the presence of mutated FLT3-ITD allele. Since FLT3-ITD mutation occurs in about 25% of all ALL patients and is associated with a worst prognosis, MG28 and MG46 could be considered promising anticancer agents to treat this aggressive ALL form, eventually in combination with FLT3 inhibitors. Moving to AD05, instead, its ability to trigger both apoptotic pathways and inhibit cell cycle showed that AD05 is characterized by a pleiotropic anticancer activity. Finally, ending with SFN, our results reflect the complexity that characterizes non-canonical cell deaths. Indeed, all programmed cell deaths, including non-canonical cell deaths, are strictly connected each other and are driven by a cancer type-dependent occurrence together with mutations eventually

carried by cancer cells. For instance, several other natural compounds showed to induce different non-canonical cell death pathways, but very rarely in a selective manner and rather depending on cancer type, concentrations tested, or treatment times. Thus, all these pieces of evidence may lead to conclude that there is a coexistence of all these cell death pathways, imaging them as many musicians who take part of the same orchestra, and which could start to play as "reserves" depending on cancer type or cancer cells status. Finally, the three new semi-synthetic derivatives showed a different toxicological profile. If AD05 was not genotoxic, MG28 and MG46 were found to be mutagenic.

Abbreviations

4-HNE	4-hydroxy-2-nonenal
γGCL	γ-glutamylcysteine ligase
ABC	adenosine triphosphate-binding cassette
AIF	apoptosis inducing factor
Apaf-1	Apoptotic protease activating factor-1
ARE	antioxidant responsive element
ASG	ascorbigen
ATF6	activating transcription factor 6
Atg	autophagy related gene
ATP	adenosine triphosphate
Bad	Bcl-2-associated death promoter
Bax	Bcl-2-associated X protein
Bak	Bcl-2 homologous antagonist/killer
Bcl-2	B-cell lymphoma 2
Bcl-B	Bcl-2-like protein 10, Bcl2L10
Bcl-xL	Bcl extralarge
Bcl-W	Bcl-2-like protein 2, BCL2L2
BCRP	breast cancer resistance protein (ABCG2)
BH3	Bcl-2 homology 3
Bid	BH3 interacting-domain death agonist
Bim	Bcl-2-like protein 11, BCL2L11
Bok	Bcl-2 related ovarian killer
BSA	bovine serum albumin
c-FLIP	cellular FLICE (FADD-like IL-1β-converting enzyme)-inhibitory protein
CAD	caspase-activated DNase
CARD	caspase activation and recruitment domain
CDK	cyclin-dependent kinase
CHAC1	glutathione-specific gamma-glutamylcyclotransferase 1
CHOP	CCAAT-enhancer-binding protein homologous protein
cIAP 1/2	cellular inhibitor of apoptosis protein 1/2
CoQ10	coenzyme Q10
CrmA	cytokine response modifier A
CPT	choline phosphate cytidylyltransferase
CRT	calreticulin
CSA	cyclosporine A
CYP	cytochrome 450
CX3CL1	CX3C motif chemokine ligand 1
DAMPs	damage-associated molecular patterns
DCF	2',7'-dichlorofluorescein
DD	death domain
DED	death effector domain
DilC1(5)	1,1',3,3,3',3'-hexamethylindo dicarbo-cyanine iodide
DISC	death-inducing signaling complex
DIM	3,3'-diindolylmethane
DR	death receptor
EMT	epithelial mesenchymal transition
ER	endoplasmic reticulum
FADD	Fas-associated death domain
FAS	Fas cell surface death receptor
FDA	Food and Drug Administration
FHT1	ferritin heavy chain 1
FLT3	FMS-like tyrosine kinase 3
FTL	ferritin light chain
GLUD1	glutamate dehydrogenase 1
GPX4	glutathione peroxidase 4
GRP78	glucose-regulated protein 78

GSH	glutathione
GSSG	oxidized glutathione
GST	glutathione S transferase
H_2DCF	2',7'-dichlorohydrofluorescein
H_2DCFDA	2',7'-dichlorodihydrofluoresceine
H_2O_2	hydrogen peroxide
HIF-1α	hypoxia-inducible factor-1alpha
HMGB1	high-mobility group box 1
HMOX1	heme-oxyhenase 1
HNC	head and neck cancer
HSP	heat-shock protein
HSPB1	heat shock protein beta-1
IAPs	inhibitors apoptosis proteins
ICAD	inhibitor of CAD (caspase-activated Dnase)
ICAM3	intercellular adhesion molecule-3
IKE	imidazole ketone erastin
ILP-2	IAP-like protein 2
IMM	Inner mitochondrial membrane
IRE1-α	inositol-requiring transmembrane kinase/endoribonuclease 1-alfa
IREB2	iron response element binding protein 2
ITD	internal tandem duplication
Keap1	Kelch-like ECH-associated protein 1
L•	lipid radical
LC3	microtubule-associated protein 1 light chain 3
LC3B	microtubule-associated protein 1 light chain 3 beta (also known as MAP1LC3B)
LIP	labile iron pool
LPS	lipopolysaccharides
LO•	alkoxyl radical
LOO•	lipid peroxyl radical
LOOH	lipid hydroperoxide
LOXs	lipoxygenases
LPC	lysophosphatidylcholine
MDA	malondialdehyde
MDR	multiple drug resistance
MFI	mean fluorescence intensity
MLKL	mixed lineage kinase domain-like
MMP	matrix metalloproteinase
MN	Micronuclei
MOMP	mitochondrial outer membrane permeabilization
MPT	mitochondrial permeability transition
MRP1	MDR-associated protein (ABCC1)
NAIP	neuronal apoptosis inhibitory protein
NCO4	nuclear receptor coactivator 4
NDI	naphtalene diimide
Nec-1	necrostatin-1
Nec-1s	necrostatin-1s (7-Cl-O-Nec1)
NF-kB	nuclear factor kappa-light-chain-enhancer of activated B cells
NQO1	NADPH-quinone oxidoreductase 1
Nrf2	nuclear factor (erythroid-derived)-like 2
O_2	oxygen
OH•	hydroxyl radical
OMM	outer mitochondrial membrane
Omi/HtrA2	high-temperature requirement protein A2
PARP-1	poly-(ADP-ribose)-polymerase-1
PC	phosphatidylcoline
PCD	programmed cell death
PCYT1A	phosphate cytidylyltransferase 1 alpha
PDT	photodynamic therapy
PE	piperazine erastin
PERK	protein kinase RNA-like endoplasmic reticulum kinase
PGAM5	mitochondrial serine/threonine protein phosphatase family member 5
P-gp	P-glycoprotein (MDR1/ABCB1)

PI3K	phosphatidylinositol 3-kinase
PS	phosphatidylserine
PTPC	permeability transfer pore complex
PUFAs	polyunsaturated fatty acids
Puma	p53 upregulated modulator of apoptosis, BBC3
RARRES3	retinoic acid receptor responder 3 (also known as RIG1)
RIP	homotypic interaction motif (RHIMs)
RIP1	receptor-interacting protein 1
RIP3	receptor-interacting protein 3
ROS	reactive oxygen species
RSL3	1S,3R)-RSL-3, RAS-selective lethal 3
RTK	receptor tyrosine kinase
S1P	sphingosine-1-phosphate
SfA	sanglifehrin A
SMAC	diablo IAP-binding mitochondrial protein (also known as second mitochondrial activator of caspase
SQS	squalene synthase
STAT3	signal transducer and activator of transcription 3
TCTP	translationally controlled tumor protein
TKD	tyrosine kinase domain
TLR3	tool-like receptor 3
TLR4	tool-like receptor 4
TMEM173	transmembrane protein 173 (also known as STING)
TNFα	tumor necrosis factor α
TNFR	tumor necrosis factor receptor
TRADD	TNF receptor-associated death domain
TRAIL	TNF-related apoptosis-inducing ligand
TRIF	TIR-domain-containing adapter inducing interferon-β
TRPM7	transient receptor potential cation channel, subfamily M, member 7
TRF1	transferrin receptor 1
UGT	UDP-glucuronosyl transferase
UPR	unfolded protein response
UTP	uridine-5'-triphosphate
VEGF	vascular endothelial growth factor
VEGFR	VEGF receptor
XBP-1	X-box binding protein-1
XIAP	X-linked inhibitor of apoptosis protein
Z-VAD-FMK	benzyloxycarbonyl-Val-Ala-Asp (OMe)-fluoromethylketone
ZBP1	Z-DNA-binding protein 1

List of Figures

Figure 4.6 Percentage (%) of viable (annexin V^-/7-AAD^-), early apoptotic (annexin V^+/7-AAD^-), and late apoptotic or necrotic (annexin V^+/ 7-AAD^+) cells after 24h treatment of Jurkat cells with increasing concentrations of AD05. ** $p < 0.01$; **** $p < 0.0001$ *versus* untreated cells.

Figure 4.7 Activity of caspase-3 (A) and caspase-8 (B) and percentage (%) of cells with decreased mitochondrial potential (C) after 24h of treatment of Jurkat cells with increasing concentrations of AD05. Cpt (camptothecin) 2μM and CCCP (carbonyl cyanide 3-chlorophenylhydrazone) 50mM were used as positive controls. ** $p < 0.01$; *** $p < 0.001$; **** $p < 0.0001$ *versus* untreated cells.

Figure 4.8 Percentage (%) of viable cells after pre-treatment for 1h with Z-VAD-FMK (Z-VAD), olaparib (Ola), necrostatin-1s (Nec-1s), ferrostatin-1 (Ferr-1), deferoxamine mesylate (DFO), and vitamin E (VitE) following 24h and 48h treatment with AD05 8μM. * $p < 0.05$; *** $p < 0.001$; **** $p < 0.0001$ *versus* untreated cells. # $p < 0.05$ *versus* AD05-treated cells.

Figure 4.9 Intracellular ROS levels, expressed as fold increase *versus* untreated cells, of Jurkat cells treated with increasing concentrations of AD05 for different time points. H_2O_2 0.5 and 1mM was used as positive control. ** $p < 0.01$ *versus* untreated cells.

Figure 4.10 Histograms (A) and cytograms (B) of cell-cycle distribution after Jurkat cells treatment with AD05 for 24h. *** $p < 0.001$; **** $p < 0.0001$ *versus* untreated cells.

Figure 4.11 Expression of cyclin A (A), cyclin B1 (B), and CDK1 (C), indicated as fold increase *versus* untreated cells, following 24h treatment of Jurkat cells with increasing concentration of AD05. ** $p < 0.01$ *versus* untreated cells.

Figure 4.12 Percentage (%) of viable (annexin V^-/7-AAD^-), early apoptotic (annexin V^+/7-AAD^-), and late apoptotic or necrotic (annexin V^+/7-AAD^+) cells (A) and cell-cycle distribution (B) following 6h treatment of Jurkat cells with increasing concentrations of AD05. * $p < 0.05$; ** $p < 0.01$ *versus* untreated cells.

Figure 4.13 Relative expression of P-H2AX following 5h treatment of Jurkat cells with increasing concentrations of AD05. Etoposide (ETO) 10μg/mL was used as positive control. ** $p< 0.01$ *versus* untreated cells.

List of Tables

Chapter 1
Introduction

1.1 Cancer

Cancer had a record of 9.6 million deaths worldwide in 2018, becoming the second leading cause of death [1]. Cancer burden still continue to raise globally, causing a great deal of pressure on people, families, societies, and health systems, mentally, socially, and financially [1].

Carcinogenesis is a multifactorial and multistep process. It involves three stages: the first, called initiation, which is characterized by the acquisition of mutations in multiple genes (oncogenes); the second phase, called promotion, which involves the selective clonal spreading of initiated cells, leading to the formation of a pre-neoplastic lesion, which may phenotypically develop into a malignant lesion during the final stage of carcinogenesis, named progression [2].

1.1.1 Hallmarks of cancer

During the multistep development of human tumors, six biological capabilities are acquired by cancer cells, that are called "hallmarks of cancer". In 2000, Hanahan and Weinberg drafted for the first time the six capabilities acquired by cancer cell, illustrated in Figure 1, which comprise: sustaining proliferative signaling, evading growth suppressors, resisting cell death, enabling replicative immortality, inducing angiogenesis, and activating invasion and metastasis (Figure 1.1) [3].

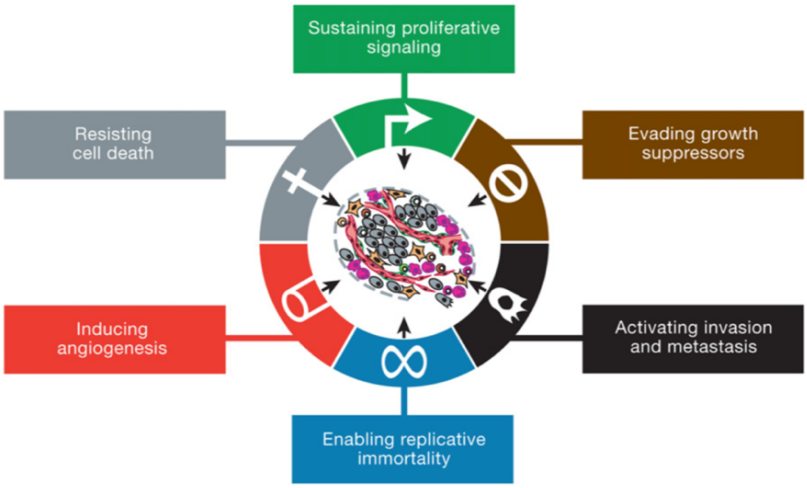

Figure 1.1 The originally six hallmarks of cancer proposed in 2000 [4]

However, these six hallmarks of cancer were revisited and updated in 2012, since the remarkable progress in cancer research unveiled new observations which clarify and modify the original formulation [4]. Indeed, to the already known six hallmarks, two new capabilities, called "emerging hallmarks", have been

added: one is the potential of cancer cells of altering or reprogramming cell metabolism to most efficiently promote neoplastic proliferation; the second one is the ability of cancer cells to escape immune destruction, particularly by lymphocytes T and B, macrophages, and natural killer cells (Figure 1.2) [4]. In addition, the acquisition of both core and emerging hallmarks was allowed by two consequential features of tumors: 1) genomic instability and mutability, which endow cancer cells with genetic alteration driving tumor progression, and 2) the tumor-promoting effects of inflammation driven by immune cells (Figure 1.2) [4].

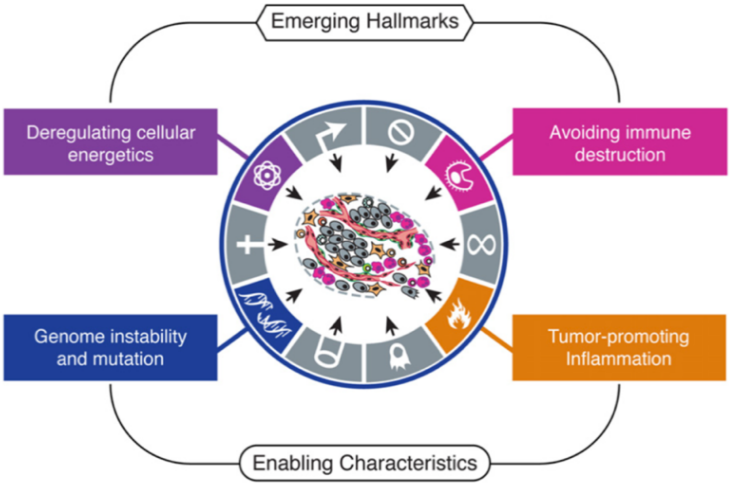

Figure 1.2 The two emerging hallmarks of cancer within the two enabling characteristics described by Hanahan and Weinberg in 2012 [4]

1.2 Programmed cell death

Historically, different cell-death modalities were defined based on morphological alterations associated with specific mechanisms whereby dead cells are eliminated. These modalities include three types of cell demise: type I cell death or apoptosis, where cells exhibit cytoplasmic shrinkage, chromatin condensation (*pyknosis*), nuclear fragmentation (*karyorrhexis*), and plasma membrane blebbing leading to the formation of apparently intact small vesicles (*i.e.,* apoptotic bodies). These latter are efficiently eliminated by neighbouring cells with phagocytic activity and lysosomal degradation [5]. In type II cell death, often indicated as autophagy-dependent cell death, cells display extensive cytoplasmic vacuolization ending with phagocytic uptake and lysosomal degradation. Although autophagy mainly promotes cell survival, in certain circumstances, it may also cause cell death, namely autophagic-dependent cell death [5]. Finally, type III or necrosis, corresponds to a process lacking type-I or -II cell-death features and culminating with cell corpse removal without obvious phagocytic and lysosomal activities [5].

Of note, apoptosis and autophagy are both forms of programmed cell death (PCD), or canonical cell death, while necrosis was for a long time considered as a non-physiological process (*i.e.,* non-PCD) that occurs as a result of infection or injury [5].

1.2.1 Apoptosis

Among all types of programmed cell death, apoptosis is certainly the most studied and known mechanism of cell demise. From a morphological point of view, apoptotic cells display several features that have been well identified and documented. These morphological changes include cytoplasmic shrinkage, chromatin condensation (*pyknosis*), and plasma membrane blebbing followed by nuclear fragmentation (*karyorrhexis*) and the formation of apoptotic bodies during a process called "budding" [5].

Apoptotic cells generate different engulfment signals, the so called "find-me" and "eat-me'" signals, that allow them to interact with the neighbouring cells with phagocytic activity and, therefore, to be degraded within phagolysosomes [6]. On one hand, the "find me" signals are secreted by cells undergoing apoptosis in order to attract phagocytes and are represented by lysophosphatidylcholine (LPC), sphingosine-1-phosphate (S1P), CX3C motif chemokine ligand 1 (CX3CL1, also known as fractalkine), and nucleotides (adenosine triphosphate, ATP; and uridine-5'-triphosphate, UTP) [6]. On the other hand, the "eat-me" signals, expressed on the cell surface by dying cells, are represented by a wide range of signals, including phosphatidylserine (PS), carbohydrates (amino sugars or mannose), intercellular adhesion molecule-3 (ICAM3), and calreticulin (CRT) [7]. Among these, the best characterized is PS which is a membrane phospholipid that normally resides in the cytoplasmatic leaflet of the plasma membrane and translocates on the cell surface in response to apoptotic stimuli [7].

Considering that in most cases, phagocytosis of apoptotic cells occurs without activating the immune system, it has been thought for a long time that apoptosis does not induce any inflammatory reaction unlike death by necrosis [8]**.** However, in 2007, a study revealed that certain anticancer agents, such as γ irradiation, are able to kill cancer cells by apoptosis while making them to enhance a tumor-specific immune response [9], opening the scenario of immunogenic cell death (ICD).

In the apoptotic machinery, a pivotal role is played by caspases, a family of intracellular cysteine proteases. In humans, 12 different caspases have been identified. Based on their functions and domain architecture, caspases are classified into two main categories: inflammatory and apoptotic. Caspase-1, -4, and -5 are involved in the inflammatory response as pro-cytokine activators, while the apoptotic caspases can be further subdivided into initiator (caspase-2, -8, -9, and -10) and executioner caspases (caspase-3, -6, and -7) [10].

Caspases are widely expressed in cells in an inactive pro-enzyme form (pro-caspases) containing an N-terminal pro-domain and a catalytic domain. Initiator caspases, after their activation by auto-proteolysis, sequentially activate executioner caspases that subsequently interact with specific cellular components to orchestrate the final apoptotic cell death. The cleavage of specific cellular components by executioner caspases reflects the final results of the two apoptotic pathways, which, therefore, converge both to the activation of caspase-3, -6 or -7. Then, activated effector caspases by interacting with distinct cellular substrates, trigger apoptotic cell death within all its typical biochemical and morphological changes [10].

Apoptosis is mainly mediated by two pathways: the extrinsic, or death receptor pathway, and the intrinsic, or mitochondrial pathway, which will be discussed below (Figure 1.3).

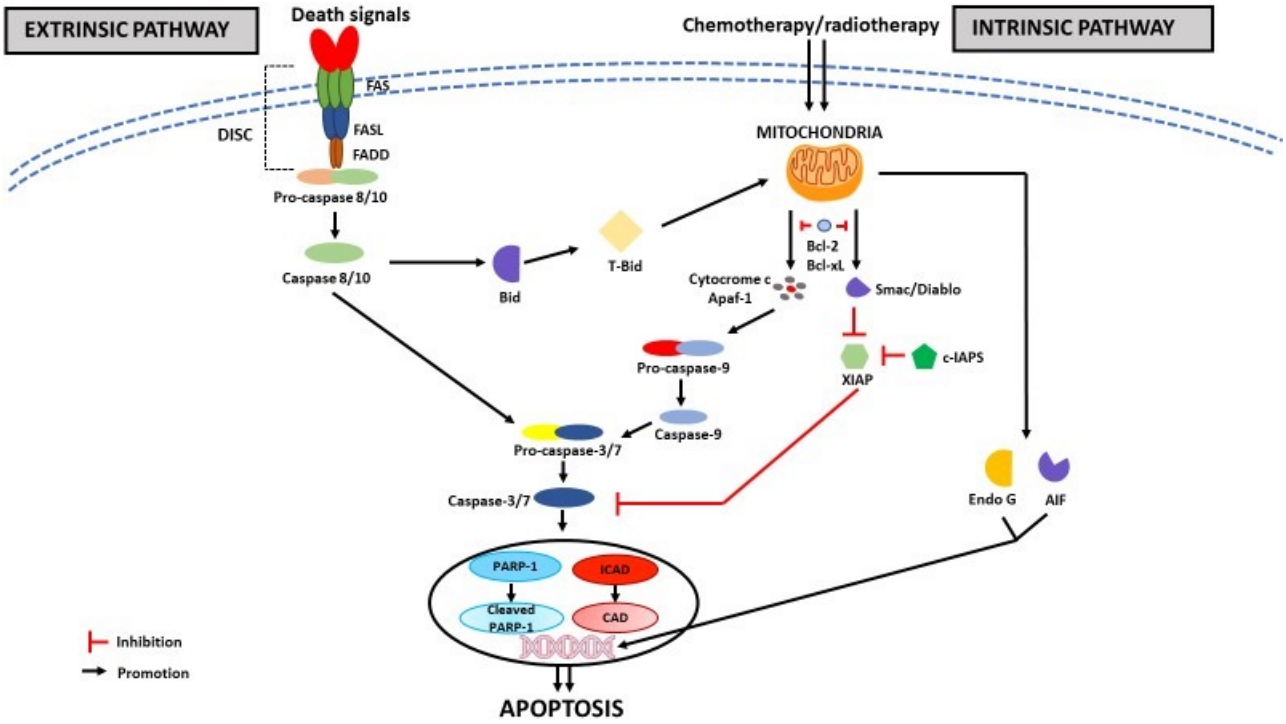

Figure 1.3 Schematic representation of apoptotic cell death pathways.

AIF: apoptosis inducing factor; Apaf-1: apoptosis protease activating factor-1; Bcl-2: B-cell lymphoma 2; Bcl-xL: Bcl-2 related protein, long isoform; Bid: BH3 interacting-domain death agonist; c-IAPs: cellular inhibitors of apoptosis; CAD: Caspase-activated DNase; DISC: death-inducing signaling complex; endo G: endonuclease G; FADD: Fas-associated death domain; FAS: death receptor; FASL: Fas-associated ligand; ICAD: inhibitor of caspase-activated DNase; PARP-1: poly(ADP-ribose)polymerase-1; SMAC/diablo: second mitochondrial activator of caspases/direct IAP binding protein; TRADD: TNF receptor-associated death domain; XIAP: X-linked inhibitor of apoptosis protein.

Extrinsic apoptotic pathway

The extrinsic apoptotic pathway is triggered by extracellular ligands that bind to specific transmembrane death receptors (DRs) belonging to the tumor necrosis factor receptor (TNFR) superfamily [11]. Members of TNFR family share an intracellular protein-protein interaction domain, called death domain (DD) which plays a critical role in apoptosis signaling pathway [11]. To date, the most characterized signaling systems of DRs-ligands include: TNFR1-TNFα, FAS (CD95, APO-1)-FasL, TRAILR1 (DR4)-TRAIL, TRAILR2 (DR5)-TRAIL [5]. Once death receptors are bound to their respective ligands, they bind to their corresponding adaptive cytoplasmic protein, such as Fas-associated death domain (FADD), and TNF receptor-associated death domain (TRADD) [5]. These adaptor proteins contain also another protein interaction domain, called the death effector domain (DED) and, since this domain is also present within pro-caspase-8, the interaction between the DED of FAAD or TRAAD with the DED of pro-caspase-8 leads to the development of a death-inducing signaling complex (DISC) responsible for the auto-catalytic activation of pro-caspase-8 (Figure 1.3) [5]. Once activation of caspase-8 occurs, execution of apoptosis proceeds by two different sub-pathways depending of cell type: in type I cells (*i.e.,* thymocytes and mature lymphocytes) caspase-8 directly cleaves and activates effector caspases, triggering apoptotic cell death; in type II cells (*i.e.*, hepatocytes, pancreatic β cells, and the majority of cancer cells),

where inhibitors apoptosis proteins (IAPs) inhibit caspase-3/-7 activation, execution of apoptosis requires the suppression of IAPs by proteins released from mitochondria [5].

Intrinsic apoptotic pathway

The intrinsic apoptotic pathway (or mitochondria-mediated pathway) is triggered by a wide variety of extracellular and intracellular stress stimuli such as DNA damage agents, irradiations, growth factor deprivation, virus infection, growth factor withdrawal, replication stress, endoplasmic reticulum stress (ER stress), hypoxia, extremely high concentrations of cytosolic Ca^{2+} and severe oxidative stress [5].

The crucial step of the intrinsic apoptotic pathway is represented by the irreversible and diffuse mitochondrial outer membrane permeabilization (MOMP) [5]. This process is strictly controlled by Bcl-2 (B-cell lymphoma 2) family proteins, a group of proteins partaking one to four BCL2 homology (BH) domains (*i.e.*, BH1, BH2, BH3, and BH4) [12]. Depending on the content of typical BH domains, the Bcl-2 proteins are classified into three sub-categories: one group with anti-apoptotic functions and two groups with pro-apoptotic functions. The anti-apoptotic multi-domain group includes Bcl-2, Bcl-xL (Bcl extralarge, BCL2L1), Bcl-W (Bcl-2-like protein 2, BCL2L2), Mcl-1, A1/Bfl-1, and Bcl-B (Bcl-2-like protein 10, Bcl2L10). These proteins contain from three to four BH domains and block apoptotic signaling through the inhibition of their pro-apoptotic counterparts by a protein-protein interaction [12]. The pro-apoptotic multidomain group, which contains three BH domains (BH1, BH2, and BH3), includes: Bax (Bcl-2-associated X protein), Bak (Bcl-2 homologous antagonist/killer) and Bok (Bcl-2 related ovarian killer) proteins. Instead, the other pro-apoptotic protein family, the so called BH3-only family members, includes Bid (BH3 interacting-domain death agonist), Bim (Bcl-2-like protein 11, BCL2L11), Bad (Bcl-2-associated death promoter), Puma (p53 upregulated modulator of apoptosis, BBC3), Noxa (PMAIP1), Bmf, Hrk and Bik [12].

After their activation, pro-apoptotic multidomain proteins, such as Bax and Bak, through their pore-forming activity induce the alteration of mitochondrial permeability and cause extensive rearrangements of the mitochondrial ultrastructure, resulting in mitochondrial outer membrane permeabilization. Once the mitochondrial permeability is destroyed, those proteins that normally reside in the mitochondrial intermembrane space are released, spreading into the cellular cytoplasm [13]. These proteins comprise cytochrome c, AIF (apoptosis inducing factor), SMAC (second mitochondrial activator of caspase, also known as diablo, IAP-binding mitochondrial protein), the serine protease Omi/HtrA2 (high-temperature requirement protein A2), and endonuclease G (Figure 3) [13]. Cytochrome c, after its release into the cytosol, binds to the apoptosis protease activating factor-1 (Apaf-1) leading to the formation of a complex known as apoptosome, which, through its exposed caspase recruitment domain (CARD), recruits and

activate pro-caspase-9. Consequently, active caspase-9 catalyzes the proteolytic activation of executioner caspase-3 and -7, leading to apoptotic cell death (Figure 1.3) [13].

Apoptosis execution

As mentioned above, both intrinsic and extrinsic apoptotic pathways converge to the cleavage of caspase-3/-7, thus initiating the execution of apoptotic process (Figure 3). Executioner caspases trigger apoptosis by cleaving several key proteins involved in different cell functions and in cell survival, leading to all the morphological and biochemical features of apoptotic cells [5]. Caspase-3 is considered the most important executioner caspase, and it is responsible for the activation of the caspase-activated DNase (CAD), which is normally inactivated by its inhibitor (ICAD) [14]. CAD, possessing a DNA-specific and a double-strands-specific endonuclease, generates double-stranded breaks in the internucleosomal chromatin regions, thus leading to the degradation of chromosomal DNA (Figure 3) [14] and to the subsequent morphological features of apoptotic dead cells.

Among all the other substrates of caspase-3, cleaved poly-(ADP-ribose)-polymerase-1 (PARP-1) represents one the most characteristic hallmarks of apoptosis execution [14]. Executioner caspase-3, after its activation, proteolytically cleaves PARP-1, generating two fragments: a 24 kDa fragment and a 89 kDa fragment. If the 89-kD fragment has a low DNA binding activity and is released from the nucleus into the cytosol, the 24kD cleaved fragment remains in the nucleus, where it irreversibly binds DNA, acting as inhibitor of active PARP-1 (Figure 3) [14]. It is important to note that the binding of 24 kD fragment to DNA strand breaks leads to the inhibition of DNA repair enzymes, including PARP-1, and reduces DNA repair [15].

Finally, also mitochondria-released factors endonuclease G and AIF could induce DNA fragmentation, occurring during apoptosis execution. Indeed, both, after their release from mitochondria upon the irreversible loss of mitochondrial potential, translocate to the nucleus where concur to the apoptotic DNA fragmentation (Figure 3). In particular, endonuclease G triggers chromatin cleavage into DNA fragments, thus possessing the same DNase activity of other nucleases [14]. AIF, instead, did not show to trigger oligonucleosomal DNA fragmentation, but rather to induce chromatin condensation and DNA cleavage by interacting with other nucleases [14].

1.3 Evasion of apoptosis as tumor-resistance mechanism

Despite several drugs exhibit their anticancer activity by inducing apoptosis in cancer cells, it is now widely known that tumor cells could develop the ability to evade apoptosis. Indeed, the intrinsic or acquired resistance to apoptosis is considered one of the hallmarks of human cancers, as mentioned before [4]. Since most of the current anticancer treatments, including chemotherapy, radiotherapy, and immunotherapy, display their anticancer activity by inducing apoptotic cell death, it is clear that evasion of apoptosis may lead to tumor growth and resistance to anticancer treatments [16].

Regarding the evasion of mitochondrial apoptotic pathway, overexpression of anti-apoptotic proteins like Bcl-2 and downregulation of pro-apoptotic proteins such as Bax represent one of the mechanisms whereby cancer cells evade apoptosis. Overexpression of many anti-apoptotic proteins have been found in different cancer types including pancreatic, ovarian, lymphoma, multiple myeloma, and others [16]. Moreover, also the overexpression of Mcl-1 has been associated with resistance to chemotherapeutic agents [16]. Indeed, by downregulating Mcl-1, induction of apoptosis and sensitivity of cancer cells towards chemotherapy has been enhanced [16].

While anti-apoptotic proteins are overexpressed, the pro-apoptotic proteins are downregulated or inhibited. Inactivation of the pro-apoptotic protein Bax, due to somatic mutations, has been found in solid and hematological tumors; in addition, homozygous deletion of Bim was detected in mantle cell lymphoma, while promoter hypermethylation of Bim was identified in Burkitt lymphoma [17]. Moreover, mutation or epigenetic silencing of Noxa have been observed in large B-cell lymphoma, while in renal carcinoma, transcriptional silencing through the deletion of the Bik gene at 22q13.2 or DNA methylation led to the loss of Bik expression [17]. Defections of the mitochondrial apoptotic pathway can also occur at the post-mitochondrial level. Indeed, impairment of the assembly of a functional apoptosome has been found in melanoma, leukemia, glioblastoma, and gastric cancer, due to a downregulation or absent expression/activity of Apaf-1 [17]. In addition, overexpression of Translationally controlled tumor protein (TCTP), which possesses anti-apoptotic activity by interacting with Apaf-1, is often related to chemoresistance through the modulation of apoptosome formation [18].

Another important mechanism involved in cancer resistance to apoptosis is the aberrant expression or function of IAPs [17]. IAPs are a family of endogenous caspase inhibitors. In humans, eight members belong to IAPs family: X-linked inhibitor of apoptosis protein (XIAP), cIAP1, cIAP2, survivin, livin, neuronal apoptosis inhibitory protein (NAIP), Bruce (apollon), and IAP-like protein 2 (ILP-2) [19]. Among all, XIAP, which inhibits apoptosis by binding to active caspase-3 and -7 and by preventing caspase-9 activation, is the most active anti-apoptotic member [19]. Moreover, besides its role in

apoptosis and caspases modulation, XIAP regulates also the Nf-kB (nuclear factor kappa-light-chain-enhancer of activated B cells) pathway [19]. In acute myeloid leukemia XIAP has been found to be overexpressed, which is probably the cause of chemoresistance and of a poor prognosis [20].

Alterations in the death receptor apoptotic pathway are responsible for cancer resistance to apoptosis as well. In human cancers, the death receptor signaling can be impaired at different levels. At the receptor level, the transmission of death signals from the cell surface to intracellular signaling cascades could be prevented by the downregulation or the absence of the surface expression of death receptors [17]. Indeed, in leukemia and in neuroblastoma cancer cells which are resistant to chemotherapy, a decreased expression of CD95 has been observed, supporting the critical role played by the intact expression of CD95 toward drug sensitivity [17]. In addition, mutations in the CD95 gene have also been documented in hematological malignancies as well as in various solid tumors [17]. Alternatively, epigenetic changes such as CpG-island hypermethylation of gene promoters may affect the surface expression of death receptors [17].

The aberrant expression of anti-apoptotic proteins that prevent the activation of caspase-8 could also functionally block the signal transduction of the death receptor apoptotic pathway. For example, elevated expression of cellular FLICE (FADD-like IL-1β-converting enzyme-inhibitory protein, c-FLIP), suppressed TRAIL-mediated apoptosis induced by chemotherapeutic drugs by inhibiting caspase-8 recruitment [17].

Finally, the inactivation of caspase-8, by genetic or epigenetic mechanisms, is involved in the cancer resistance to the extrinsic apoptotic pathway as well, even if the frequency of caspase-8 mutations in human cancers is fairly low [17]. However, mutated forms of caspase-8 observed, for example, in colorectal and head and neck carcinoma, could inhibit apoptosis by preventing the recruitment of the wild type of caspase-8 to activated death receptors [17]. Moreover, in leukemia and in neuroblastoma cancer cells caspase-8 expression was found to be transcriptionally regulated by splicing. For example, caspase-8L, which is generated by an alternative splicing of intron 8 of the caspase-8, could inhibit apoptosis by interfering with the recruitment of wild type caspase-8 [17].

To conclude, several mechanisms are involved in the cancer resistance to apoptosis, thus limiting the effectiveness of anticancer therapies solely based on apoptosis induction. Therefore, the search for new anticancer agents capable of modulating not only the apoptotic pathway, but also of inducing other mechanisms of cell death is pressing.

1.4 Non-canonical cell death

In recent years, accumulating evidence increasingly pointed out that various non-apoptotic forms of PCD, also called non-canonical, can be triggered independently of apoptosis or when the apoptotic process appears to be altered or inhibited. Non-apoptotic cell death pathways differ from the apoptotic process not only in morphological terms, but also in biochemical terms and include various PCD pathways, such as ferroptosis and necroptosis [21].

Since therapeutic approaches based solely on induction of apoptosis led to a number of therapeutic failures due to the activation of resistance mechanisms, as discussed before, the recent discovery of additional pathways acting as potential intervention targets could certainly improve cancer treatment modalities.

Figure 1.4 illustrates some of the non-canonical cell death mechanisms (Figure 1.4). Among them, ferroptosis and necroptosis will be described in detail below.

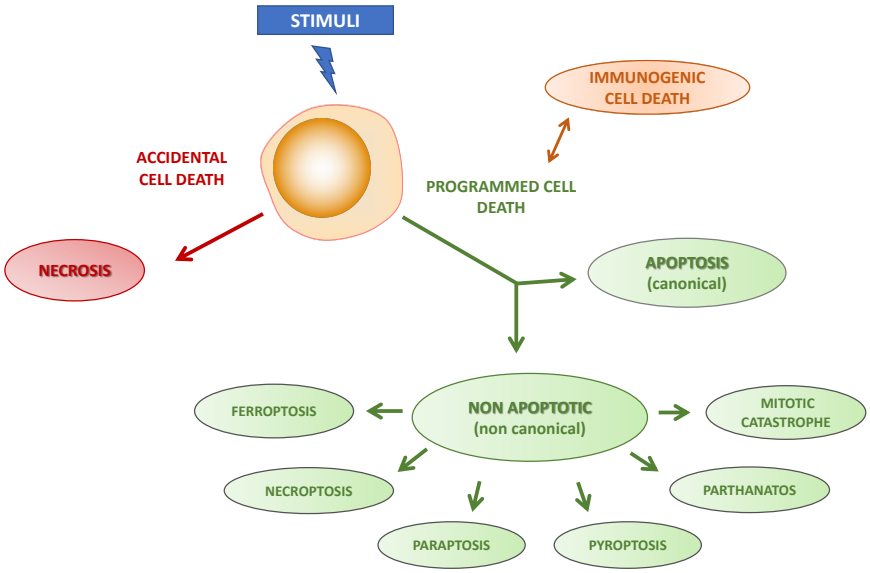

Figure 1.4 Overview of non-canonical cell death mechanisms.

1.4.1 Ferroptosis

The term ferroptosis was used for the first time in 2012 by Dixon *et al* to describe a new form of programmed non-apoptotic cell death [22]. Briefly, ferroptosis is characterized by an iron-dependent accumulation of lipid reactive oxygen species (ROS) which leads to cell demise (Figure 1.5) [23]. This type of programmed cell death clearly differs from other forms of cell death both in morphological and biochemical terms. Morphologically, ferroptosis does not involve chromatin condensation, cell shrinkage, chromatin condensation, formation of apoptotic bodies, which are typical apoptotic features;

ferroptosis is not characterized by cytoplasmatic swelling and disruption of cell membrane, as instead happens in necrosis, and, finally, the formation of typical autophagic vacuoles is not observed [22,24]. Therefore, from a morphological point of view, ferroptosis typically occurs as a distinct shrinkage of mitochondria with enhanced membrane density and decrease or depletion of mitochondrial cristae, which is really a distinct mechanism from other types of cell death [22].

Ferroptosis is involved in a great deal of disease such as ischemia/reperfusion-induced organ injury and stroke [25–27]. Moreover, by controlling the growth and proliferation of tumor cells, ferroptosis plays a critical role in the development and progression of multiple tumor diseases [28]. For this reason, inducing cancer cells death by triggering ferroptosis is now considered a promising strategy to fight cancer [29–31].

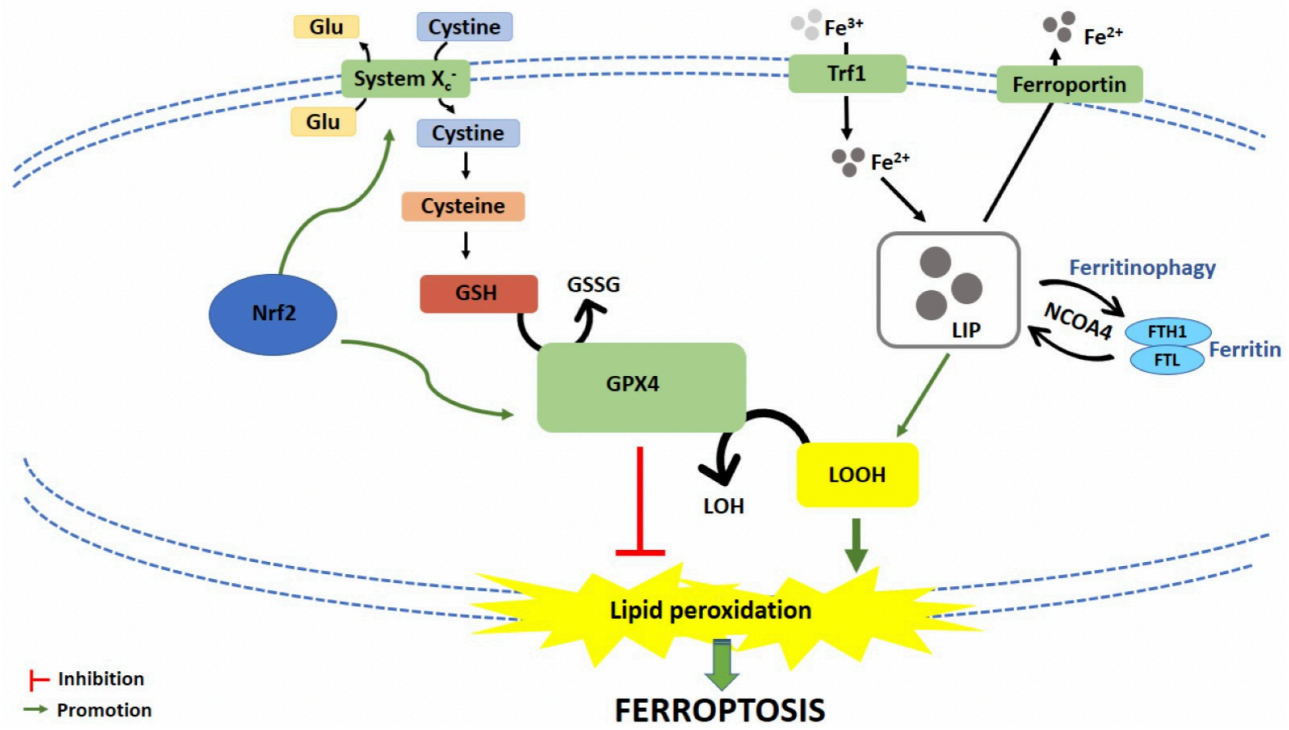

Figure 1.5 Schematic representation of ferroptotic cell death pathway [32].

Inhibition of system X_c^- or glutathione peroxidase 4 (GPX4) induce ferroptosis. The glutamate-cystine antiporter system X_c^- transports cystine inside the cell by exchanging intracellular glutamate (Glu). Inside the cell, cystine is reduced into cysteine, used to synthesize glutathione (GSH). GPX4 reduces lipid hydroperoxides into lipid alcohols (LOH) by converting GSH into oxidized glutathione (GSSG), hence protecting cells from lipid peroxidation. Inhibition of GPX4, directly or through the depletion of GSH, leads to accumulation of lipid ROS and to ferroptotic cell death. The transcription factor nuclear factor erythroid 2-related factor 2 (Nrf2) could modulate the expression of both system X_c^- and GPX4, thus regulating ferroptosis.

Excessive levels of free iron promote ferroptosis. Fe^{3+} is transported inside the cell by Trf1 (transferrin receptor 1). In the cytosol, Fe^{3+} is converted into Fe^{2+} that is stored in the iron storage protein ferritin, composed by a ferritin light chain (FTL) and ferritin heavy chain 1 (FTH1). LIP (labile iron pool) constitutes the amount of free Fe^{2+}. The NCO4 (nuclear receptor coactivator 4)-mediated autophagic degradation of ferritin (ferritinophagy) could increase the levels of LIP and promote ferroptosis.

Mechanisms of ferroptosis induction

Accumulation of lipid peroxides, which is responsible for ferroptotic lethal cell fate, can be caused by two different mechanisms: inhibition of the System X_c^-, and subsequent inactivation of glutathione peroxidase 4 (GPX4), or direct inhibition of GPX4.

System X_c^- is an amino acid antiporter that transports inside the cells the extracellular cystine, the oxidized form of cysteine, by exchanging intracellular glutamate [33]. Once inside the cells, intracellular cystine is reduced to cysteine, which is an essential substrate for glutathione (GSH) synthesis. Since GSH plays a key role in cellular antioxidant defenses, cellular uptake of cysteine represents a critical step in GSH synthesis and, therefore, in protecting cells from oxidative stress [28]. Hence, inhibition of the System X_c^- blocks the biosynthesis of GSH, thus reducing the antioxidant activity of GSH, selenium-dependent, peroxidases (GPXs) and leading to accumulation of lipid ROS, and, therefore, cell death [28]. Among GPXs, GPX4 is the only isoform able to reduce hydrogen peroxides or organic hydroperoxides to water or corresponding alcohols by converting GSH, which represents an essential cofactor of GPX4, into oxidized glutathione (GSSG) (Figure 1.5) [34]. Then, inhibition of GPX4 leads to accumulation of lipid ROS and to ferroptotic cell death (Figure 1.5). GPX4 can be inactivated through direct inhibition or indirect mechanisms such as depletion of GSH [34].

According to the different inducing mechanisms, ferroptosis inducers (FINs), could be divided into 4 different classes (Table 1).

Table 1. Classification of ferroptosis inducers (FINs)

Class	Mechanism of action	Compounds
Class I	Depletion of GSH	Erastin, PE, IKE, sulfasalazine, sorafenib
Class II	Direct inhibition of GPX4	RSL3, ML210, ML162,
Class III	Depletion of GPX4 protein and CoQ10	FIN56
Class IV	Induction of iron and lipids oxidation, indirect inhibition of GPX4	$FINO_2$

PE, piperazine erastin; IKE, imidazole ketone erastin; GSH, glutathione; GPX4, glutathione peroxidase 4; RSL3, (1S,3R)-RSL-3, RAS-selective lethal 3; CoQ10, coenzyme Q10

Class I of FINs triggers ferroptosis by depleting intracellular levels of GSH. Erastin and its analogues, such as imidazole ketone erastin (IKE) and piperazine erastin (PE), belong to class I of FINs [35]. These molecules induce GSH depletion by inhibiting System X_c^-: for instance, as mentioned before, by blocking the transport of cystine inside the cells, the synthesis of GSH is compromised. Thus, depletion of GSH leads to the inhibition of GPX4 antioxidant activity, resulting in a lethal accumulation of lipid peroxides

and subsequent cell death by ferroptosis. Other class I ferroptosis inducers are represented by the Food and Drug Administration (FDA)-approved drugs sulfasalazine and sorafenib [34].

Moving on to the class II, RSL3 (RAS-selective lethal 3) is a compound able to directly inhibit GPX4. RSL3 contains an electrophilic moiety and a chloroacetamide moiety, which covalently interact with selenocysteine, the nucleophilic amino acid residue at the active site of GPX4, leading to the irreversible inactivation of GPX4 [36]. Induction of ferroptosis by RSL3 does not involve the inhibition of System X_c^-, since the import of cystine is not affected, as well as the depletion of GSH content [36]. In addition to RSL3, other molecules such as ML210, (also known as DPI10) and ML162 (also known as DPI7) are able to inhibit GPX4 through the interaction between their electrophile moiety with the GPX4 selenocysteine [37]. Ultimately, it has been observed that also altretamine, an FDA-approved anticancer drug, can induce ferroptosis by directly inhibiting GPX4 activity [38].

Class III includes those compounds whose trigger ferroptosis by decreasing the abundance of GPX4 and simultaneously causing depletion of coenzyme Q10 (CoQ_{10}), a lipid-soluble coenzyme with an antioxidant activity towards proteins, lipids and DNA oxidation products [39]. For instance, FIN56 promotes ferroptosis through two different mechanisms: depletion of GPX4 protein from cells and reduction of the levels of CoQ_{10}, by binding and activating squalene synthase (SQS), an enzyme implicated in the mevalonate pathway [34].

Currently, only one ferroptosis inducer can be included in class IV: endoperoxide ($FINO_2$). $FINO_2$ promotes ferroptosis through two distinct mechanisms. It indirectly inhibits GPX4 activity, even if the specific inactivation mechanism is still unclear, and it directly oxidizes ferrous iron through the reaction of 1,2-dioxolane, contained in the molecule, with ferrous iron to produce oxygen-centered radicals; moreover, $FINO_2$ can also oxidize lipids [40].

Recently, Hassannia *et al* have suggested a "non-canonical" induction of ferroptosis related to an increase of the labile iron pool (LIP) [34,41]. LIP increase could be triggered, for example, by an excessive activation of heme-oxygenase 1 (HMOX1), a reduced ferroportin expression or an enhanced transferrin expression [34,41]. Moreover, even if the mechanism of action is still uncertain, iron chloride, hemoglobin, hemin, or ferrous ammonium sulfate could also trigger ferroptosis by overloading cells with iron [34].

Role of iron and lipid peroxidation in ferroptosis

As can be observed from the name given to this particular form of non-canonical cell death, iron plays an essential role in ferroptosis. Intracellular iron is strictly controlled, in order to maintain a correct

homeostasis in the body, by a wide range of proteins which are involved in the modulation of cellular Fe^{2+} amount, and in the control of iron intake, transport, release, and export [42]. The most of intracellular Fe^{2+} is stored in ferritin, an iron storage protein complex composed by a ferritin light chain (FTL) and ferritin heavy chain 1 (FTH1). Instead, the amount of free Fe^{2+}, also known as LIP, which is very limited, is placed in mitochondria, cytoplasm, nucleus, and lysosomes [42].

Several studies confirmed that the modulation of proteins involved in iron homeostasis, including its uptake, storage, export of iron, regulates ferroptosis through the modulation of the intracellular levels of iron. In particular, heat shock protein beta-1 (HSPB1) can decrease the levels of intracellular iron by inhibiting transferrin receptor 1 (TRF1); consequently, overexpression of HSPB1 could inhibit ferroptosis while its inactivation could enhance ferroptosis induction through iron accumulation [43]. Moreover, the inhibition of the expression of iron response element binding protein 2 (IREB2), one of the most important transcription factors involved in the control of iron homeostasis, increased the expression of FTL and FTH1, therefore limiting erastin-induced ferroptosis [44]. Besides the role of proteins involved in iron metabolism in modulating ferroptosis, a pivotal role in ferroptosis is played by the free-iron pool, LIP, particularly in accumulation of lipid ROS [45].

Iron-dependent accumulation of lipidic ROS can occur through non-enzymatic and/or enzymatic lipid peroxidation. Non-enzymatic lipid peroxidation, also called autoxidation of lipids, consist in a free radical-driven chain reaction where ROS initiate the oxidation of polyunsaturated fatty acids (PUFAs). Fenton or Fenton-like reactions, that involve a reaction between hydrogen peroxide (H_2O_2) and free labile Fe^{2+}, are the main sources of hydroxyl radical (OH•) formation. The first step of lipid autoxidation is triggered by hydroxyl radical which dissociate a hydrogen atom from PUFAs to form a lipid radical (L•) that immediately reacts with oxygen (O_2) to generate a lipid peroxyl radical (LOO•). Then, peroxyl radical can abstract hydrogen from an adjacent PUFA generating a new lipid radical that starts another lipid radical chain reaction, and a lipid hydroperoxide (LOOH) that is transformed in presence of Fe^{2+} in an alkoxyl radical (LO•), which reacts with another adjacent PUFA to initiate an additional chain reaction. Within this autocatalytic process, autoxidation can be freely propagated leading to membrane destruction and subsequent cell death [35,46].

Enzymatic lipid peroxidation, instead, is mostly driven by lipoxygenases (LOXs). LOXs are non-heme-iron enzymes possessing a dioxygenases activity. They can catalyze the insertion of oxygen into PUFAs lipid membrane generating different lipid hydroperoxides that, therefore, can start the autocatalytic process of lipid autoxidation mentioned above [46].

It is not totally clear whether LOXs are crucial in ferroptosis induction. Indeed, even if the inhibition or knockdown of LOXs, in some cell types, inhibit ferroptosis [47], thus showing the involvement of LOXs

in ferroptosis induction, different studies suggested that lipoxygenases, even if their expression can sensitize to ferroptotic cell death, and their activity contribute to ferroptosis occurrence, are not essential in ferroptosis cell death, unlike lipid autoxidation [48].

Ferroptosis execution

If the link between lipid metabolism and ferroptosis induction is well known, how lipid peroxidation leads to ferroptotic cell death remains still not clarified. Two mechanisms through which the accumulation of lipid peroxides leads to cell death have been hypothesized. The first hypothesis is that lipid hydroperoxides, produced by PUFAs peroxidation, generate reactive toxic products such as 4-hydroxy-2-nonenal (4-HNE) or malondialdehyde (MDA) [49]. The highly reactive 4-HNE contains an electrophilic functional group by which can alkylates and inactivates different survival proteins, involved in crucial cellular processes, thus leading to ferroptotic cell death. For instance, a study on DU145 erastin-resistant prostate cancer cells unveiled that resistant cells had a drastic upregulation of AKR1C genes, that are associated to the detoxification of aldehydes such as 4-HNE [45,50]. Moreover, a recent study, using a quantitative protein carbonylation profiling approach, confirmed that proteins could be modified during ferroptosis by electrophilic products derived from lipid peroxidation, as, indeed, by those detoxified by AKR1C, as 4-HNE [51].

The second hypothesis is that the extensive peroxidation of phospholipids during ferroptosis leads to structural and functional modification of cellular membrane [35]. Accumulation of lipid peroxides, indeed, might produce deformation of the lipid bilayer, forming pore-like structures that increase membrane permeability and decrease membrane fluidity [52]. For instance, Agmon and colleagues observed that the accumulation of lipid peroxides causes a reduction of the membrane thickness and an increase in membrane curvature. These alterations lead to an increased access of oxidants causing, therefore, an irreversible damage to the integrity of the membrane and, consequently, cell death [52].

Regulation of ferroptosis and its crosstalk with other forms of PCD

Recently, several studies confirmed the interplay between ferroptosis and autophagy, even if this link is not yet clear. On one hand, it has been observed that quinacrine suppressed autophagy and increased the sensitivity of glioblastoma stem cells to temozolomide by inducing ferroptosis [53]. On the other hand, induction of autophagy promoted ferroptosis activation. Activation of autophagy provokes degradation of ferritin, thus increasing the levels of free labile iron that boosts accumulation of ROS and triggers ferroptosis, a process called ferritinophagy. Ferritinophagy is a peculiar form of autophagy related to the NCO4 (Nuclear receptor coactivator 4)-mediated autophagic degradation of ferritin [54]. Ferritinophagy degrades the iron storage protein ferritin, thus increasing the release of free iron and promoting

ferroptosis [54]. NCO4 knockdown inhibited ferroptosis in fibrosarcoma, pancreatic cancer cells, and other cancer cell types, thus confirming the promoting activity of ferritinophagy towards ferroptosis [54]. Moreover, also the genetic knockout of autophagy-related gene (Atg) 5 and Atg7, which are crucial genes for autophagosome formation, weakened erastin-induced ferroptosis through the inhibition of ferritin, thus reducing the intracellular levels of Fe^{2+} and lipid peroxidation [54]. However, in certain cancer cell lines, bafilomycin A1 and chloroquine, which are two autophagy inhibitors, did not inhibit erastin-induced ferroptosis, probably because they are not specific inhibitor of autophagy but also for lysosomal processes and endocytic pathways [54]. In addition, two recent studies further show how autophagy could enhance ferroptosis induction: in fact, it has been observed that the degradation of a circadian clock regulator by autophagy, promotes *in vitro* and *in vivo* ferroptosis in cancer cells [55,56]. Finally, also BECN1, which is another key component involved in autophagy, enhanced ferroptosis induction: for instance, BECN1 increased lipid peroxidation in an autophagy-independent manner, by interacting with the SLC7A11 member of System X_c^- [57].

Besides autophagy, a crosstalk between ferroptosis and apoptosis has also been observed. For instance, Hong and colleagues found that in human pancreatic cancer PANC-1 and BxPC-3 and human colorectal cancer HCT116 cells, erastin and artesunate could enhance TRAIL-mediated apoptosis [58]. The underlying mechanism of this effect is the promotion of ER stress together with ferroptosis. Indeed, erastin and artesunate, by promoting ER stress, enhanced the expression of Puma by CHOP (CCAAT-enhancer-binding protein homologous protein) [58]. Hence, the ER stress-mediated activation of CHOP/Puma axis seems to play a crucial role in the sensitization to TRAIL-mediated apoptosis by ferroptotic agents [58].

Additionally, tumor suppressor factor p53 which is the master regulator of cell cycle and apoptosis induction, is also involved in ferroptosis [59,60].

In particular, it was reported that $TP53^{3KR}$ an acetylation-defective mutant p53, is not effective in inducing cell senescence, cell-cycle arrest, and apoptosis, but it can repress the expression of SLC711A, a subunit of System X_c^-, thus inducing ferroptosis [59,60]. In addition, $p53^{R273H}$ and $p53^{R175H}$, other two mutant forms of p53 resulting from missense mutations in TP53 gene, can repress SLC7A11 expression through the inhibition of Nrf2 (Nuclear factor (erythroid-derived)-like 2)-mediated upregulation of SLC7A11 [59,60]. Lastly, a novel type of p53 complex, called metal organic network-p53 (MON-p53) was designed by Zheng *et al.* This complex of tannin acid integrated with ferric ions, form MON on the external of the p53 plasmid; after its internalization, ferric ion induce ROS generation by activating Fenton reaction, thus promoting ferroptotic cell death, besides apoptosis, as observed in MON-p53 treated cells [61].

However, p53 can act also as negative regulator of ferroptosis: mutations in the N-terminal domain of the gene were not able to suppress SLC7A11 [59,60]. Moreover, acetylation-defective mutant $p53^{4KR98}$ is not able to suppress SLC711A but holds its activity against the other p53 target genes, as $TP53^{S47}$, a p53 mutated form of gene TP53 with single nucleotide polymorphism on Serine 47, which is not able to repress the transcription of SLC711A, making cells resistant to ferroptosis induction [59,60]. Additionally, it was found that the stable wild type p53 reduces the sensitivity of fibrosarcoma, renal cancer, and osteosarcoma cells against ferroptosis induced by the inhibition of System X_c^-; this protection is due to the activation of p53-p21 axis, which weakens the depletion of intracellular GSH and limits the accumulation of lipid ROS [59,60].

Another negative regulator of ferroptosis is represented by Nrf2. Normally, Nrf2 is kept inactivated by Kelch-like ECH-associated protein 1 (Keap-1)-dependent proteasomal degradation. Under increased oxidative stress conditions, Nrf2 dissociates from Keap1, translocates into the nucleus, and starts the transcription of antioxidant responsive element (ARE)-dependent genes [62]. Most of the Nrf2 target genes are implicated in the maintenance of redox homeostasis, including regulation of System X_c^-, and also in iron and heme homeostasis, by regulating HMOX1, ferroportin, and FTL/FTH1 [62]. Hence, since Nrf2 pathway activation endorses iron storage, limits cellular iron uptake and ROS production, Nrf2 is considered as a negative ferroptosis regulator [63]. Indeed, in hepatocellular carcinoma cells the exposure with ferroptosis inducers induces the binding between p62 and Keap1, leading to the disruption of Keap1-Nrf2 interaction and the consequent activation of Nrf2 pathway, conferring resistance to cancer cells against ferroptosis induction [64]. Moreover, also the activation of Nrf2 pathway by artesunate was supposed to be related to ferroptosis resistance in HNC cells [65]. However, in contrast with the afore-mentioned reports, activation of Nrf2 pathway could also promote ferroptotic cell death, as observed for withaferin A [41], and supposed for artesunate [66], thus presuming that Nrf2 could act as a double-edge sword. This opposite role of Nrf2 in ferroptosis could be probably cell-type specific [67], since activation of Nrf2 pathway protected hepatocellular carcinoma cells against ferroptosis [64], while in neuroblastoma it promoted ferroptosis induction [41].

Lastly, among the negative regulators of ferroptosis, there is HSPA5, better known as GRP78 (glucose-regulated protein 78) or BiP. HSPA5 is a molecular chaperone located in the ER and is considered the master regulator of the Unfolded Protein Response (UPR) signaling process, which is activated in response of perturbations in the ER folding machinery, a condition better known as ER stress [68]. Besides its role in UPR regulation, HSPA5 negatively regulates ferroptosis [69], as showed in pancreatic cancer cells where activating transcription factor 6 (ATF6)-induced HSPA5, bound and upregulated GPX4 activity, therefore limiting its degradation, and, subsequently, lipid peroxidation [69].

1.4.2 Necroptosis

Since 1980s, it was known that TNFα is capable of inducing necrosis in addition to apoptosis in certain cell lines [70]. Few years later it was found that TNF-induced necrosis could be further enhanced by the inhibition of caspases through the chemical pan-caspases inhibitor benzyloxycarbonyl-Val-Ala-Asp (OMe)-fluoromethylketone (Z-VAD-FMK) or by cytokine response modifier A (CrmA) which induce a viral inhibition of caspase-8 [71]. When in 2000 it was observed that the activity of receptor-interacting protein (RIP) kinase RIP1 was essential in regulating cell death induced by TNF-α, TRAIL, or FasL/CD95L in a kinase- activity-dependent manner, it became increasingly clear that necrosis triggered by death receptors is highly regulated by the kinase activity of RIP1 [72]. Then, in 2005, the term necroptosis was coined when Degterev *et al* discovered that necrostatin-1 (Nec-1), a specific chemical inhibitor, was able to inhibit TNF-induced necrosis by blocking RIP1 kinase activity [73].

From the morphological point of view, despite being a finely regulated mechanism of cellular death, necroptosis shares the typical morphological features of necrosis, such as cellular rounding, swelling, cytoplasmic granulation, and plasma membrane rupture [74]. However, despite necroptosis is a caspase-independent cell death mechanism, it bears some similarities with apoptosis. In particular, part of the extrinsic apoptotic pathways is shared with necroptosis (Figure 1.6) [5].

It is currently known that necroptosis can be triggered by a plethora of stimuli, as activation of death receptors (*e.g.* FAS and TNFR1), tool-like receptors (*e.g.* tool-like receptor 3, TLR3, and TLR4), nucleic acid sensor (*e.g.* Z-DNA-binding protein 1, ZBP1, also called DAI), retinoic acid receptor responder 3 (RARRES3, also known as RIG1), transmembrane protein 173 (TMEM173, also called STING), and adhesion receptor. Moreover, also the same ligands that trigger apoptosis (*e.g.* Fas ligand, TNF, TRAIL) could initiate necroptosis in specific conditions such as inhibition of caspase-8 activation by viral proteins, genetic defects, and treatment with the pan-caspase inhibitor Z-VAD-FMK [5].

Among the aforementioned initiation mechanisms, the best characterized inducer of necroptosis is the TNFα/TNFR signaling pathway, which could be considered as a prototype of necroptosis induction mechanism (Figure 1.6) [74].

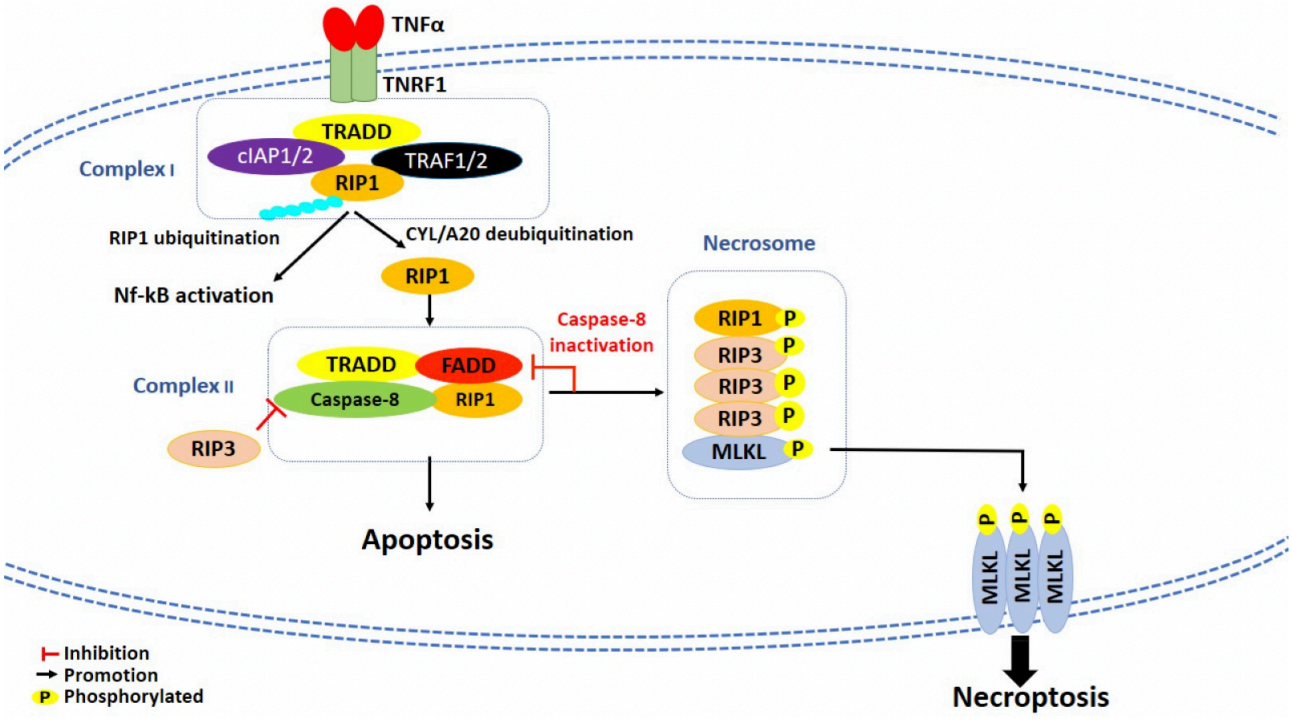

Figure 1.6 Schematic representation of necroptotic cell death pathway [32].

The binding of TNFα (tumor necrosis factor α) to TNFR1 (tumor necrosis factor receptor 1) promotes the formation of complex I, composed by RIP1 (receptor-interacting protein 1), TRADD (TNF receptor-associated death domain), TRAF1/2 (TNFR-associated factors 1/2) and cIAP1/2 (cellular inhibitors apoptosis proteins). Within complex I, cIAP1/2 induces Lys63-linked polyubiquitination of RIP1, which eventually leads to the activation of NF-ϰB (nuclear factor kappa-light-chain-enhancer of activated B cells) pathway and cell survival. Deubiquitination of RIP1 by CYLD (cylindromatosis) or A20, instead, induces the dissociation of RIP1 from complex I and the formation of complex II, composed by TRADD, FADD, RIP1 and caspase-8. When the activity of caspase-8 is inhibited, RIP1 after its phosphorylation interacts with RIP3 (receptor-interacting protein 3) promoting the formation of necrosome. In the necrosome, phosphorylated RIP1 leads to the phosphorylation of RIP3, which subsequently phosphorylates mixed lineage kinase domain-like (MLKL). Phosphorylation of MLKL induces its oligomerization and its translocation to plasma membrane to execute necroptosis.

After the binding with TNFα, TNFR1 undergoes its activation through a conformational change; then, activated TNFR1 recruits TRADD, cellular inhibitors of apoptosis (cIAP1 and cIAP2), TNFR-associated factors (TRAF1 and TRAF2), and RIP1, to create a membrane-signaling complex, called complex I. In this complex, cIAP1/2 induces Lys63-linked polyubiquitination of RIP1, which consequently leads to the activation of canonical NF-kB pathway and, eventually, cell survival (Figure 1.6) [75]. Conversely, inhibition of cIAPs activity by Smac/Diablo proteins or Smac mimetic compounds promotes the deubiquitination of RIP1 by the deubiquitinating enzymes cylindromatosis (CYLD) and A20, which both hydrolyze Lys63-linked ubiquitin chains [75]. Subsequently, deubiquitination of RIP1 induces its dissociation from complex I and the formation of either cytosolic complex IIa or complex IIb, depending on the proteins content: complex IIa is formed by TRADD, RIP1, FADD and caspase-8; complex IIb is formed by RIP1, FADD, and caspase-8, but it does not contain TRADD. If in the complex IIa, activation of caspase-8 by cleavage is independent from RIP1 kinase activity, in complex IIb, where

TRADD is not present, RIP1 kinase activity is required for caspase-8 activation to induce RIP1-dependent apoptosis [75]. However, complex IIa and IIb are both capable of inducing apoptosis or necrosis depending on cell status [76,77]. Indeed, when caspase-8 is inhibited by caspase inhibitors or virally expressed proteins, RIP1 after its activation by autophosphorylation of the serine residue 161 (S161) [76], interacts with RIP3 (receptor-interacting protein 3) through their RIP homotypic interaction motif (RHIMs) leading to the formation of a protein complex called necrosome (Figure 1.6) [76].
RIP3, beside its activation through RIP1, could be directly activated also by other stimuli. For instance, lipopolysaccharides (LPS) or double-stranded (dsRNA), after their association with TL3/TL4 receptors, can straight activate RIP3 through TIR-domain-containing adapter inducing interferon-β (TRIF), a RHIM-containing protein [5,75]. Additionally, DNA-dependent activator of interferon-regulatory factor DAI, called also ZBP1, after its activation in response of exogenous DNA, is capable to interact with RIP3 through its RHIM [5,75].

The formation of the necrosome complex induces the activation and phosphorylation of both RIP1 and RIP3: in humans, RIP1 is phosphorylated at Ser14/15 and Ser161/Ser166, and RIP3 at Ser227. Then, the active phosphorylated RIP3 subsequently phosphorylates mixed lineage kinase domain-like (MLKL) at Ser358. In this regard, it has been observed that phosphorylation of RIP3 at Ser227 has an essential role in the recruitment of MLKL [75]. Hence, phosphorylation of MLKL induces its oligomerization, mostly trimers or tetramers, and its translocation to plasma membrane (Figure 1.6), which is crucial for necroptosis execution [75].

To date, the mechanism by which necroptosis is executed is still controversial. Some studies report that oligomerized MLKL could create pore structures into the plasma membrane by interacting with negatively charged phospholipids. In particular, an initial interaction of MLKL with phosphorylated phosphatidylinositol phosphate (PIP) phospholipids, which have low-affinity binding sites, induces a conformational rearrangement of MLKL that yields additional higher affinity binding sites for PIPs, causing a massive association of MLKL to the plasma membrane and multiple interactions with the membrane phospholipids that ultimately lead to membrane permeabilization [75]. Other studies, in contrast, reported that MLKL could induce a dysregulation of ionic fluxes at the plasma membrane. Cai *et al* demonstrated that phosphorylated MLKL forms trimers that, by interacting with the kinase TRPM7 (transient receptor potential cation channel, subfamily M, member 7), induce a massive extracellular Ca^{2+} influx responsible for breaking plasma membrane [78]. Additionally, it has been found by Chen *et al* that the rupture of plasma membrane is due to an influx of Na^{+}, but not Ca^{2+} ions triggered by MLKL tetramers; however, the mechanism through with tetramers induce this Na^{+} influx has not been identified [79].

1.5 Natural compounds as non-canonical cell death inducers

Nature is a never-ending source of preventive and curative agents, used since ancient times in traditional medicines to prevent many human diseases [80]. Nature continues to represent an exhaustible source of pharmacologically active compounds, especially in the field of anticancer therapy. Indeed, of the 136 new anticancer drugs discovered between 1981 and 2019, the 65% are represented by natural or natural-based compounds [81]. The enormous potential of natural products in the context of cancer therapy relies on their great biodiversity. Indeed, as they are composed of innumerable molecules, natural products could interact with various molecular targets and regulate different biological pathways. Therefore, it is not surprisingly that many different natural compounds were discovered to be effective anticancer agents by promoting non-canonical cell death mechanisms.

1.5.1 Natural products as ferroptosis inducers

Many different natural products, summarized in Table 2, elicit ferroptosis in various cancer models both *in vitro* and *in vivo* (Table 2).

Table 2. Overview of natural *in vitro* and *in vivo* ferroptosis inducers

Natural compound	Source compound	*In vitro* models	*In vivo* models	Reference
Albiziabioside A	*Albizia inundata* Mart.	MCF-7	/	[82]
Ardiacrispin B	*Ardisia kivunensis*	CCRF-CEM	/	[83]
Amentoflavone	*Selaginella* spp. and other plants	U251/U373	BALB/c nude mice inoculated with U251 cells	[84]
Artesunate	*Artemisia annua* L.	DAUDI/CA-46	NOD/SCID mice inoculated with CA-46 cells	[85]
		MT-2/HUT-102	/	[86]
		HN9/NH9-cisR	/	[65]
		PaTU8988/AsPC-1	/	[87]
		HEY1/HEY2/SKOV-3	/	[88]
		Panc-1/BxPC-3/AsPC-1	/	[66]
Methanolic extract of *Betula etnensis* bark	*Betula etnensis* Raf.	CaCo2	/	[89]
Dihydroartemisinin	*Artemisia annua* L.	HL60	/	[90]
		G0101/G0107/U251/U373	/	[91]
		MEFs/HT1080	Foxn1nu/ Foxn1+ athymic mice inoculated with GPX4 iKO H292 cells	[92]
Dihydroisotanshinone I	*Salvia miltiorrhiza* Bunge	MCF-7/MDA-MB-231	/	[93]
Epunctanone	*Garcinia epunctata* Stapf.	CCRF-CEM	/	[94]
Ferroptocide	Semi-syntetic derivative of Pleuromutilin (*Pleurotus passeckerianus* and others spp.)	ES-2/HCT116/4T1	/	[95]
Gallic acid	Phenoliuc compound found in different plants/food	A375/MDA-MB-231	/	[96]
Physcion 8-O-β-glucopyranoside	*Rumex japonicus* Houtt.	MGC-803/MKN-45	/	[97]
Piperlongumine	*Piper longum* L.	Panc-1/MIAPaCa-2	/	[98]
Ruscogenin	*Ruscus aculeatus* L. *Radix Ophiopogon japonicas* (Thunb.) *Ker Gawl.*	BxPC-3/SW1990	/	[99]
Typaneoside	*Pollen Typhae*	Kas-1/HL60/NB4	/	[100]

Ungeremine	*Crinum zeylanicum* L.	CCRF-CEM	/	[101]
Withaferin A	*Withania somnifera* L.Dunal	IM-32/SK-N-SH	BALB/c nude mice inoculated with IMR-32 cells	[41]

Amentoflavone

Amentoflavone is a flavonoid mainly found in *Selaginella tamariscina* (P.Beauv.) Spring and in other species of *Selaginella*, as well as in many other plant species [102]. In U251 and U373 glioma cell lines, amentoflavone promoted ferroptotic cell death by reducing GSH and FTH intracellular levels, thus leading to lipid ROS and MDA accumulation, and subsequent cell death (Table 2) [84]. Interestingly, amentoflavone promoted the degradation of FTH by triggering ferritinophagy, therefore suggesting the induction of autophagy-dependent ferroptosis. Indeed, FTH overexpression, which would otherwise have been degraded through ferritinophagy, reduced ferroptotic cell death, by diminishing MDA and lipid ROS levels [84]. Amentoflavone confirmed its ability to promote ferroptosis also *in vivo*. Indeed, in a glioma xenograft mouse model, amentoflavone increased MDA levels, and decreased GSH levels (Table 2) [84]. Moreover, amentoflavone increased LC3B, Beclin1, Atg5, and Atg7 levels, and decreased FTH levels in tumor tissue, thus confirming the induction of autophagy-dependent ferroptosis also *in vivo* [84].

Artesunate

Artesunate is a semi-synthetic derivative of artemisinin, a sesquiterpene lactone derived from *Artemisia annua* L. Artesunate showed to promote ferroptosis in pancreatic [66,87], ovarian [88], head and neck cancer (HNC) [65], in T-cell leukemia/lymphoma (ATLL) [86], and in Burkitt's Lymphoma [85], by modulating different molecular targets (Table 2).

In Burkitt's Lymphoma DAUDI and CA-46 cells, artesunate triggered ferroptosis and ER stress, by activating ATF4 (activating transcription factor-4)-CHOP-CHAC1 (glutathione-specific gamma-glutamyl-cyclotransferase 1) pathway [85]. Depending on cell type, artesunate showed to possess different effects towards ER stress induction. Indeed, Dixon *et al* already demonstrated that certain ferroptosis inducers, but not artesunate, induced ER stress within the activation of ATF4 and the upregulation of CHAC1, by inhibiting System X_c^- [103]. Conversely, in Burkitt's Lymphoma cells, artesunate, together with ferroptosis induction, boosted ER stress by activating ATF4-CHOP-CHAC1 cascade reaction [85]. Moreover, upregulation of CHAC1, that possess also a GSH degradation activity [104], probably contributes to ferroptosis induction in DAUDI and CA-46 cells, as proposed by the authors [85].

In *kras* mutant pancreatic cancer cells PaTU8988 and AsPC-1, artesunate induced ferroptosis by increasing MDA levels, used as a marker of lipid peroxidation. In this study, authors showed that the artesunate-induced ferroptosis was enhanced by the knockdown of GRP78 [87]. Indeed, as mentioned before, GRP78 possesses a negative role towards ferroptosis induction [69,103].

In HNC cells, artesunate induced ferroptosis by decreasing GSH intracellular levels and increasing lipid ROS production [65]. In HNC cells, but also in cisplatin-resistant NHC cells, artesunate activated the Nrf2 pathway, which has been related to ferroptosis resistance [65]. Indeed, by silencing Keap1, the sensitivity of cancer cells towards artesunate-mediated ferroptosis has been enhanced [65]. However, in Panc-1 pancreatic cancer cells, induction of ferroptosis by artesunate was accompanied by an increase of HOMX1 protein expression, thus supposing that artesunate, by increasing ROS levels, could activate Nrf2-mediated antioxidant response [66]. Promotion of ferroptosis by artesunate has been reported also *in vivo* (Table 2). In a Burkitt's Lymphoma xenografted mouse model, artesunate suppressed tumor growth by inducing lipid peroxidation, as suggested from the observed increase of MDA levels in tumor tissues (Table 2) [85].

Whitaferin A

Withaferin A (WA) is a naturally occurring steroidal lactone derived from *Withania somnifera* (L.) Dunal, a popular herbal medicinal plant used in Ayurvedic medicine for its many health benefits [105]. In a variety of cancer cells, WA showed to possess anticancer activity through a plethora of mechanisms, including proteasomal inhibition, cell-cycle inhibition, modulation of oxidative stress, and induction of apoptotic cell death [105]. In neuroblastoma cells, WA promoted ferroptosis through a dual mechanism: at high dose, WA directly binds and inactivates GPX4, thus inducing canonical ferroptosis; at medium dose, WA activates the Nrf2 pathway by targeting Keap1, leading to an excessive upregulation of HMOX1, and a subsequent increase of intracellular labile iron [41], the ferroptotic mechanism referred to as "non-canonical" ferroptosis induction [41].

The ability of WA to induce ferroptosis was confirmed also *in vivo*. In a neuroblastoma xenograft mouse model, WA suppressed tumor growth, showing the same effectiveness of the chemotherapeutic agent etoposide [41]. WA eradicated neuroblastoma xenografts by triggering ferroptosis, since a decrease of GPX4 expression, an increase of HMOX1 expression, and accumulation of lipid peroxides has been observed in tumor tissues [41].

1.5.2 Natural products as necroptosis inducers

Many different natural products, summarized in Table 3, elicit necroptosis in various cancer models *in vitro* and *in vivo* (Table 3).

Table 3. Overview of natural necroptosis inducers

Natural compound	Source compound	*In vitro* models	*In vivo* models	References
2-Methoxy-6-acetyl-7-methyljuglone	*Polygonum cuspidatum* Sieb. et Zucc	A549	BALB/c nude mice inoculated with A549 cells	[106]
		A549/H1299	/	[107]
		U87/U251	U251-derived xenograft zebrafish model	[108]
11-methoxytabersonine	*Tabernaemontana bovina* Lour.	A549/H157	/	[109]
***Acridocarpus orientalis* dichloromethane/n-butanol fractions**	*Acridocarpus orientalis* A. Juss	HeLa	/	[110]
Arctigenin	*Arctium lappa* L., *Saussurea heteromalla*	PC-3/PC3-AcT	/	[111]
		RPMI-2650	/	[112]
Aridanin	*Tetrapleura tetraptera* (Schum. & Thonn) Taub.	CCRF-CEM	/	[113]
Berberine	*Coptis chinensis* Franch., and *Hydrastis Canadensis* L.	OVCAR3/POCCLs	/	[114]
		DB/RAMOS	/	[115]
Celastrol	*Tripterygium wilfordii* Hook. f.	HGC-27/AGS	/	[116]
Columbianadin	*Angelica decursiva Fr. Et Sav*	HCT116	/	[117]
Deoxypodophyllotoxin	*Pulsatilla koreana* (Yabe ex Nakai) Nakai ex T. Mori	NCI-H460	/	[118]
Emodin	*Rheum Palmatum* L.	U251	BALB/c nude mice inoculated with U251 cells	[119]
Gomisin J	*Schisandra chinensis* (Turcz.) Baill.	MCF7/MDA-MB-231	/	[120]
Jujuboside B	*Zizyphus jujube Mill var. spinosa* (Bunge) Hu ex H. F. Chow	U937	/	[121]
Matrine	*Sophora flavescent s* Aiton	Mz-ChA-1/QBC939	/	[122]
Neoalbacol	*Albatrellus confluens*	C666-1/HK1	/	[123]
Ophiopogonin D'	*Ophiopogon japonicus* (Thunb.) Ker Gawl	LnCaP	/	[124]
Pristimerin	*Celastraceae* and *Hippocrateaceae* spp.	C6/U251	BALB/c nude mice inoculated with C6 cells	[125]
Progenin III	*Raphia vinifera P.* Beauv.	CCRF-CEM	/	[126]
Quercetin	Flavonoid found in different plants/food	MCF7	/	[127]
Resibufogenin	Venom of *Bufo gargarizans*	HCT116	/	[128]
		SW480	BALB/c nude mice inoculated with eGFP-SW480 cells	[128]
			C57BL6/j mice inoculated with eGFP-MC38 cells	
Sanguilutine	*Papaveraceae, Fumariaceae, Ranunculaceae* and *Rutaceae* spp.	Mel-JuSo/A375/A375-Bcl-2	/	[129]
Shikonin	*Lithospermum erythrorhizon* Siebold & Zucc.	F-47D	/	[130]
		AsPC-1	/	[131]
		CNE-2Z	Nude mice inoculated with CNE-2Z cells	[132]
		A549	BALB/c athymic nude mice inoculated with A549 cells	[133]
		KMS-12-PE/ RPMI-8226/U266	/	[134]

		K7/K12/K7M3/U20S/ 143B	BALB/c nude mice inoculated with K7 cells	[135]
		U937	/	[136]
		C6/U87/SHG-44/U251	BALB/c nude mice inoculated with C6 cells	[137–140]
		5-8F	BALB/c nude mice inoculated with 5-8F cells	[141]
		AGS	/	[142]
		NIH3T3	/	[143]
		MCF7	/	[144]
		MDA-MB-468	/	[145]
Tanshinol A	*Salvia mltiorrhiza* Bunge	H1299/A549	/	[146]
Tanshinone IIA	*Salvia mltiorrhiza* Bunge	HepG2	/	[147]
Ungeremine	Ethanol extract of *Crinum zeylanicum* and of *Ungernia oligostroma* Popov & Vved	CCRF-CEM	/	[101]

Berberine

Berberine is the mayor component of different plants belonging to *Berberis* species, and many other plants including, among all, *Coptis chinensis* Franch., and *Hydrastis canadensis* L. [148]. Berberine promoted necroptosis in ovarian cancer cells and in three patient-derived primary ovarian cancer cell lines (POCCLs) by activating RIP3 and MLKL, as showed by the increased expression of RIP3 and MLKL and their phosphorylated forms (Table 3) [114]. Berberine triggered necroptosis also in diffuse large B-cell lymphoma (DLBCL) cancer cells (Table 3), by promoting mitophagy-dependent necroptosis through the induction of the RIP1/RIP3/MLKL necrosome complex formation, and by promoting the mRNA degradation of PCYT1A (phosphate cytidylyltransferase 1 alpha), thus reducing its expression in cancer cells [115]. PCYT1A is an isoform of the key enzyme CTP (choline phosphate cytidylyltransferase), which is crucial for PC (phosphatidylcoline) synthesis [149]. Authors showed that PCYT1A was overexpressed in 44% of the analysed DLBCL patients, and that PCYT1A overexpression occurred in parallel within the enhanced gene and protein expression of MYC [115], one of the oncogenes mostly involved in lymphoma cell chemoresistance [150]. Moreover, MYC-induced overexpression of PCYT1A led to inhibition of necroptotic cell death in DLBCL cells [115]. In this context, berberine effectively suppressed DLBCL cancer cells growth by inhibiting the MYC-driven downstream effector PCYT1A, and by inducing mitophagy-dependent necroptosis [115].

Shikonin

Shikonin is a natural naphtoquinone isolated from the root of of *Lithospermum erythrorhizon* Sieb. et Zucc, [141]. Shikonin promoted necroptosis in a wide range of cancer cells, including pancreatic [131], nasopharyngeal carcinoma [132,141], gastric [142], lung [133], and breast cancer cells [130,144,145], osteosarcoma [135](, lymphoma [136], multiple myeloma [134], and glioma [137–140] (Table 3).

In AGS gastric cancer cells, shikonin induced necroptosis in a time-dependent manner: short treatment time led to necroptosis induction, while longer treatment time led to apoptotic cell death [142]. In MCF-

7 breast cancer cells, shikonin promoted necroptosis when the apoptotic machinery was inhibited by the pan-caspase inhibitor Z-VAD-FMK [144], as observed also in tanshinone IIA-induced necroptosis [147]. Interestingly, most of natural compounds illustrated in Table 3, induced both necroptosis and apoptosis (Table 3), confirming the existing interrelation between these cell death programs. Indeed, cell fate (apoptosis *versus* necroptosis) decision is primarily affected by available caspase-8 and cIAP1, cIAP2 and XIAP, since their deficiency favors necroptosis induction by suppressing RIP/RIP3 proteolytic cleavage, or ubiquitination of RIP1, respectively [151–153].

Besides the activation of RIP1, and RIP3, and the promotion of necrosome complex formation, the crucial event involved in shikonin-induced necroptosis is the production of ROS and mitochondrial ROS, observed in nasopharyngeal carcinoma [132], glioma [138–140], gastric cancer cells [142], and breast cancer cells [144].

In glioma cancer cells shikonin boosted ROS and mitochondrial superoxide generation [138–140]. Inhibition of RIP1 and RIP3 reduced ROS and mitochondrial superoxide production, showing that RIP1 and RIP3 regulate shikonin-oxidative stress, by targeting mitochondria [138]. In line with this evidence, RIP3 triggered oxidative stress by activating different metabolic enzymes, such as mitochondrial GLUD1 (glutamate dehydrogenase 1) [154]. Indeed, Han *et al* observed that resibufogenin, another natural-derived necroptosis inducer, activates GLUD1 in a RIP3-dependent manner [128].

Moreover, oxidative stress triggered by shikonin led to the collapse of mitochondrial membrane potential, within the release of AIF into the cytoplasm and its nuclear translocation [140]. Activated MLKL seems to be the responsible for shikonin-induced mitochondria collapse, since its inhibition reduced ROS and superoxide production, and AIF mitochondrial release [140]. This hypothesis is further supported by the observed accumulation of MLKL in mitochondria, and the enhanced expression of both mitochondrial MLKL and activated MLKL [140]. Indeed, MLKL could bind mitochondrial-specific lipid cardiolipin [155], in addition to its ability to boost the catalytic activity of PGAM5 (mitochondrial serine/threonine protein phosphatase family member 5), leading to mitochondrial fragmentation [5]. However, if mitochondria are essential in necroptotic cell death is not yet clear. Indeed, in mitochondria-deficient cells, due to mitophagy occurrence, as well as in cells from PGAM5$^{-/-}$ mice, necroptosis still occurred [156,157].

Shikonin confirmed its ability to promote necroptosis also *in vivo*. In nasopharyngeal carcinoma xenograft mice, and in lung cancer xenograft mice, it reduced tumor growth within increasing tumor necrosis [132,133,141], which have been related to an increase of RIP1 expression in lung cancer xenografted mice tumor tissue (Table 3) [133].

In osteosarcoma xenograft mice, shikonin reduced tumor growth by increasing RIP1 and RIP3 expression, and reduced lung metastasis, showing that shikonin also possesses antimetastatic activity (Table 3) [135]. However, the role of necroptosis in cancer metastasis is controversial. Indeed, Strilic *et*

al reported that necroptosis of endothelial cells, induced by tumor cells, promotes cancer cells extravasation and cancer metastasis by interacting with DR6 (death receptor 6) [158], hence showing that necroptosis could also promote cancer cell metastasis.

Finally, in glioma xenograft mice, shikonin promoted necroptosis by inducing the binding of MLKL with mitochondria and the subsequent release of AIF (Table 3) [140].

Chapter 2
Research aim

Therapeutic approaches based solely on induction of apoptosis are often unsuccessful due to the activation of resistance mechanisms. The identification and characterization of compounds capable of triggering further mechanisms of programmed cell death could represent an important strategy that may integrate or offer alternative approaches to the current anticancer therapies based exclusively on the induction of the apoptotic process.
Among all the investigated compounds as potential inducers of non-canonical cell death there are naturally occurring compounds. This should come as no surprise as more than 50% of anticancer drugs are derived from natural compounds or scaffolds found in nature. In addition, they are useful both for preventive and therapeutic purposes as they can modulate numerous targets involved in neoplastic transformation, and could therefore, more likely than "monotarget" compounds, activate different forms of cell death.

Hence, the aim of my research project was to explore the *in vitro* anticancer activity of certain natural compounds and their semisynthetic derivatives belonging to isothiocyanates and indoles classes, with the main purpose to investigate the potential induction of non-canonical cell death.

Isothiocyanates are a class of molecules present in form of precursors in many cruciferous plants. Isothiocyanates showed a marked antitumor activity, validated through *in vitro* and *in vivo* studies, and clinical trials [159]. Indoles are widely present in nature, produced by plants and bacteria; moreover, indoles also represent a class of alkaloids produced as secondary metabolites by marine organisms [160]. The first part of my research explored *in vitro* the anticancer effects of three isothiocyanates: the natural isothiocyanate sulforaphane and two novels synthetic isothiocyanates, *i.e.,* MG28 and MG46. The second part of my PhD work covered the *in vitro* study of the anticancer activity of AD05, a newly synthetic indole derivative.

Chapter 3
ISOTHIOCYANATES AND THEIR DERIVATIVES

3.1 Introduction

Cruciferous vegetables are a class of vegetables belonging to the *Brassicaceae* family (also called *Cruciferae*) and comprise many different food products including cabbage, broccoli, cauliflower, and Brussels sprout [161].

Clinical and pre-clinical studies have stated that cruciferous vegetables possess anti-carcinogenic, anti-inflammatory, and antioxidant activity largely due to the presence of many bioactive components, including flavonoids, minerals, and vitamins [162]. However, the most studied active compounds of crucifers are glucosinolates, which are thought to be the compounds most involved into the cancer protection activity of *Brassicaceae* plants [163].

In cruciferous vegetables, more than 120 different glucosinolates have been discovered, even if only some of them could be found in large amounts. Indeed, the amount of glucosinolates in cruciferous vegetables depends on different factors such as plant variety, cultivation, and growing conditions, and can also differ depending on the specific parts of the plant [163].

3.1.1 Biosynthesis of isothiocyanates

Glucosinolates are composed by a β-*D*-thioglucose group, a sulfonated oxime moiety, and a variable side chain R. The plant enzyme myrosinase, responsible for glucosinolates metabolism into active products, normally cannot interact with glucosinolates, since they are located in two different plant comparts [164]. When the plant is attacked by insects, but also by chewing, cooking, and heating, the rupture of plant tissues leads to the release of myrosinase which catalyzes the hydrolysis of glucosinolates [164]. Additionally, myrosinase originated from the gastrointestinal tract bacteria is responsible for the isothiocyanates absorption from ingested plant material [164]. The interaction between myrosinase and glucosinolates produces a molecule of glucose and the unstable aglycone thiohydroximate-O-sulfonate, which, depending on the nature of aglycone, reaction temperature and pH, and the presence of ferrous ions, rearranges to produce different breakdown products, including isothiocyanates (Figure 3.1) [163].

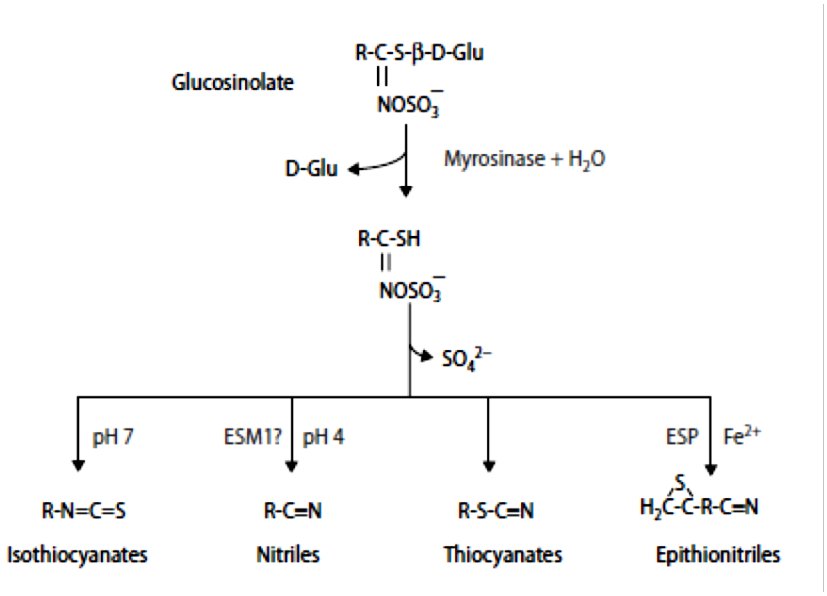

Figure 3.1 Mechanism of isothiocyanates formation from hydrolysis of glucosinolates [165].
ESM: epithiospecifier modifier; ESP: epithiospecifier protein.

3.1.2 Sulforaphane

Many different isothiocyanates (ITCs), produced by the myrosinase activity on glucosinolates (Figure 3.2), have shown interesting biological activities, including a marked antitumor activity, validated through *in vitro* and *in vivo* studies, and clinical trials, against various human neoplasms [159].

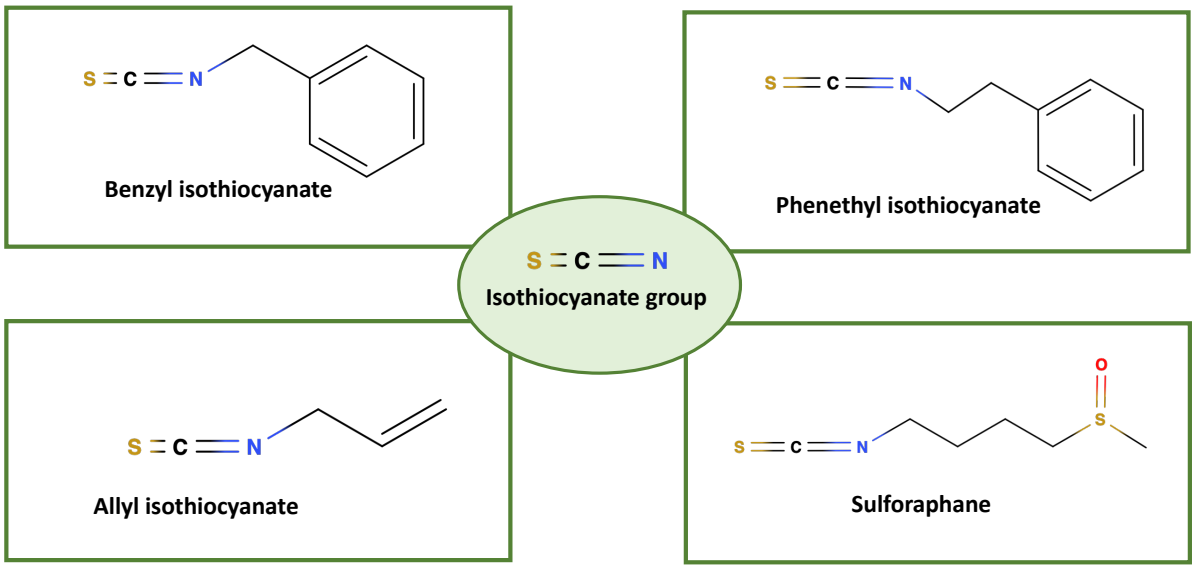

Figure 3.2 Chemical structures of some isothiocyanates.

Among these, the most investigated ITC is sulforaphane (SFN). SFN is able to simultaneously modulate several cellular targets involved in cancer development including cell proliferation, apoptosis, autophagy,

and angiogenesis; it is, therefore, able to prevent, delay or reverse preneoplastic lesions, thus acting as chemopreventive agents, as well as to act on cancer cells as a therapeutic agent (Figure 3.3) [161].

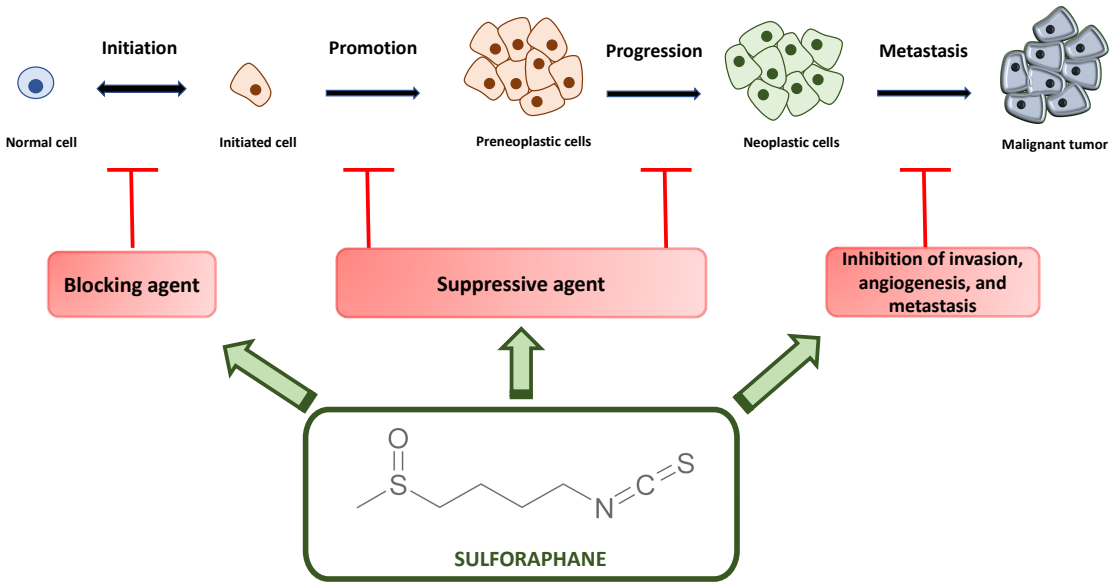

Figure 3.3 Chemopreventive and chemotherapeutic activity of SFN.

Sulforaphane as chemopreventive agent

Several epidemiological studies demonstrated the relation between consumption of cruciferous and a lower risk of diverse cancer diseases occurrence [166].

The chemopreventive activity of SFN relies upon its ability to modulate the initiation phase through different mechanisms, as the modulation of phase I and phase II detoxification pathways, the direct inhibition of carcinogens binding to DNA, and by possessing anti-inflammatory effects.

Since phase I enzyme are responsible for the bioactivation of chemical carcinogens, compounds able to modulate their expression and activity could decrease carcinogens activation, thus reducing carcinogenesis initiation [161]. Cytochrome 450 (CYP) comprise a superfamily of drug-metabolizing enzymes responsible for xenobiotics bioactivation, including carcinogenic chemicals [167]. SFN showed to inhibit different isoforms of CYP. In rat hepatocytes, SFN inhibited the activity of CYP1A1, and CYP2B1/2, while in human hepatocytes SFN decreased CYP3A4 activity, by reducing its mRNA levels [168].

In addition to the phase I enzymes inhibition, SFN carries out its chemopreventive activity also by inducing phase II enzymes, which are related to cell/tissue defense against exogenous/endogenous carcinogenic intermediates. Indeed, UDP-glucuronosyl transferase (UGT) 1A1, glutathione S transferase (GST) A1, and NADPH-quinone oxidoreductase 1 (NQO1) activity, together with UGT1A1 protein and bilirubin glucuronidation, were dose- and time-dependently increased by SFN in hepatocellular HepG2 carcinoma and in colon HT-29 and CaCo2 cancer cells [166]. Finally, in human prostate cancer cells, SFN increased NQO1 and GSTA1 mRNA levels, GST microsomal, and NQO1 activity [168]. Moreover, by increasing phase II enzymes, SFN enhances carcinogenic detoxification, thus reducing damage caused by highly reactive metabolites, including DNA damage. Indeed, SFN showed to reduce the number and the levels of DNA-adducts after exposure with different chemical carcinogens [166,169]. Upregulation of phase II enzyme by SFN has been related to its ability to enhance Nrf2 activity. By disrupting the bind between Nrf2 and its suppressor Keap1, SFN promotes Nrf2 cytoplasmatic and nuclear accumulation, and the consequent transcription of antioxidant response elements (ARE) [170]. For instance, it is well-known that SFN could promote the expression of NQO1, heme-oxygenase (HO-1), and γ-glutamylcysteine ligase (γGCL) [170], which are all related to the cellular antioxidant machinery. Indeed, among all the ARE-target genes, also the above-mentioned phase II enzymes are comprised.

Sulforaphane as chemotherapeutic agent

Due to its pleiotropic activity, SFN could also inhibit tumor promotion through many different mechanisms, including apoptosis, autophagy, and cell-cycle arrest induction, thus acting as antitumor agent. Moreover, SFN showed also to inhibit angiogenesis and metastasis formation, hence inhibiting tumor progression.

Sulforaphane induces apoptosis

A huge plethora of studies reported the pro-apoptotic activity of SFN. SFN could trigger apoptosis by regulating several molecular targets involved in the apoptotic machinery. Indeed, as widely reviewed, SFN showed to downregulate the expression of antiapoptotic proteins Bcl-2 and Bcl-XL and increase the expression of pro-apoptotic protein Bax; to promote the release of cytochrome c; to downregulate the expression of inhibitor of IAP family (*i.e.,* cIAP1, cIAP2, and XIAP); to induce the activation of Apaf-1; to activate caspase-3/-9/-7/-8, and to promote the cleavage of PARP [171,172]. Additionally, SFN upregulates the protein expression of TRAIL-R1/ DR4, and TRAIL-R2/DR5 [172].

In a wide variety of cancer cell lines, generation of ROS has been linked to SFN-induced disruption of mitochondrial membrane potential, caspase-3/-9 activation, downregulation of Bcl2 expression, and upregulation of Bax expression [162]. Since one of the targets of ROS is nuclear DNA, SFN-induced

ROS generation also leads to DNA damage, which could therefore promote cell death. ROS generation induced by SFN is not caused by its direct oxidation or reduction reactions. Instead, SFN leads to ROS accumulation through the promotion of mitochondrial events onset [162]. For instance, by using pharmacological inhibitors of mitochondrial respiratory chain complexes, ROS formation by SFN has been prevented [162].

Besides ROS generation, SFN could trigger apoptosis also by inducing ER stress. The endoplasmic reticulum is a central eukaryotic cellular organelle that provides crucial biosynthetic, stress-sensing, and signalling functions [173].
UPR, the signalling process activated in response to ER stress [68], is governed by three ER stress sensors: inositol-requiring transmembrane kinase/endoribonuclease 1-alfa (IRE1-α), activating transcription factor 6 (ATF6), and protein kinase R-like ER kinase (PERK) [68]. The three ER stress sensors, in physiological conditions, are kept in an inactive state by the master regulator of the UPR, GRP78 [68]. However, in case of loss of ER proteostasis or Ca^{2+} dysregulation, GRP78 disassociates from those ER stress sensors, thereby activating the UPR signalling pathway. Under tolerable stress conditions, UPR signalling induces pro-survival pathways, while, in the presence of severe, highly toxic and irreversible stress conditions, the same UPR pathway induces pro-cell death pathways [68]. Indeed, in bladder cancer cells SFN induced apoptosis together with an increase of the expression of GRP78 and CHOP [174]. Additionally, in HepG2 cells SFN increased the protein expression levels of GRP78, Bid, XBP-1 (X-box binding protein-1), and CHOP [175]. Since CHOP and Bid are related to ER stress-induced apoptosis, authors proposed that their upregulation by SFN could concur to its pro-apoptotic activity in liver cancer cells [175].

Sulforaphane induces autophagy

Cells have evolved an evolutionary conserved mechanism for destroying long-lived cytoplasmatic proteins and organelles, called autophagy, to provide energy and recycle nutrients. Usually, autophagy is considered an adaptation mechanism activated in response to a wide range of stress stimuli, such as nutrients starvation, hypoxia, ER stress, and oxidative stress, in order to activate a pro-survival process, thus preventing cell death [5]. Moreover, not only in physiological conditions, but also in pathological conditions as cancer, autophagy is activated as an adaptive response to advance cell survival [5]. However, a continuous activation of autophagy, occurring in certain conditions, leads to a collapse of cellular sources and, therefore, cell demise. Cell death driven by the molecular machinery of autophagy is called "autophagic cell death" or "autophagy-dependent cell death" [5].

Besides induction of apoptosis, SFN could also trigger autophagy in cancer cells. PC-3 and LNCap prostate cancer cells exposed to SFN displayed characteristic autophagic features such as cytoplasmatic membranous vacuoles and formation of acidic vesicular, together with an increase in the expression, the processing and the recruitment of LC3 (microtubule-associated protein 1 light chain 3) [176]. Moreover, by inhibiting SFN-induced autophagy an increase of cytochrome c release and, subsequently, apoptotic cell death has been reported [176]. Similar results were obtained also in human breast cancer cell [177], where inhibition of autophagy potentiated SFN-induced apoptosis, thus suggesting that autophagy possess a cytoprotective activity against SFN-induced apoptosis.

Sulforaphane induces cell-cycle arrest

Numerous studies reported that SFN could alter cell-cycle progression in several cancer cell lines. In LnCaP and DU-145 human prostate cancer cells, SFN treatment blocked cell-cycle progression in G1 phase, while in PC-3 human prostate cancer cells, SFN induced an arrest in G2/M phase [178]. In HT-29 human colon cancer line, a G2/M arrest accompanied by an increase in cyclin A and cyclin B1 protein levels and Rb hyperphosphorylation has been observed after SFN exposure [166]. An arrest of cell-cycle progression during G2/M has been reported in many other cell lines, including human breast, ovarian, lung, and T-cell leukemia cells [171,172].

Several mechanisms are involved in SFN-induced cell-cycle inhibition, such as downregulation of cyclin B1, Cdc25B and Cdc25C, together with activation of checkpoint 2 kinase [161]. Additionally, a transcriptome analysis reported that SFN promotes cell-cycle arrest by regulating other proteins involved in cell-cycle regulation, including kruppel-like factor 4, GADD45b, BTG family member 2 (PC3TIS21/BTG2), BTG3-associated nuclear protein (SMAR1), and CDC28 protein kinase 2 (CKSHS2) [161]. Finally, also the tumor suppressor and cell-cycle inhibitor p21 plays a role in SFN-induced cell cycle arrest. Indeed, p21 resulted upregulated after SFN treatment together with an increase in p53 expression in human prostate cancer cells [179], and in p53 negative colon cancer cells [180]. Moreover, in acute lymphoblastic leukemia cells obtained from human patients, SFN induced cell-cycle arrest in G2/M phase through the p53-independent upregulation of p21 [181].

Sulforaphane inhibits angiogenesis, endothelial cell functions, and metastatic process

The terminal stage of carcinogenesis is called progression. Progression stage is characterized by a high rate of genetic and phenotypic changes, and by high cell proliferation, which leads to a rapid increase of tumor size, where tumor cells could acquire further mutations within invasive and metastatic potential [182]. Instead, during metastatic process, cancer cells could escape from the primary tumor site through blood and lymphatic vessels, being supported by the growth of a vascular network that could efficiently

supply nutrients, oxygen, and remove waste products [182]. The process through which new blood vessels are formed is called angiogenesis.

SFN could modulate different steps involved in angiogenesis. In human umbilical vein endothelial cells (HUVECs), used as angiogenesis model, SFN inhibited tube formation on matrigel, and dose-dependently decreased the proliferation of endothelial cells, by inducing cell apoptosis [183]. In an immortalized human microvascular endothelial cell line (HMEC-1), SFN regulated all the essential steps of neovascularization [184]. Indeed, under hypoxic conditions, SFN inhibited mRNA expression of VEGF (vascular endothelial growth factor), HIF-1α (hypoxia-inducible factor-1alpha) and c-Myc, which are angiogenesis-associated transcription factors. Additionally, SFN inhibited also vascular endothelial growth factor receptor KDR/flk-1 at the transcriptional level, and prevented migration of HMEC-1 cells, together with their tube formation on basement membrane matrix [184].

The ability of SFN to inhibit metastasis formation has been reported by Thejass and Kuttan [185]. B16F-10 melanoma cells are characterized by a high metastatic ability by forming colonies of tumor nodules in lung, where they promote lung fibrosis and deposition of collagen [185]. In C57BL/6 mice, SFN inhibited lung metastasis induced by B16F-10 melanoma cells, as showed by a reduction of specific markers of lung fibrosis, malignant transformation, proliferation, adhesion and migration of endothelial cells [185].

3.2 Materials and methods

Cell cultures

Human acute myeloid leukemia (AML) cell lines (U-937, OCI-AML3, MOLM-13, MV4-11) and human acute lymphoblastic leukaemia (ALL) cell line (Jurkat) were purchased from the Deutsche Sammlung für Mikroorganismen und Zellkulturen, Braunschweig (DSMZ; Braunschweig, Germany). Human normal B lymphoblastoid cells (TK6) were purchased from LGC (LGC Group, Middlesex, UK).

U-937, MOLM-13, MV4-11 and Jurkat cells were cultured in Roswell Park Memorial Institute (RPMI) 1640 medium (BioWhittaker, Lonza, Verviers, Belgium) supplemented with 10% heat-inactivated fetal calf serum (FCS; Sigma Aldrich, Bornem, Belgium) and 1% antibiotic–antimycotic (BioWhittaker). OCI-AML3 cells were cultured in α-Minimum Essential Medium Eagle (α-MEM; BioWhittaker) supplemented with 10% heat-inactivated FCS and 1% antibiotic–antimycotic. TK6 cells were cultured in RPMI 1640 medium (Sigma Aldrich) supplemented with 10% heat-inactivated fetal bovine serum, 1% glutamine, 1% sodium pyruvate, 1% penicillin/streptomycin, and glucose to final concentration of 4.5 g/liter (all obtained from Sigma). All cells were maintained at 37°C and 5% CO_2 in a humidified atmosphere.

Chemicals and treatments

MG28 and MG46 (Figure 3.4) are two newly developed ITCs, synthetized by Professor Andrea Milelli from University of Bologna, Department for Life Quality Studies. In MG28 and MG46, the ITC group was condensed with rhodol, a fluorophore capable of targeting and delivering small molecules to subcellular organelles[186].

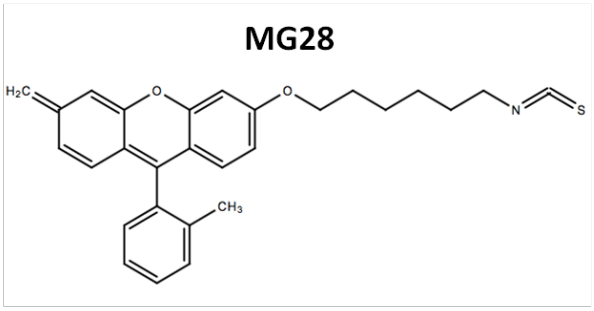

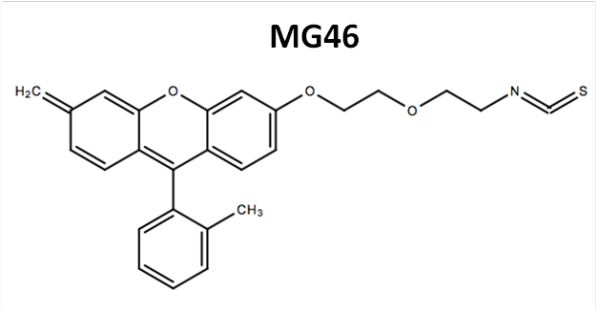

Figure 3.4 Chemical structure of MG28 and MG46.

SFN (Sigma Aldrich) was dissolved in DMSO at the concentration of 100mM; N-Benzyloxycarbonyl-Val-Ala-Asp (O-Me) fluoromethyl ketone (Z-VAD-FMK; Calbiochem, EMD Millipore Corp., Billerica, MA, USA) and necrostatin-1 (Nec-1; Sigma Aldrich) were dissolved in DMSO at the concentration of 50mM; cyclosporin A (CSA), olaparib (Ola; Selleck, Houston, TX, USA), necrosulfonamide (NSA; Tocris Bioscience (Bristol, UK) and ferrostatin-1 (Ferr-1; Sigma Aldrich) were dissolved in DMSO at the concentration of 10mM; rhodol (Sigma Aldrich) was dissolved in water at the concentration of 5mM.

Exponentially growing cells were used for all experiments. Cells were treated with increasing concentration of SFN (0-200μM), MG28 and MG46 (0-25μM), and rhodol (200μM, *i.e.,* the highest tested concentration of MG28 and MG46) for 3, 5, 6, 9, 16, 24, 48 or 72h depending on experimental conditions.

To evaluate the induction of non-canonical cell death pathways, cells were pre-treated for 1h with different chemical inhibitors and then treated with increasing concentrations of SFN for 24h. For this purpose, the following blockers were used: the pan-caspase inhibitor Z-VAD-FMK (50μM); the PARP-1/-2 inhibitor Ola (1μM); the inhibitor of mitochondrial permeability transition pore CSA (5μM), the RIP1 inhibitor Nec-1 (50μM); the MLKL inhibitor NSA (1μM), and the inhibitor of ROS generation and lipid peroxidation Ferr-1 (1μM), in order to inhibit apoptosis, parthanatos, mitochondrial permeability transition (MPT)-driven necrosis, necroptosis and ferroptosis, respectively.

Analysis of cell viability and cell proliferation

Cells were processed through a semi-automated image-based cell analyser Cedex XS Innovatis, (Roche, Penzberg, Germany), which provides information about cells concentration and viability based on the Trypan Blue exclusion method. Trypan Blue, for its chemical-physical properties, is not able to penetrate cells with intact cell membrane (*i.e.,* viable cells), penetrating exclusively in dead cells with damaged membrane [187].

Analysis of nuclear morphology by fluorescence microscopy

Nuclear morphology was investigated by fluorescence microscopy using a cell^M imaging station (Olympus, Aartselaar, Belgium) on cells incubated for 15 min at 37°C with the DNA-specific dye 1μg/mL Hoechst 33342 (Sigma Aldrich) and stained with 1μg/mL propidium iodide (PI; Sigma Aldrich). For each sample, at least 100 cells were counted. Quantification of the percentage of apoptotic cells was performed on the basis of their fragmented nuclei and the condensed chromatin around the periphery of the nucleus: cells with distinct condensed nuclei, segregated nuclei and apoptotic bodies were counted as apoptotic and determined as a fraction of the total number of cells; cells, excluding PI, were categorized as viable cells; PI-stained cells with a round morphology and homogeneously stained nucleus were termed PI-positive (necrotic).

Whole cell extracts and immunoblotting

For the preparation of whole cell extracts, cells were harvested, washed in ice-cold 1X Phosphate-buffered saline (PBS) and lyzed in 1X Mammalian Protein Extraction Reagent (M-PER®; Thermo Fisher Scientific, Rockford, USA) supplemented with 1X protease inhibitor cocktail (Complete EDTA-free; Roche, Basel, Switzerland) and 1X phosphatase inhibitor (PhosphoStop™; Roche) according to the manufacturer's instructions. Protein concentration was measured using the Bradford assay (Bio-Rad, Nazareth Eke, Belgium) by a SpectraMax ID3 Multi-Mode Microplate Reader (Molecular Devices, LLC, San Jose, CA, USA) and extrapolated by using the standard curve obtained from bovine serum albumin (BSA). Proteins were aliquoted and stored at -80°C.

Proteins (10 or 20 µg) were subjected to sodium dodecyl sulfate (SDS)–polyacrylamide gel electrophoresis (PAGE) and transferred onto a HybondTM-P 0.2/0.45 nm pore size membrane (GE Healthcare, Diegem, Belgium). Membranes were then incubated in 1X PBS supplemented with 10% Tween (PBS-T) containing the appropriated blocking agent [5% non-fat dry milk (NFDM) or 5% bovine serum albumin (BSA)] with the following primary antibodies: anti-caspase-3 (no. 9668, Cell Signaling, Beverly, MA, USA), anti-PARP-1 (no. 9542, Cell Signaling or no. 53643, Santa Cruz Biotecnology, Santa Cruz, CA, USA), anti-MLKL (no. 184718, Abcam, Cambridge, UK), anti-MLKL (phospho S358, no. 187091, Abcam), anti-GRP78 (no. 13968, Santa Cruz Biotechnology), and anti-β Actin (no. A2228 Sigma Aldrich). After washing with PBS-T blots were incubated with Horseradish Peroxidase (HRP)-conjugated secondary antibody (no. 516102, Santa Cruz Biotechnology; no. 6721, Abcam) in PBS-T containing 5% NFDM or 5% BSA. After washing in PBS-T, proteins of interest were detected with Amersham™ ECL™ Prime Western Blotting Detection reagent (GE Healthcare) using the ImageQuant ™LAS 4000 camera system (GE Healthcare).

Quantification of high-mobility group box 1 (HMGB1) release

After treatments, cells were centrifuged, and the supernatant was collected and immediately stored at -80°C. Quantification of HMGB1 release in the cell culture supernatants was assessed by an enzyme-linked immunosorbent assay (ELISA) kit from IBL International (Hamburg, Germany), according to the manufacturer's instructions.

Micronucleus assay

Micronucleus assay was performed following the OECD guidelines for the testing of chemicals [188]. TK6 cells were seeded at a concentration of 350 000 cells/mL and treated for 4h with concentrations of MG28 and MG46 that induce less than 50% of mortality (1, 2 and 4µM for both compounds). Vinblastine 2µg/mL and mitomycin C 0.8µg/mL were used as positive controls. After 4h, cells were centrifuged and resuspended in 10 mL of complete medium supplemented with cytochalasin B (final concentration of 6µg/mL) for 20h. At the end of incubation period (*i.e.,* 24h, equal to approximately two cell cycles), TK6

were treated with an hypotonic solution [98% (RPMI 1640 : H_2O, 1:3) + 2% fetal bovine serum] and fixed with a solution of ice-cold methanol : acetic acid (1:1). Then, fixed cells were directly put on slides using a cytospin and stained with May Grünwald – Giemsa. All slides were coded before scoring. At least 2000 binucleated lymphocytes were examined for each concentration (two cultures *per* concentration) for the presence of micronuclei.

Statistical analysis

All experiments are expressed as the mean ± SEM of at least three independent experiments. IC_{50} (concentration of drug responsible for the inhibition of 50% of cell viability) values of drugs against cellular viability were determined by non-linear regression fitting curves using GraphPad InStat 6.0 version (GraphPad Prism, San Diego, CA, USA).

Statistical analyses were assessed by using one-way or two-way ANOVA tests and Tukey or Dunnett or Bonferroni were used as post-tests, by using GraphPad Prism 6 software. *p*-values below 0.05 were considered as significant and represented as $*p<0.05$, $**p<0.01$, $***p<0.001$, and $****p<0.0001$.

3.3 Results

MG28 and MG46 exhibit cytotoxic activity towards various leukemia cell models

First, the cytotoxic potential of MG28 and MG46 compared to the parental compounds SFN and rhodol was evaluated on different cell models of leukemia. The trial was conducted on different AML cell lines (MOLM-13, MV4-11, U-937 and OCI-AML3) and on an ALL cell line (Jurkat).

Cells were treated with increasing concentration of SFN (0-200μM), MG28 and MG46 (0-25μM), or rhodol (200μM).

After treatment of 24, 48 and 72h with SFN, the viability of U-937, OCI-AML3, MOLM-13, and MV4-11 cells was analysed (Figure 3.5). In all tested cell lines, SFN reduced cell viability in a time-dependent manner. In U-937 and MV4-11 cells, the decrease in cell viability was also dose-dependent. MOLM-13 and MV4-11 were the most sensitive cells to SFN cytotoxic activity: after 24h and already at the concentration of 5μM, the recorded cell viability was about 80%, reaching about 50% at 50μM, and 5-10% at the highest tested concentration. Prolonging the treatment time from 48h to72h, already at the concentration of 25 μM cell viability dropped to about 20% (48h) and 5% (72h). On the contrary, U-937 and OCI-AML3 were less sensitive to SFN. In OCI-AML3 cells a drop of cell viability was observed after increasing SFN dose from 25 to 50μM (from about 80% to a 10%) after 24h, while after 48h and 72h almost all cells succumbed to SFN cytotoxicity at the concentration of 50μM. U-937 were highly resistant to SFN: IC_{50} values obtained after 24, 48 and 72h were 112.4μM, 71.2μM and 58.8μM, respectively, showing a difference in sensitivity of about one order of magnitude compared to the IC_{50} values obtained in MV4-11 cells (32.8μM, 11.3μM and 7.4μM, respectively after 24, 48 and 72h). To note, in all cell lines prolonging the treatment time to 48h and 72h influenced cell viability in a minor extent rather than from 24h and 48h treatment, when a drop down of cell viability was recorded.

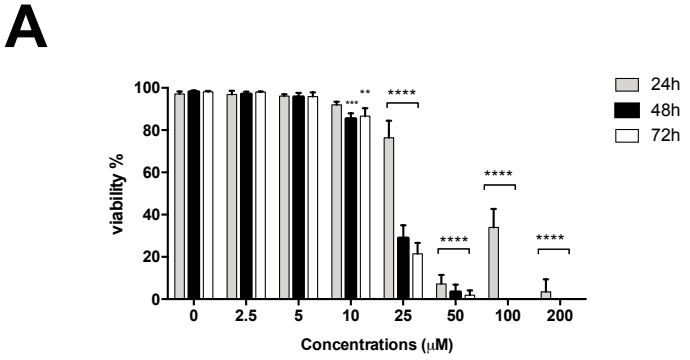

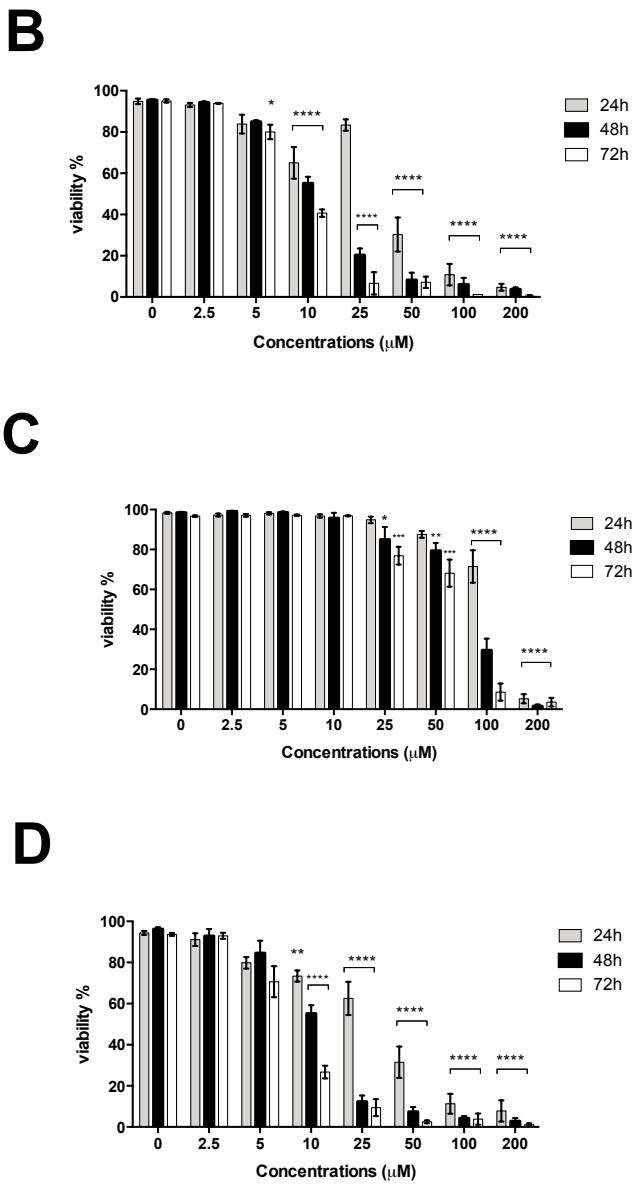

Figure 3.5 Viability of OCI-AML3 (A), MOLM-13 (B), U-937 (C), and MV4-11 (D) cells after 24-48-72h of treatment with SFN. * $p < 0.05$; ** $p < 0.01$; *** $p < 0.001$; **** $p < 0.0001$ *versus* untreated cells.

The viability of U-937, OCI-AML3, MOLM-13, MV4-11, and Jurkat cells was analysed after 24, 48 and 72h of treatment with MG28 and MG46 (Figure 3.6).

In all tested cell lines, MG28 and MG46 decreased cell viability in a dose-dependent manner, with the exception for MV4-11, where after treatment with MG46 cell viability remained constant starting from 5μM, at all tested treatment times. MG28 and MG46 caused a substantial drop down of cell viability shifting from the concentration of 10μM to 25μM after 24h, and from 5μM to 10μM after 48 and 72h of treatment in OCI-AML3, Jurkat and U-937 (in this cell line this trend was observed only with MG46 treatment). In MOLM-13 and MV4-11 cells, cell viability dramatically decreased using lower concentrations: from 2.5μM to 5μM, at all tested treatment times, thus reflecting the different sensitivity

of those cell lines toward the two ITC derivatives. MV4-11 cell line was the most sensitive, with calculated IC_{50} values of 4.1μM, 3.6μM and 3.4μM for MG28, and 3.7μM, 4.0μM and 5.1μM for MG46, respectively after 24, 48 and 72h of treatment. Also, MOLM-13 cells readily succumbed to SFN treatment, showing IC_{50} values of 5.8μM, 3.2μM and 3.8μM for MG28, and 5.8μM, 2.1μM and 3.2μM for MG46, respectively after 24, 48 and 72h of treatment. On the contrary, U-937, OCI-AML3 and Jurkat cells were less responsive to MGs cytotoxicity at all tested time points. For instance, calculated IC_{50} values of treated U-937 cells were 14.5μM, 8.1μM and 8.7μM for MG28, and 17.4μM, 6.4μM and 5.2μM for MG46, respectively after 24, 48 and 72h of treatment. Of note, in all tested cell lines, MG28 and MG46 induced a substantial decrease in cell viability only after 24h of treatment, while after 48 and 72h the two ITCs displayed a similar cytotoxic effect.

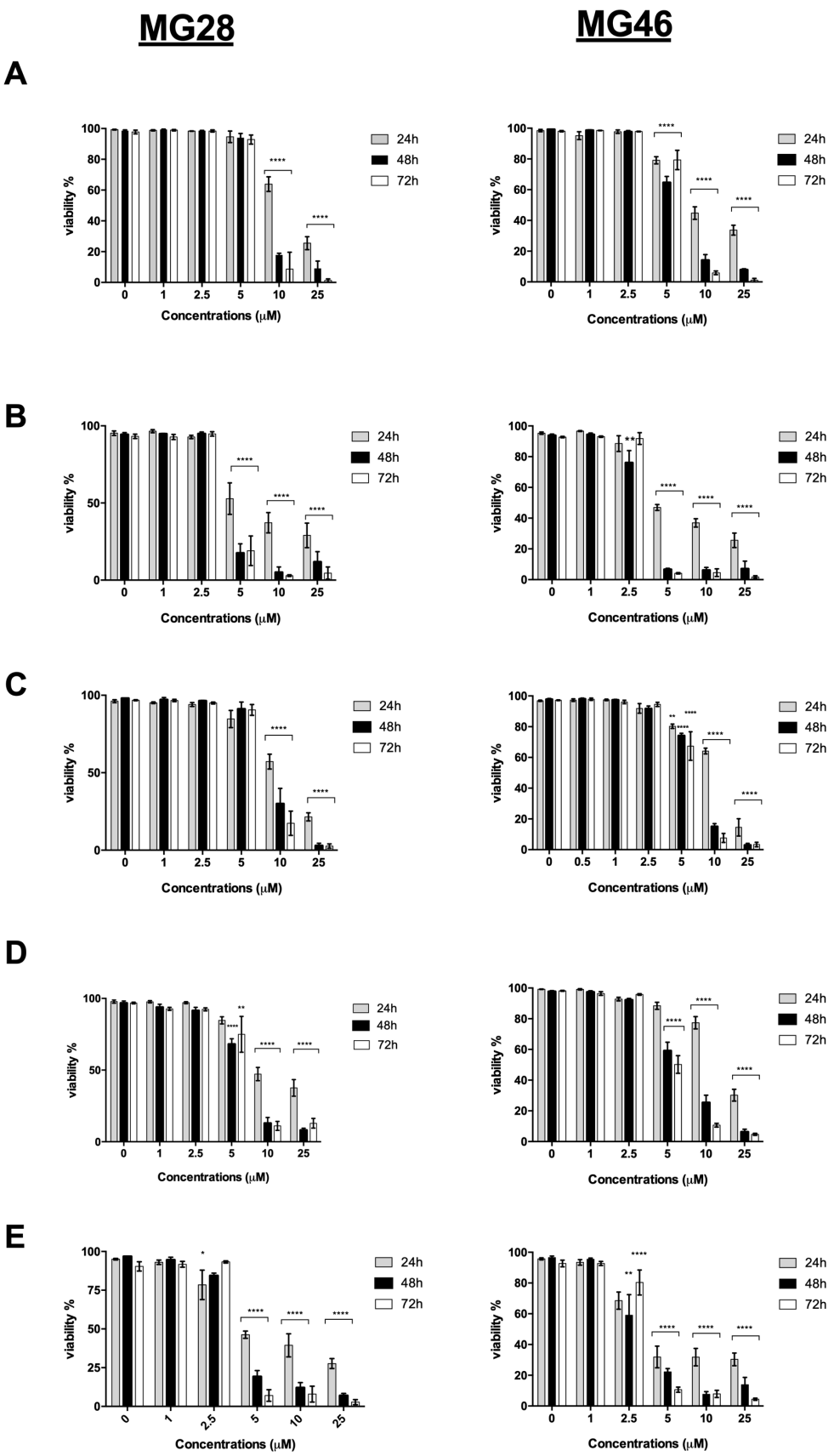

Figure 3.6 Viability of OCI-AML3 (A), MOLM-13 (B), Jurkat (C), U-937 (D), and MV4-11 (E) cells after 24-48-72h of treatment with MG28 or MG46. * $p < 0.05$; ** $p < 0.01$; *** $p < 0.001$; **** $p < 0.0001$ *versus* untreated cells.

Next, to test whether the ITC functional group was responsible for the cytotoxic activity of MG28 and MG46, the parental compound rhodol was tested. Results illustrated in Figure 3.7 show that, at the concentration of 200µM, rhodol failed to exhibit any cytotoxic effect on the five tested cancer cell lines (Figure 3.7), suggesting that the activity of MG28 and MG46 could be attributed essentially to the presence of the ITC group.

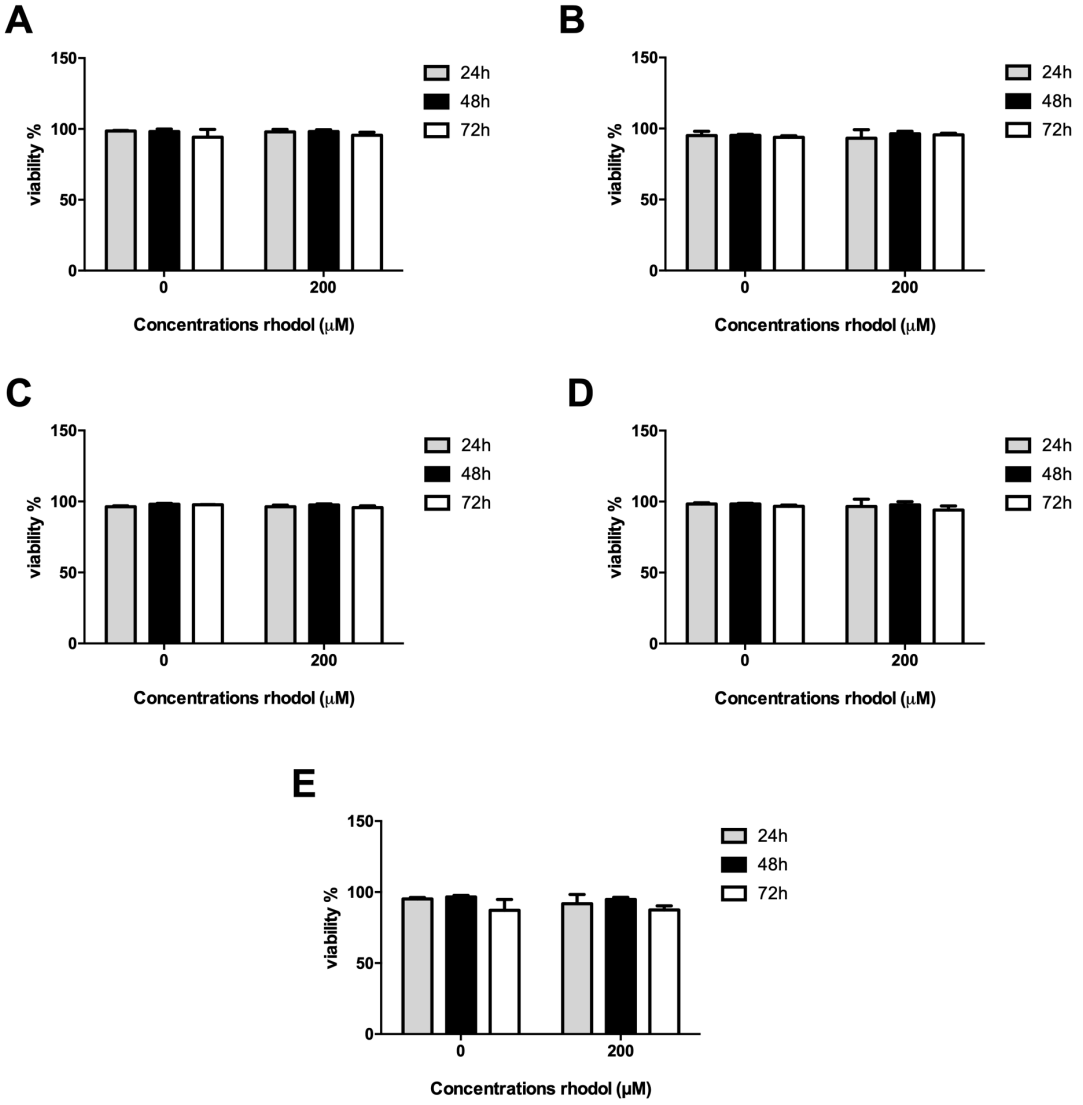

Figure 3.7 Viability of OCI-AML3 (A), MOLM-13 (B), Jurkat (C), U-937 (D), and MV4-11 (E) cells after 24-48-72h of treatment with rhodol 200µM.

Hence, to compare the cytotoxic potency of the different compounds in the different cell lines, we next determined the corresponding IC_{50} values after 24h of treatment (Table 4).

Table 4 IC_{50} values (μM) obtained after 24h of treatment with MG28, MG46 or SFN

Cell line	IC_{50} (μM) ± SD		
	MG28	MG46	SFN
U-937	14.5 ± 3.6	17.4 ± 1.2	112.4 ± 1.0
OCI-AML3	13.7 ± 0.9	12.3 ± 2.2	33.3 ± 3.9
MOLM-13	5.8 ± 1.9	5.8 ± 3.2	38.4 ± 11.2
MV4-11	4.1 ± 2.0	3.7 ± 1.9	32.8 ± 12.5
JURKAT	14.4 ± 1.5	12.7 ± 1.3	ND

IC_{50}: half maximal inhibitory concentration.
Data are the mean of at least three independent experiments.
ND: not determined.

MV4-11 and MOLM-13 cell lines were found to be the most sensitive to both MG28 and MG46 with IC_{50} values, in MV4-11 cells, of 4.1μM and 3.7μM after 24h of treatment, respectively, and in MOLM-13 cells, of 5.8μM for both MG28 and MG46. On the contrary, U-937, Jurkat and OCI-AML3 were the less sensitive cells with IC_{50} values of 14.5μM, 14.4μM and 13.7μM after 24h of treatment with MG28, respectively, and of 17.4μM, 12.7μM and 12.3μM after 24h of treatment with MG46, respectively. Of note, there was no striking difference in terms of cytotoxicity between MG28 and MG46. Nevertheless, MG compounds displayed markedly greater activity than SFN used as reference ITC, with a difference of about one order of magnitude in all tested cell lines except OCI-AML3 cell line, where MG compounds were 2- to 3-fold more potent.

Since MV4-11 and U-937 cells displayed, respectively, the highest and the lowest sensitivity, these two cell lines were further investigated in order to potentially determine the underlying mechanisms responsible for such difference of sensitivity.

MG28, MG46 and low dose of SFN induce apoptotic cell death in AML cells

Since MG28 and MG46 reduced cancer cell viability, we evaluated the type of cell death triggered by such treatments. Evaluation of cell death mechanism was carried out through the analysis of nuclear morphology by fluorescence microscopy. Marking DNA through specific fluorochromes, such as Hoechst and PI, allows to carry out a morphological evaluation of normal or apoptotic nuclei, which have specific morphological characteristics such as fragmentation of DNA, chromatin condensation and formation of apoptotic bodies [189]. Moreover, in addition to the different ways of binding to DNA, the two used markers differ also in their ability to permeate the plasma membrane: the nuclear dye Hoechst, for example, is able to intercalate to DNA indistinctly in all cells as it is permeable to the plasma membrane; PI, instead, is impermeable to the plasma membrane and is therefore capable of penetrating

only into cells that present compromised plasma membrane [189]. Since during necrotic cell death process and during the late phases of apoptosis the integrity of the plasma membrane is compromised [5,189], the simultaneous use of PI and Hoechst allows the discrimination of necrotic or apoptotic advanced cells from apoptotic ones [189].

Nuclear morphology analyses revealed a dose-dependent increase in the fraction of apoptotic cells in U-937 (Figure 3.8) and MV4-11 (Figure 3.9) cells after exposure to MG28 and MG46. However, in both cell lines the fraction of apoptotic cells reached a maximum after 24h of treatment, remaining constant after longer treatment times (*i.e.,* 48 and 72h).

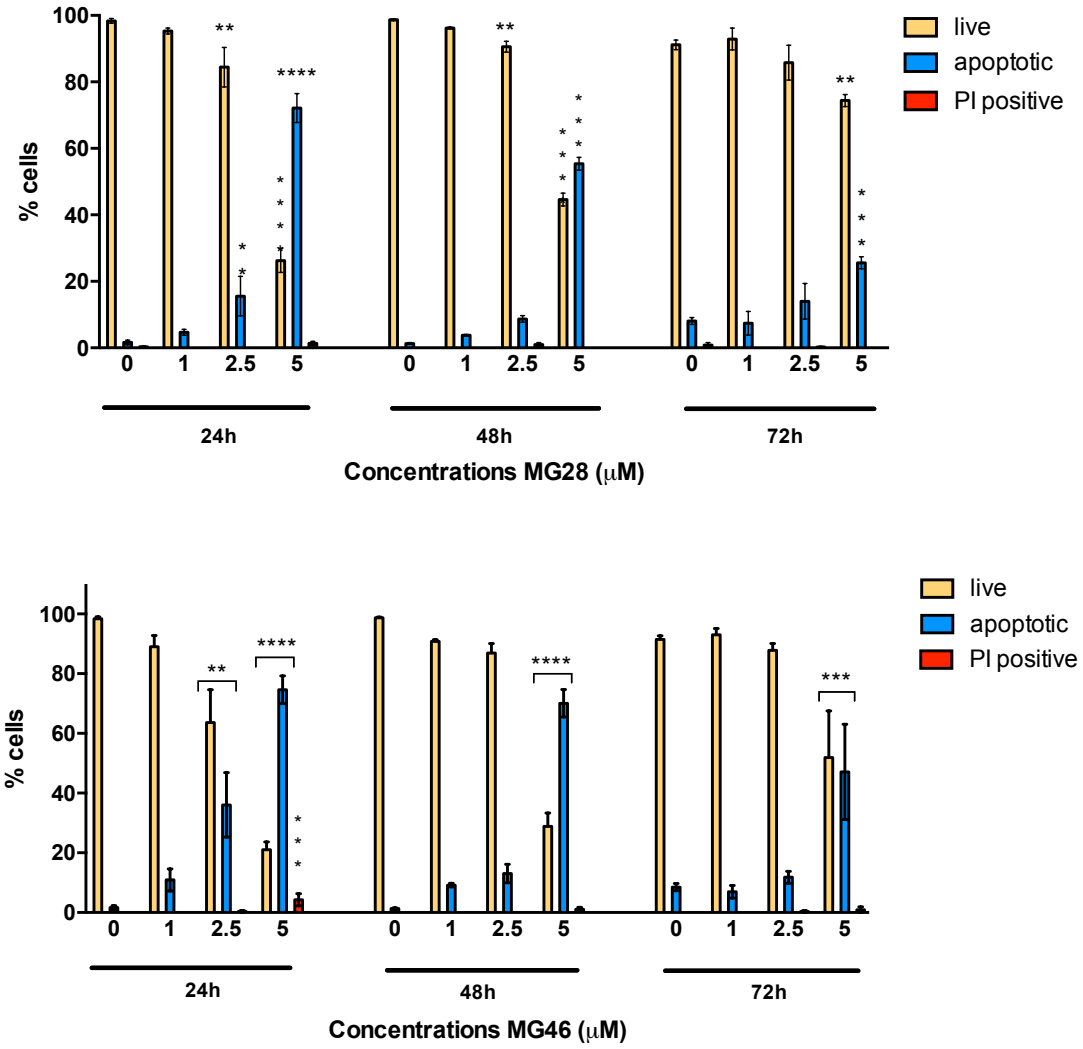

Figure 3.8 Percentage (%) of living, apoptotic, and necrotic (PI positive) cells after 24-48-72h treatment of U-937 cells with increasing concentrations of MG28 and MG46. * $p < 0.05$; ** $p < 0.01$; *** $p < 0.001$; **** $p < 0.0001$ *versus* untreated cells.

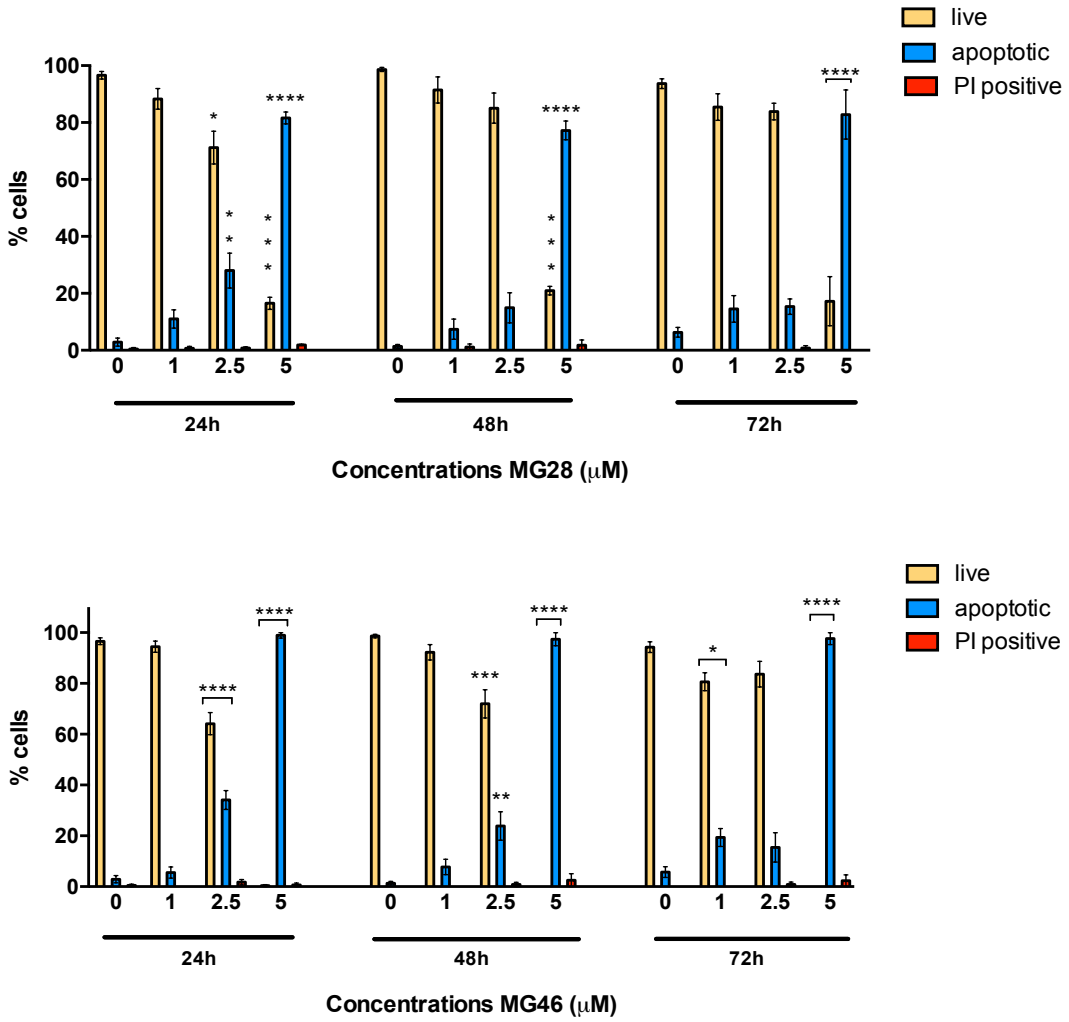

Figure 3.9 Percentage (%) of living, apoptotic, and necrotic (PI positive) cells after 24-48-72h treatment of MV4-11 cells with increasing concentrations of MG28 and MG46. * $p < 0.05$; ** $p < 0.01$; *** $p < 0.001$; **** $p < 0.0001$ *versus* untreated cells.

Hence, taking into account that the pro-apoptotic activity of MG28 and MG46 reached a maximum after 24h, we next analysed the kinetics of cell death induction, in order to better understand the time-dependent apoptosis occurrence in cancer cells after MGs treatment. For this purpose, U-937 and MV4-11 cells were treated with MG28 and MG46 for 3, 6, 9, and 24h and then nuclear morphology was analysed by fluorescent microscopy (Figure 3.10 and 3.11).

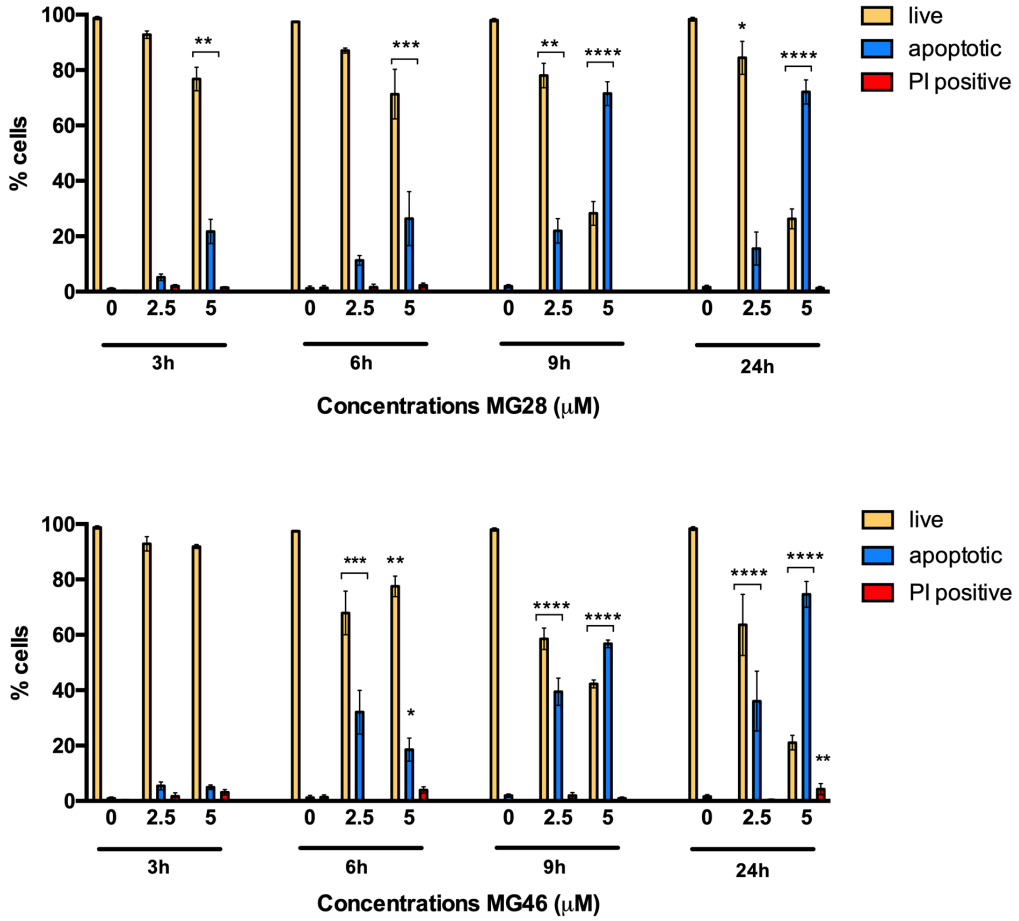

Figure 3.10 Percentage (%) of living, apoptotic, and necrotic (PI positive) cells after 3-6-9-24h treatment of U-937 cells with increasing concentrations of MG28 and MG46. * $p < 0.05$; ** $p < 0.01$; *** $p < 0.001$; **** $p < 0.0001$ *versus* untreated cells.

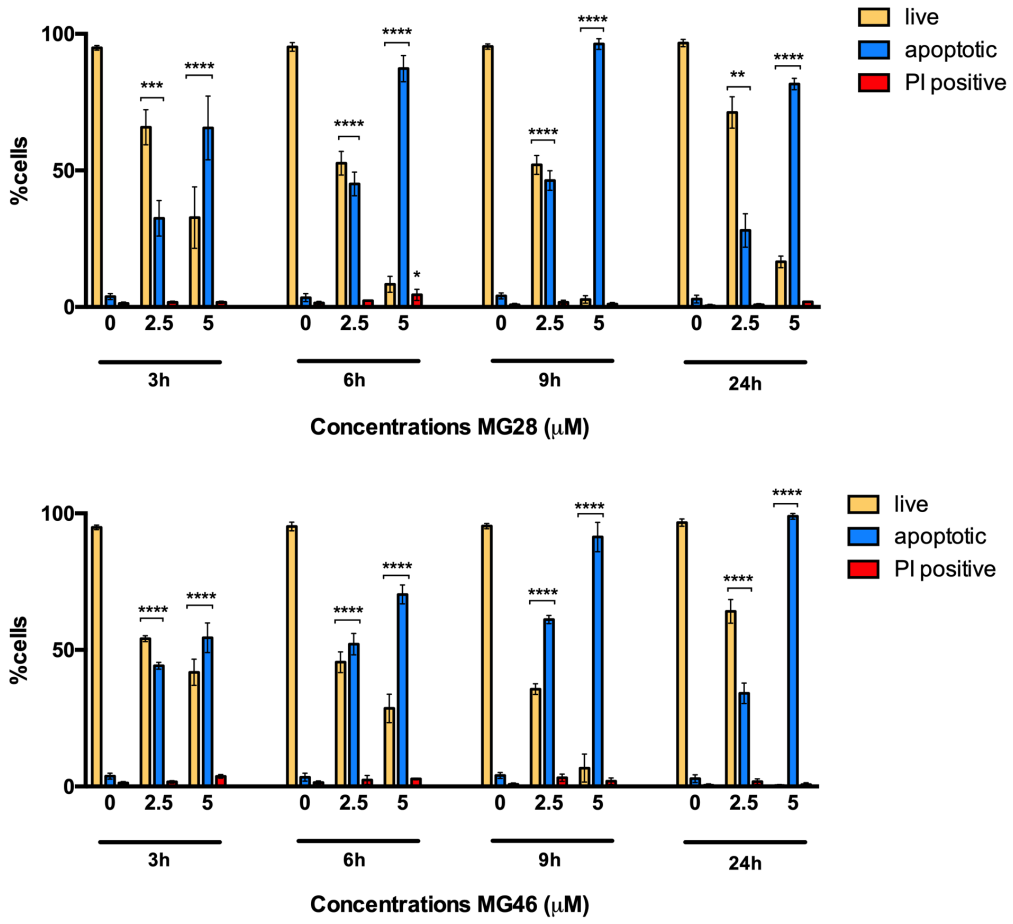

Figure 3.11 Percentage (%) of living, apoptotic, and necrotic (PI positive) cells after 3-6-9-24h treatment of MV4-11 cells with increasing concentrations of MG28 and MG46. * $p < 0.05$; ** $p < 0.01$; *** $p < 0.001$; **** $p < 0.0001$ *versus* untreated cells.

In U-937 cells (Figure 3.10), both MG28 and MG46 triggered cell death starting from 3h of treatment and the percentage of apoptotic cells achieved the maximum after 9h of treatment, remaining constant, or even decreasing, at 24h of treatment. A similar trend was observed on MV4-11 cells. However, in this cell line MG28 and MG46 were highly effective already after 3h of treatment; moreover, starting from the shorter treatment time, the apoptotic fraction was almost similar to that observed after longer exposure (Figure 3.11). Overall, MG28 and MG46 induced cell death in a time- and dose-dependent manner up to 24h of treatment, then loosing time dependence. Additionally, we can speculate that probably the higher sensitiveness exhibited by MV4-11 cells could also be due to the more rapid cell death onset triggered by the two ITC derivatives.

Next, we evaluated the type of cell death involved in SFN-induced cytotoxicity on U937 and on MV4-11 cells, analysing their nuclear morphology (Figure 3.12) after treatment with increasing concentrations of SFN for 24h, which was the treatment time where the two ITC derivatives reached their maximum

cytotoxic activity. In both cell lines, a dose-dependent increase in the apoptotic cell fraction was observed, while the percentage of PI-positive cells never exceeded the 10% of total cell population, at least up to the concentration of 25μM. However, at the highest tested concentration, the fraction of PI-positive cells strongly increased up to about 70%, suggesting the induction of a different mechanism of cell death dependent on SFN concentration. To note, MG28 and MG46 were not tested at concentrations above 5μM as at this concentration the mortality rate was already equal to or above 80% in U-937 cells and about 100% in MV4-11 cells. Most importantly, the percentage of necrotic cells was less than 5% in both U-937 and MV4-11 cells, suggesting that the cell death mechanism was only apoptotic.

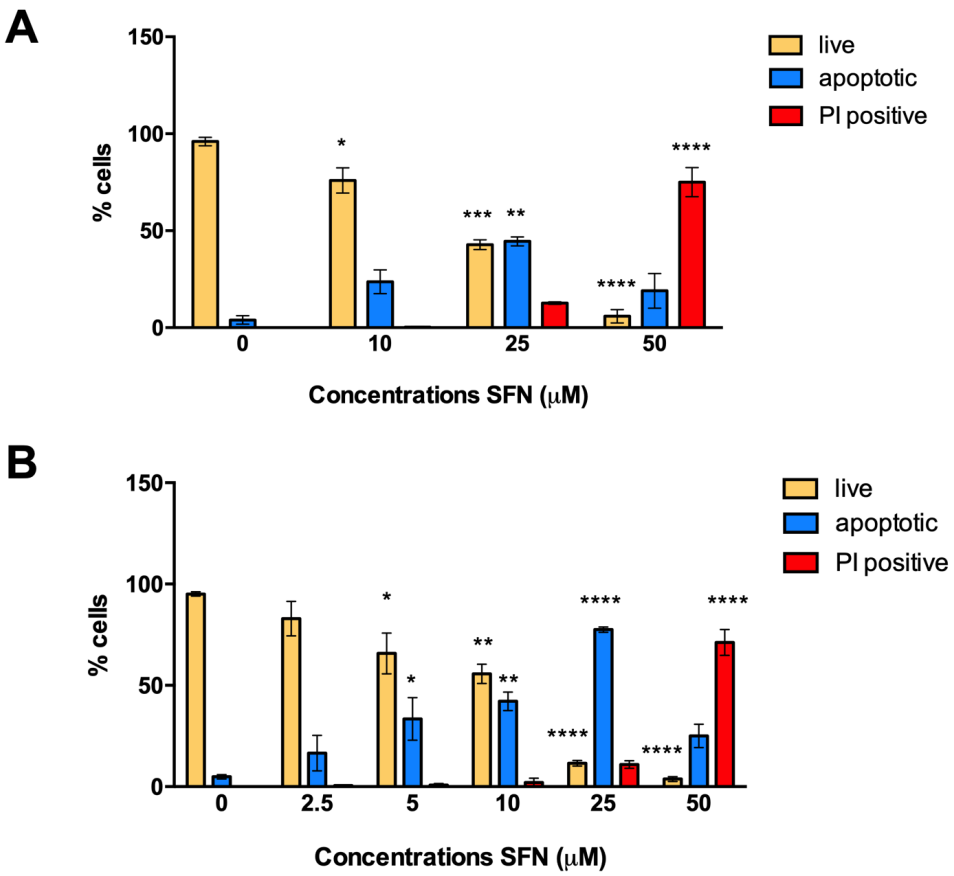

Figure 3.12 Percentage (%) of living, apoptotic, and necrotic (PI positive) cells after 24h treatment of U-937 (A) and MV4-11 (B) cells with increasing concentrations of SFN. * $p < 0.05$; ** $p < 0.01$; *** $p < 0.001$; **** $p < 0.0001$ *versus* untreated cells.

Since apoptosis is considered a caspase-dependent cell death pathway, in the next experimental setting we analysed the potential involvement of caspases in MGs- and SFN-induced apoptotic cell death. For this purpose, U-937 and MV4-11 cells were pre-incubated with the pan-caspase inhibitor Z-VAD-FMK and then treated with MGs or SFN for 24h. The obtained results demonstrated that Z-VAD-FMK almost

abrogated the induction of apoptosis triggered by treatment with MG compounds (from about 80-90% to 10%) (Figure 3.13).

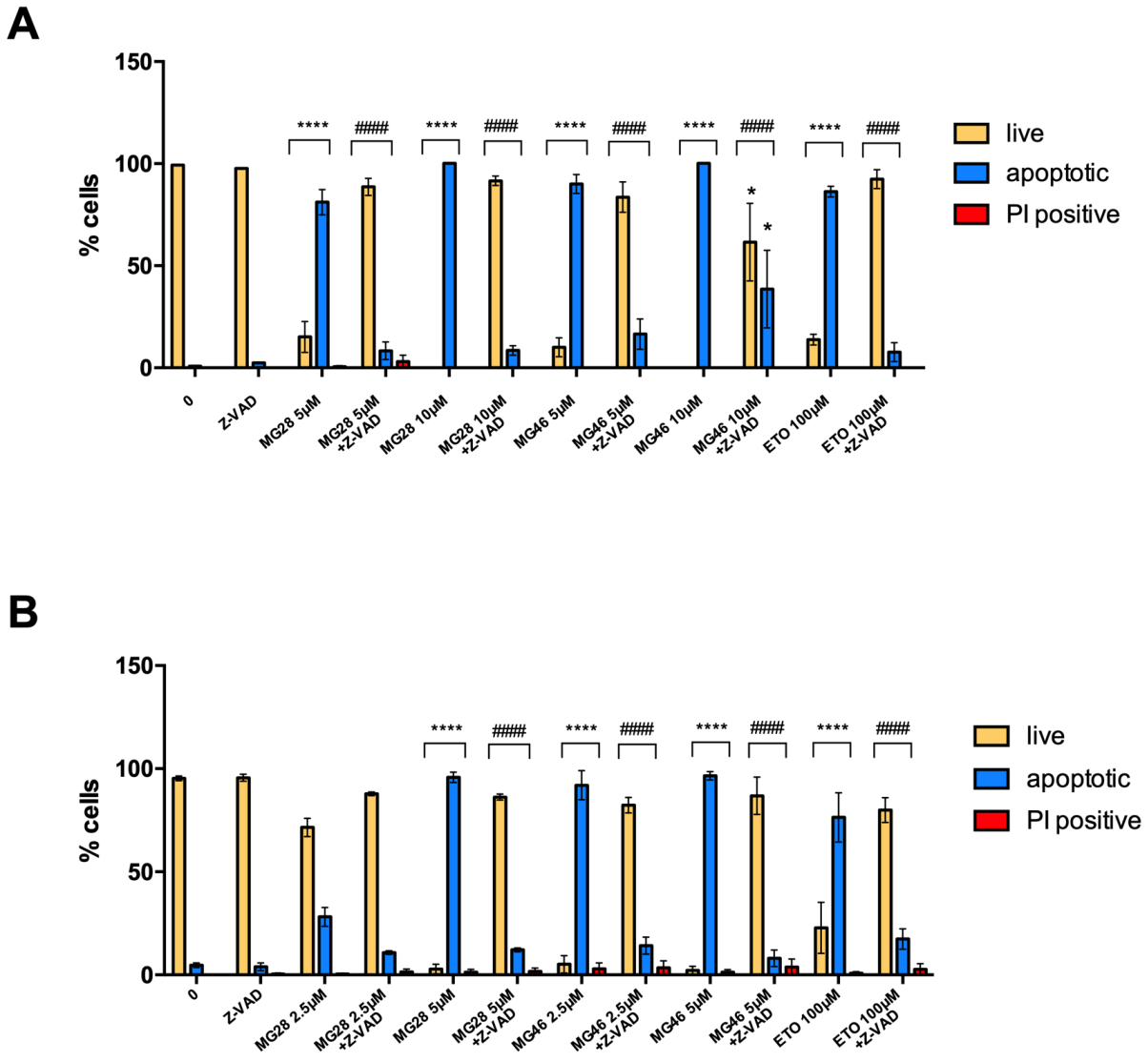

Figure 3.13 Percentage (%) of living, apoptotic, and necrotic (PI positive) cells of U-937 (A) and MV4-11 (B) cells after pre-treatment of 1h with Z-VAD-FMK and treatment with MG28 and MG46 for 24h. * $p < 0.05$; *** $p < 0.001$; **** $p < 0.0001$ *versus* untreated cells. #### $p < 0.0001$ *versus* Z-VAD-FMK untreated cells. Etoposide (ETO) 100μM was used as positive control.

Regarding SFN, the results were notably different. Indeed, in MV4-11 and U-937 cells the pre-treatment with Z-VAD-FMK almost totally abrogated the induction of apoptosis triggered by the exposure to low concentration of SFN (from about 40-70% to 5%), but it did not have any effect at the highest SFN tested concentration (Figure 3.14), hence suggesting the involvement of other forms of PCD.

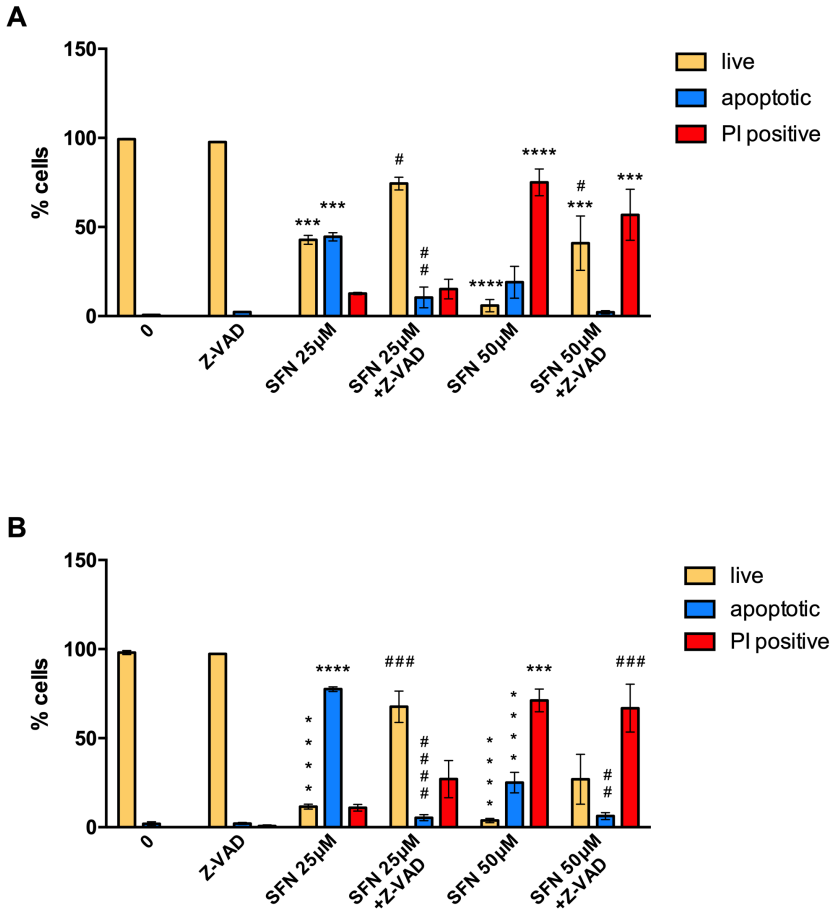

Figure 3.14 Percentage (%) of living, apoptotic, and necrotic (PI positive) cells of U-937 (A) and MV4-11 (B) cells after pre-treatment of 1h with Z-VAD-FMK and treatment with SFN for 24h. *** $p < 0.001$; **** $p < 0.0001$ *versus* untreated cells. # $p < 0.05$; ## $p < 0.01$; ### $p < 0.001$; #### $p < 0.0001$ *versus* Z-VAD-FMK untreated cells.

During the execution stage of apoptosis, cleaved executioner caspase-3 triggers apoptosis by cleaving several key proteins and, among all caspase-3 substrates, PARP-1 represents one the most characteristic hallmarks of apoptosis execution [190]. Hence, to further confirm the pro-apoptotic activity of MG28, MG46 and low concentrations of SFN, we next investigated their effect on the cleavage of caspase-3 (Figure 3.15) and its substrate PARP-1 (Figure 3.16) by Western Blotting. In MV4-11 and U-937 cells, the protein expression of cleaved caspase-3 and cleaved PARP-1 was strongly increased after treatment with MG compounds or low concentrations of SFN. In addition, Z-VAD-FMK totally prevented the cleavage of caspase-3 and PARP-1. Collectively, these results demonstrated that MG compounds and relatively low concentrations of SFN triggered caspase-dependent apoptotic cell death.

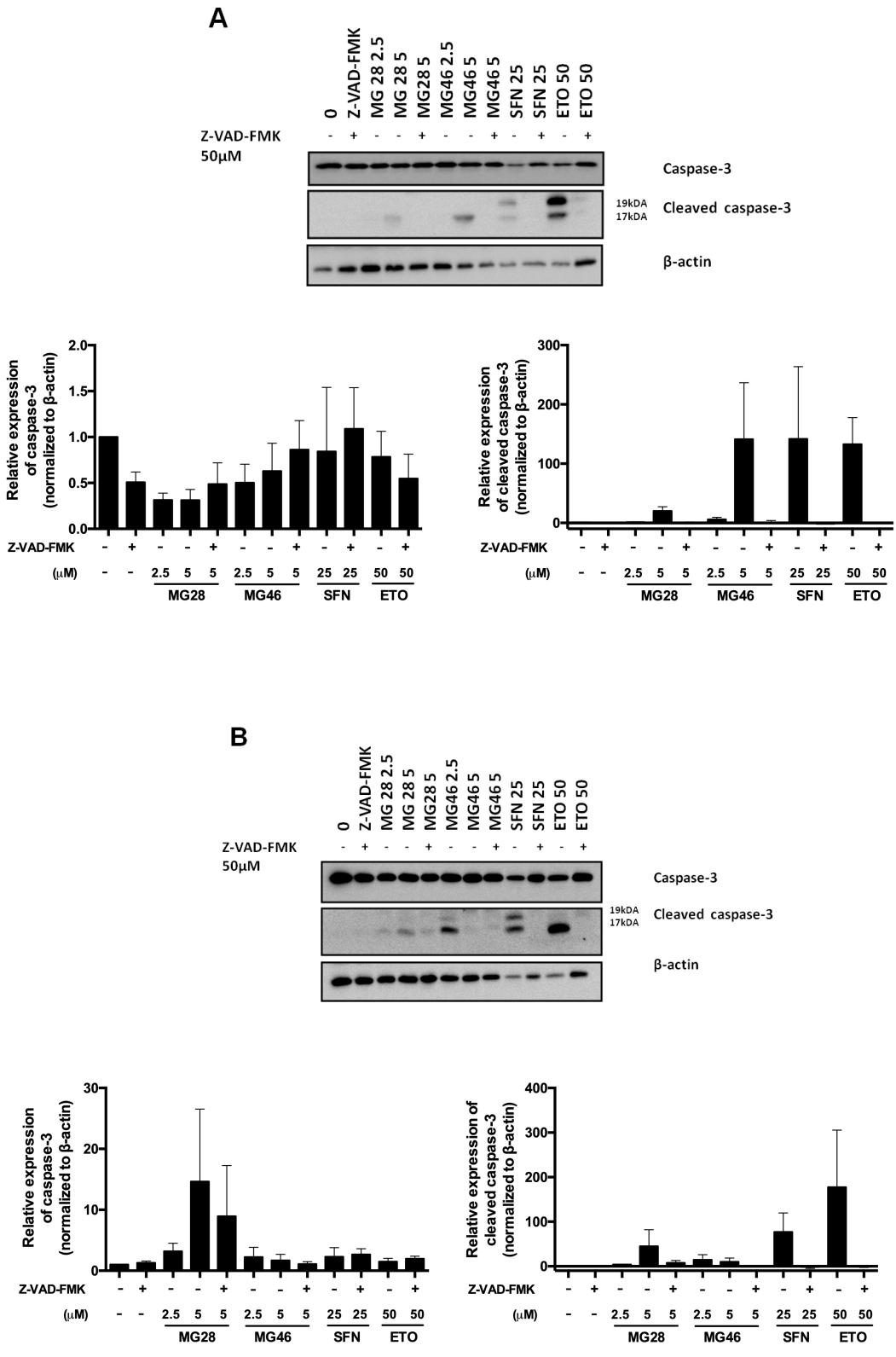

Figure 3.15 Protein expression of caspase-3 and cleaved caspase-3. U-937 cells (A) were pre-treated or not with Z-VAD-FMK and treated with MG28 and MG46 (2.5-5μM) for 16h or with SFN (25μM) for 24h. MV4-11 cells (B) were pre-treated or not with Z-VAD-FMK and treated with MG28 and MG46 (2.5-5μM) for 5h or with SFN (25μM) for 24h. Etoposide (ETO) 50μM was used as positive control. Expression of caspase-3 and cleaved caspase-3 is expressed as intensity values normalized to β-actin.

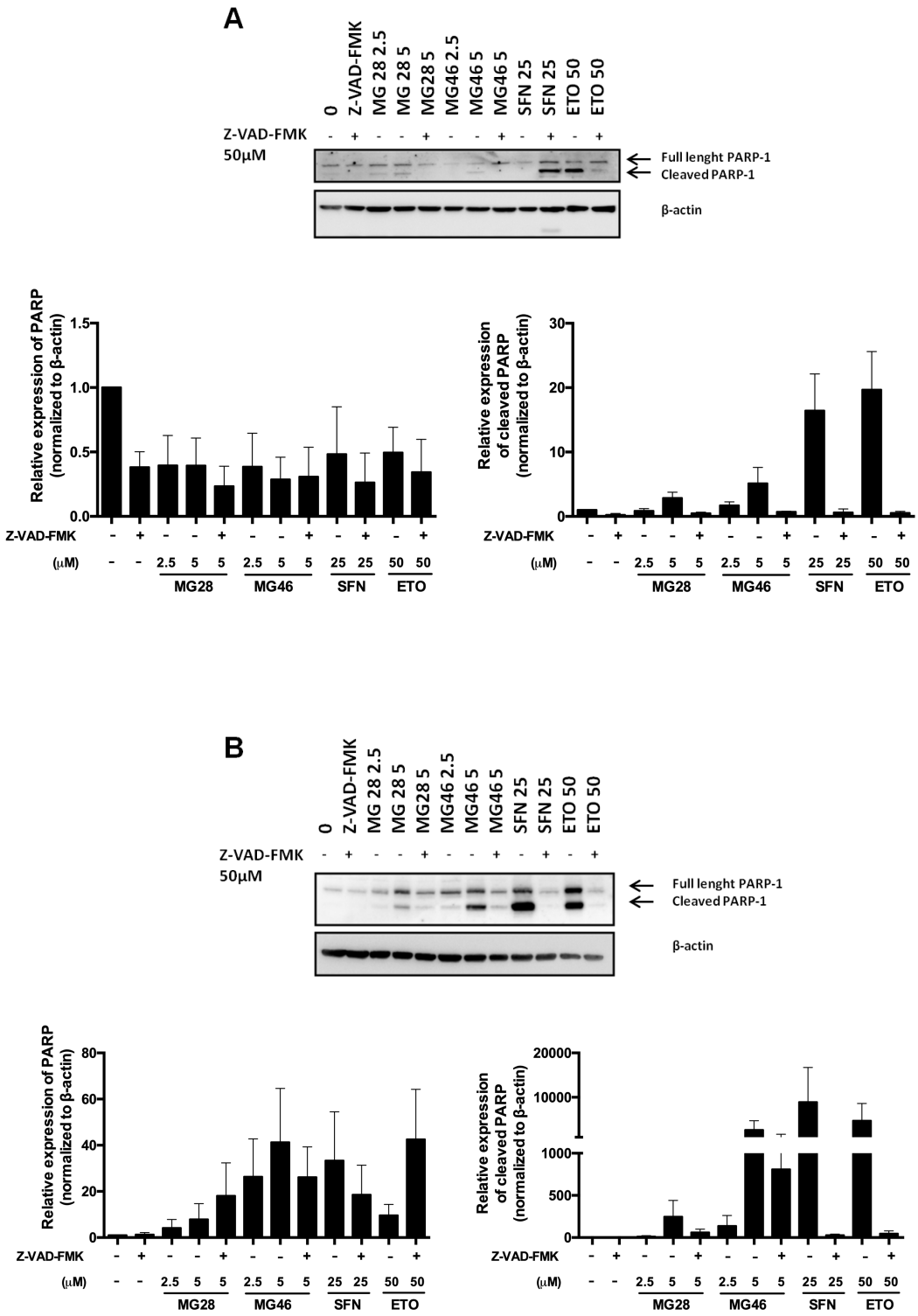

Figure 3.16 Protein expression of PARP-1 and cleaved PARP-1. U-937 cells (A) were pre-treated or not with Z-VAD-FMK and treated with MG28 and MG46 (2.5-5μM) for 16h or with SFN (25μM) for 24h. MV4-11 cells (B) were pre-treated or not with Z-VAD-FMK and treated with MG28 and MG46 (2.5-5μM) for 5h or with SFN for 24h. Etoposide (ETO) 50μM was used as positive control. Expression of PARP-1 and cleaved PARP-1 is expressed as intensity values normalized to β-actin.

SFN at high dose induces different non-apoptotic cell death mechanisms in AML cells

To characterize the cell-death pathway activated by the highest concentration of SFN, we analysed the nuclear morphology of MV4-11 and U-937 cells treated with SFN 50μM in presence of multiple pharmacological inhibitors of non-canonical PCD pathways. Necrostatin-1 is a specific inhibitor of RIP1, involved in the necroptotic cell death pathway; necrosulfonamide, instead, specifically blocks necroptosis downstream of RIP3 activation by preventing MLKL-RIP3 interaction. Ferrostatin-1 is an antioxidant that traps peroxyl radicals even more efficiently than other phenolic compounds, as vitamin E [191]; ferrostatin-1 is widely used as ferroptosis inhibitor [23,192,193]. Olaparib is a PARP-1 inhibitor and thus a parthanatos inhibitor. Cyclosporine A blocks mitochondrial permeability transition pore (mPTP) opening through the interaction with cyclophilin D [5]. Cyclophilin D is a key protein involved in mPTP and regulates certain necrotic but not apoptotic cell death mechanisms [194–196]. Therefore, the pharmacological inhibitor cyclosporine A is used to block MPT-driven necrosis [5,197].

The most interesting results were obtained by pre-treating AML cells with ferroptosis and necroptosis inhibitors.

In both AML cell lines, even if with a much remarkable effect on U-937 cells, pre-treatment with ferrostatin-1 induced a switch of cell death mechanism from necrosis to apoptosis, as shown by the almost total conversion of SFN-induced necrotic cells into apoptotic ones. Pre-treatment with ferrostatin-1 reduced the fraction of necrotic cells from 75% to 3% and from 53% to 12% in U-937 and MV4-11 cells, respectively; concomitantly, the apoptotic fraction increased from 19% to 79% and from 28% to 34% in U-937 and MV4-11 cells, respectively. Accordingly, pre-treating cells with ferrostatin-1 and Z-VAD-FMK almost totally restored cell viability on both cell lines: from 6% to 90% in U-937 cells and from 15% to 87% in MV4-11 cells (Figure 3.17).

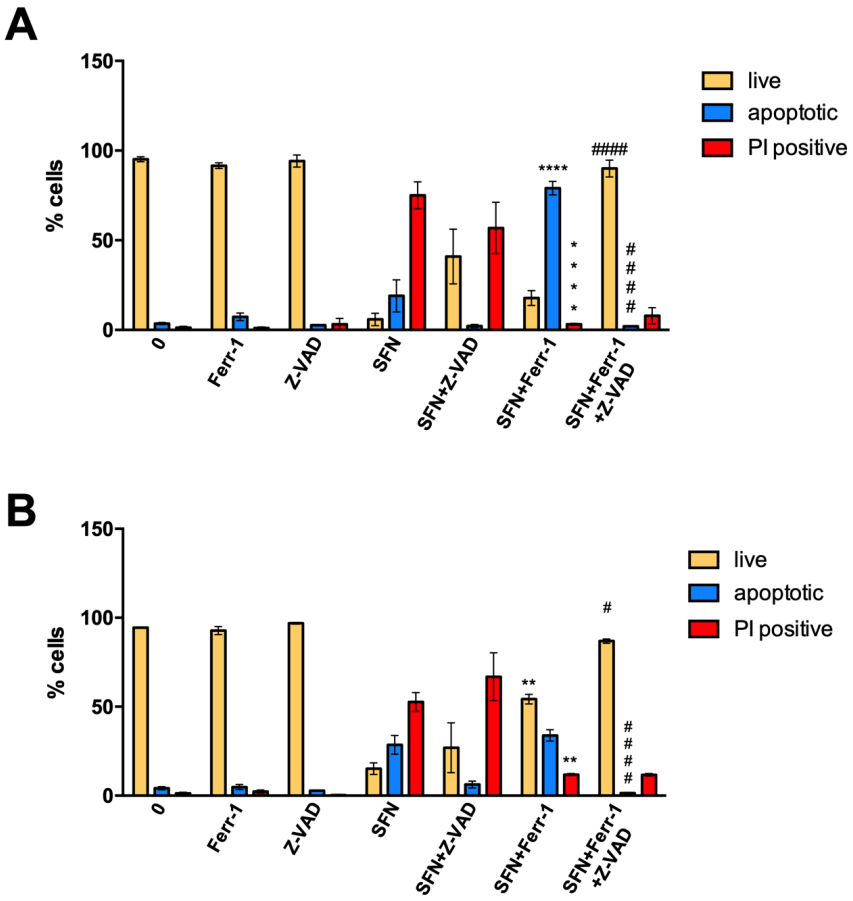

Figure 3.17 Percentage (%) of living, apoptotic, and necrotic (PI positive) U-937 (A) and MV4-11 (B) cells. Cells were pre-treated for 1h with ferrostatin-1 (Ferr-1) *plus* or not Z-VAD-FMK and then treated with SFN 50μM for 24h. ** $p < 0.01$; *** $p < 0.001$; **** $p < 0.0001$ *versus* cells treated with SFN. # $p < 0.05$; #### $p < 0.0001$ *versus* cells treated with SFN and Ferr-1.

Next, to assess whether necroptosis was involved in cell death induced by high dose of SFN, MV4-11 and U-937 cells were pre-treated with necrostatin-1 and necrosulfonamide, alone or in combination with Z-VAD-FMK, and then treated with SFN 50μM.

Pre-treatment of U-937 and MV4-11 cells with necrostatin-1 led to the conversion of necrotic cells into apoptotic ones. The effect was more pronounced in U-937 cells. The fraction of PI-positive cells was reduced from 75% to 4% and from 53% to 32% in U-937 and MV4-11 respectively; the fraction of apoptotic cells, instead, increased from 19% to 66% and from 29% to 42% in U-937 and MV4-11 cells, respectively. Moreover, pre-treatment of both AML cell lines with necrostatin-1 and Z-VAD-FMK restored cell viability (from 6% to 83% in U-937 cells and from 15% to 76% in MV4-11 cells), confirming the switch of PCD pathway (Figure 3.18, A and C).

Pre-treatment of AML cells with necrosulfonamide, instead, induced only a partial conversion of necrotic cells into apoptotic ones. In addition, pre-treatment with necrosulfonamide and Z-VAD-FMK partially restored cell viability and did not have any effect on the necrotic fraction, that was comparable to that observed in SFN-treated cells pre-treated only with Z-VAD-FMK (Figure 3.18, B and D).

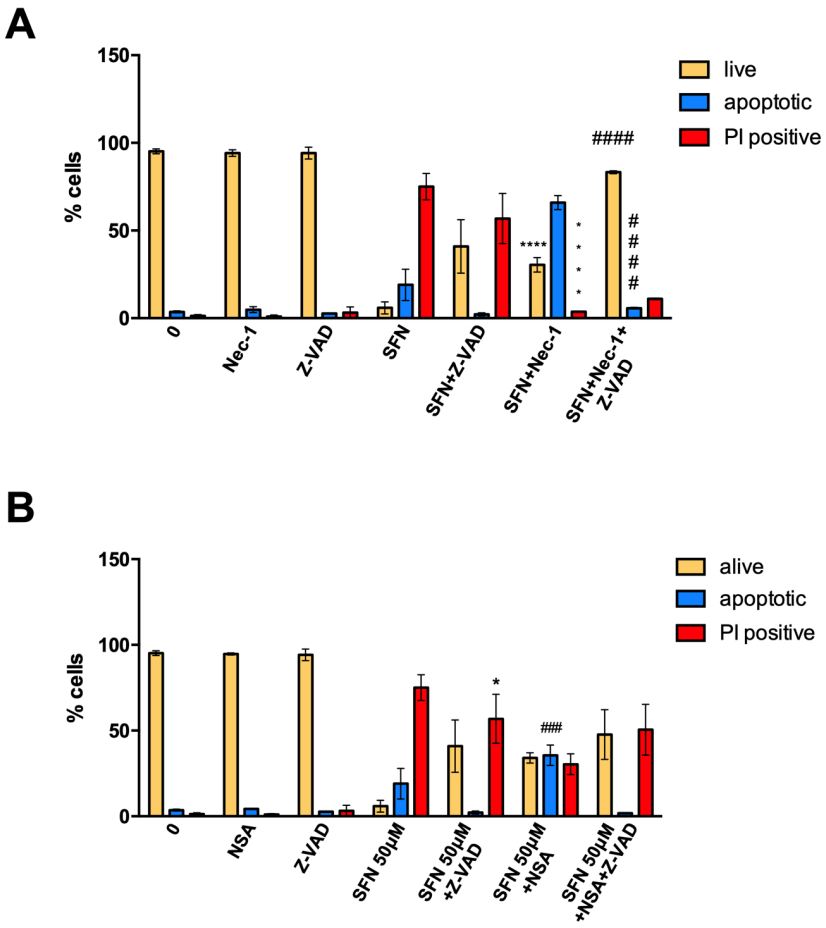

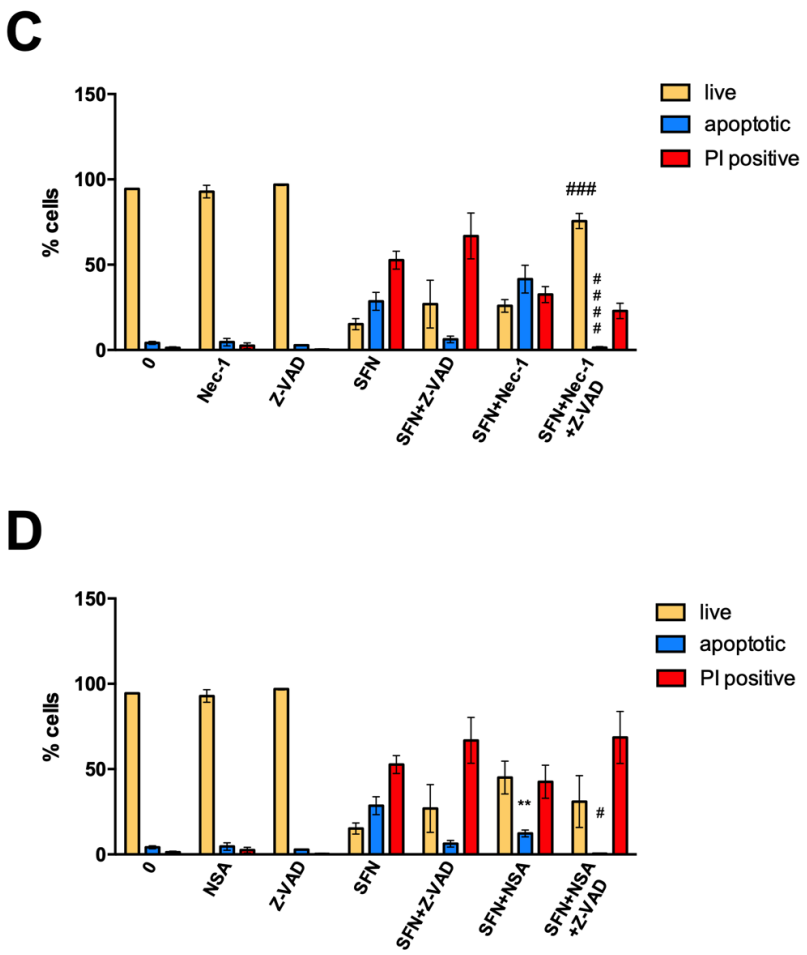

Figure 3.18 Percentage (%) of living, apoptotic, and necrotic (PI positive) U-937 (A, B) and MV4-11 (C, D) cells. Cells were pre-treated for 1h with necrostatin-1 (Nec-1) (A, C) or necrosulfonamide (NSA) (B, D), *plus* or not Z-VAD-FMK, and then treated with SFN 50μM for 24h. * $p < 0.05$; ** $p < 0.01$; **** $p < 0.0001$ *versus* cells treated with SFN. # $p < 0.05$; ## $p < 0.01$; ### $p < 0.001$; #### $p < 0.0001$ *versus* cells treated with SFN and Nec-1/NSA.

Since necrosulfonamide induced a partial switch in the cell death pattern, we hypothesized the involvement of MLKL. To unveil the mechanism of SFN-induced necroptosis, we analysed the protein expression of MLKL and its phosphorylated form (p-MLKL) by Western Blotting. Phosphorylation of MLKL allows MLKL oligomerization and translocation to plasma membrane, which is a fundamental step in necroptosis execution [78].

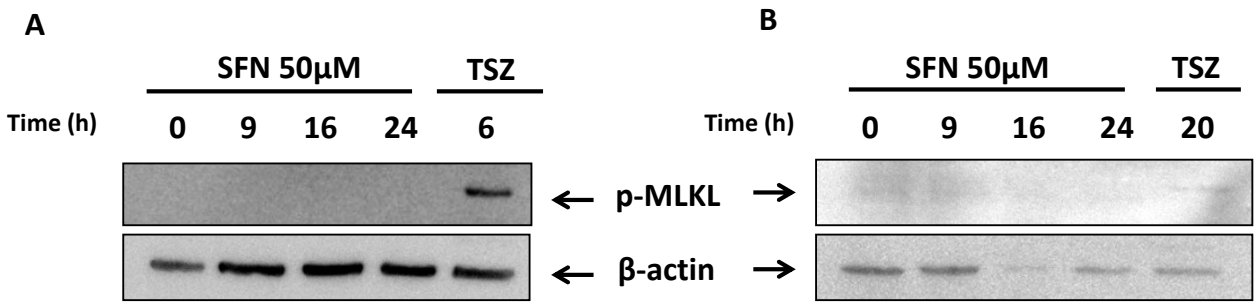

Figure 3.19 Protein expression of p-MLKL on U-937 (A) and MV4-11 (B) cells treated with SFN 50µM for 9-16-24h. TNF-α 50ng/mL (T)+SM-164 500nM (SM)+Z-VAD-FMK 50µM (Z) were used as positive control.

In both SFN-treated cell lines, we found that MLKL was expressed at all tested treatment times (data not shown). However, as illustrated in Figure 3.19, SFN treatment seems not to induce the phosphorylation of MLKL, since p-MLKL was not expressed in SFN-treated cells at any tested time points (Figure 3.19). In MV4-11 cells, the bands related to both p-MLKL and the housekeeping protein used, *i.e.,* β-actin, are significantly milder than those observed in U-937 cells. However, we did not carry out further analyses since the results obtained on U-937 cells were definitely clear. Accordingly, the pre-treatment with necrosulfonamide did not have any effect on SFN-induced cell death in MV4-11 cells.
As neither the expression of p-MLKL nor a total conversion of necrotic cells into apoptotic ones following pre-treatment with necrosulfonamide has been recorded, these observations may indicate that SFN could induce the phosphorylation of RIP-1 and/or RIP3 but is not able to fully activate the necroptotic process. However, it would be appropriate to evaluate the expression of other proteins involved in necroptosis such as RIP-1 and RIP-3, and their phosphorylated forms, to have a complete view of the phenomenon.

Besides ferroptosis and necroptosis, many other non-canonical cell death pathways were discovered. Among them, we investigated parthanatos and MPT-driven necrosis as additional cell death mechanisms eventually involved in the anticancer activity of SFN.
Parthanatos is a peculiar form of non-canonical PCD. Morphologically, it is characterized by plasma membrane rupture without the formation of apoptotic bodies and DNA fragments [5]. Biochemically, parthanatos is a PARP-1-dependent PCD pathway, as it is mediated by the hyperactivation of PARP-1, due to a DNA-base modification induced by oxidative injury as ROS, UV, and alkylating agents [5]. Hyperactivation of PARP-1 leads to parthanatos through two mechanisms: depletion of NAD^+ and ATP, which are associated with necrotic cell death, and collapse of mitochondrial membrane potential, an event related, instead, to apoptosis [5]. Additionally, parthanatos does not require caspases or endonuclease G but instead requires the mitochondrial release of AIF [198]. Hyperactivated PARP-1 binds AIF leading

to its translocation from mitochondria into the nucleus, where it induces parthanatotic chromatinolysis [5,198].

Hence, to test whether SFN at high dose was able to induce parthanatos, U-937 and MV4-11 cells were pre-treated with olaparib, alone or with Z-VAD-FMK, and then treated with SFN 50μM. Analysis of nuclear morphology revealed an almost total conversion of necrotic cells into apoptotic ones in U-937 cells pre-treated with olaparib: the fraction of PI-positive cells was reduced from 75% to 15%, while the fraction of apoptotic cells increased from 19% to 56%. On the contrary, this effect was very limited in MV4-11 cells. Even in this case, the switch of cell death mode was confirmed by using Z-VAD-FMK, which restored cell viability (74% *vs* 6% in U-937 SFN-treated cells) (Figure 3.20).

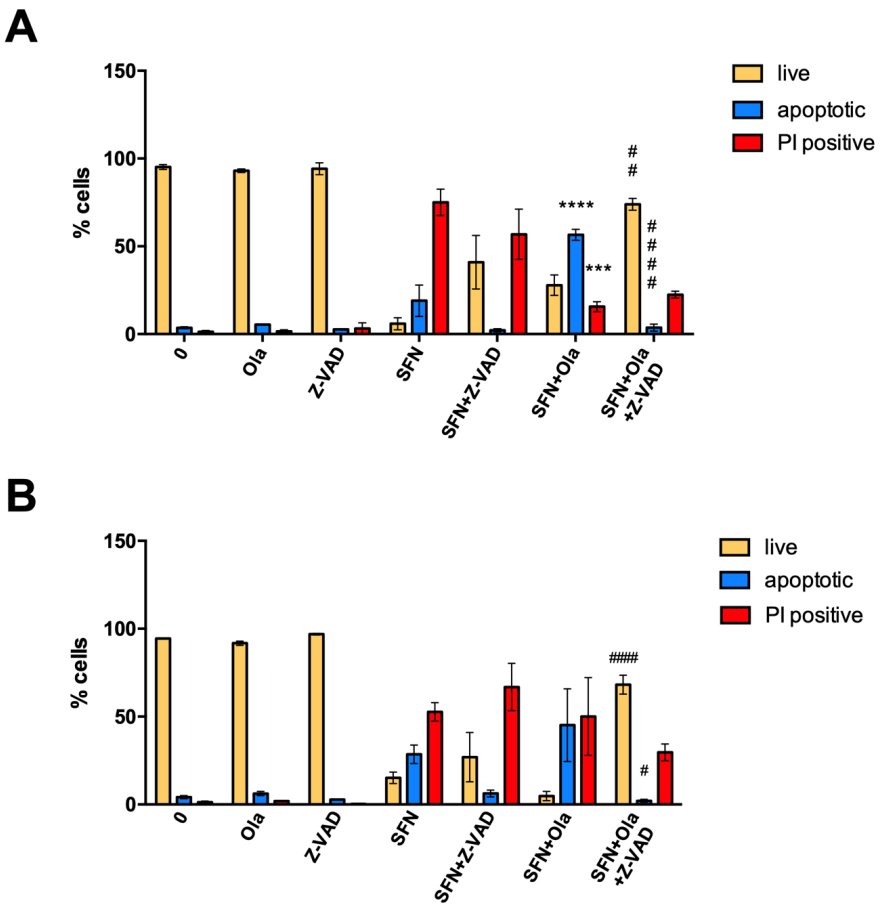

Figure 3.20 Percentage (%) of living, apoptotic, and necrotic (PI positive) U-937 (A) and MV4-11 (B) cells. Cells were pre-treated for 1h with olaparib (Ola), *plus* or not Z-VAD-FMK, and then treated with SFN 50μM for 24h. *** $p < 0.001$; **** $p < 0.0001$ *versus* cells treated with SFN. # $p < 0.05$; ## $p < 0.01$; #### $p < 0.0001$ *versus* cells treated with SFN and Ola.

MPT-driven necrosis is a form of programmed cell death induced by specific intracellular microenvironmental disturbances, such as severe oxidative stress and cytosolic overload of Ca^{2+}. This form of cell death generally occurs with a necrotic cell morphology [5]. The term MPT refers to a rapid

dissipation of mitochondrial membrane potential and consequent osmotic degradation of both mitochondrial membranes due to the sudden lack of impermeability of the inner mitochondrial membrane [199]. At biochemical level, the opening of the so-called "permeability transfer pore complex" (PTPC), a supramolecular complex assembled at the joints of IMM (inner mitochondrial membrane) and OMM (outer mitochondrial membrane), was proposed as the putative cause for MPT-driven necrosis [5]. To date, the only protein that has been validated to be required *in vivo* for MPT induction is peptidylprolyl isomerase F (PPIF; best known as cyclophilin D, CYPD). Accordingly, MPT-driven necrosis was limited by the pharmacological inhibitors cyclosporine A (CSA), sanglifehrin A (SfA) and JW47 [5].

Bearing in mind these findings, we analysed the nuclear morphology of U-937 and MV4-11 cells pre-treated with cyclosporine A, alone or with Z-VAD-FMK, and treated with SFN 50μM. The obtained results showed that pre-treatment with cyclosporine A reduced the fraction of necrotic cells from 75% to 9% and from 52% to 29% in U-937 and MV4-11 cells, respectively; concomitantly, the apoptotic fraction increased from 19% to 84% and from 28% to 64% in U-937 and MV4-11 cells, respectively (Figure 3.21). Even in this latter case, pre-treatment of cells with cyclosporine A *plus* Z-VAD-FMK almost totally and partially restored cells viability in U-937 and MV4-11 cells, respectively, even if the necrotic fraction was equal to that observed in cyclosporine A -pre-treated cells (Figure 3.21).

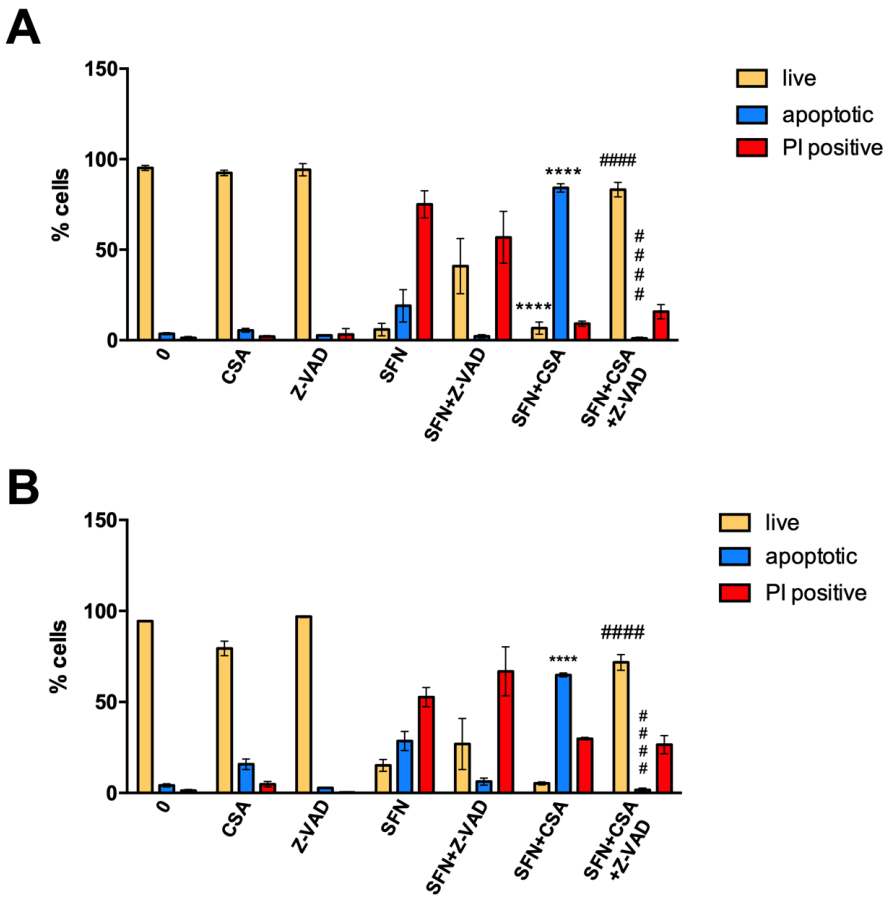

Figure 3.21 Percentage (%) of living, apoptotic, and necrotic (PI positive) U-937 (A) and MV4-11 (B) cells. Cells were pre-treated for 1h with cyclosporin-A (CSA) *plus* or not Z-VAD-FMK, and then treated with SFN 50μM for 24h. **** $p <$ 0.0001 *versus* cells treated with SFN. #### $p <$ 0.0001 *versus* cells treated with SFN and CSA.

SFN, MG28 and MG46 modulate GRP78 and HMGB1 levels

In order to evaluate whether the ability of MG28 and MG46 of activating PCD in AML cells could be mediated by the induction of ER stress, we analysed GRP78 protein expression levels by Western Blotting. Results showed that the two ITC derivatives, at the highest tested concentration, induced a slight increase in GRP78 protein expression levels in U-937 and MV4-11 cells compared to the positive control thapsigargin (Figure 3.22). On the contrary, SFN treatment (25μM) did not upregulate GRP78 protein expression. These results led us to hypothesize that the two ITC derivatives could induce apoptosis by triggering ER stress, but further studies need to be carried out to elucidate this aspect.

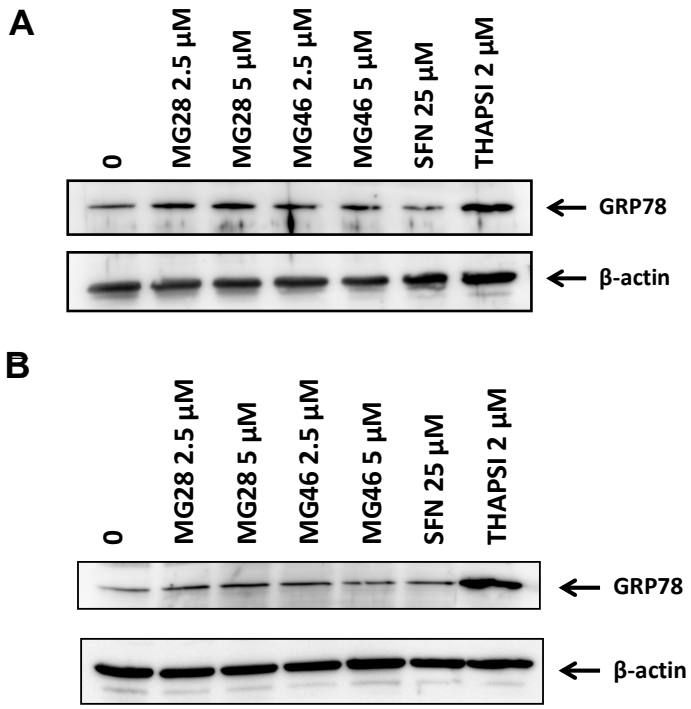

Figure 3.22 GRP78 protein expression in U-937 (A) and MV4-11 (B) cells treated with MG28 or MG46 for 3h or SFN for 24h. Thapsigargin (Thapsi) 2µM was used as positive control.

Since we observed an increase in GRP78 protein expression levels after MGs treatment and considering that ER stress is a pivotal event to elicit ICD, we decided to evaluate whether MGs-induced PCD could be immunogenic. Accordingly, we analysed the amount of HMGB1 release, one of the ICD hallmarks, in the cell-culture supernatant of AML cells treated with MG28, MG46 or high dose of SFN. The release of HMGB1 was analysed at different treatment times with the aim of evaluating this biological end point based on the kinetic of cell death induced by MG compounds and SFN. In fact, at 3 and 6h, respectively for MGs and SFN, the percentage of dead cells was less than 20% (except MG28 and MG46 on MV4-11 cells). Prolonging the treatment time to 6h for MGs and to 16h for SFN, instead, the percentage of dead cells was equal to or greater than 70%, indicating a high mortality rate. Our results showed that only SFN treatment strongly enhanced HMGB1 release (Figure 3.23), despite we did not observe an increase in GRP78 protein expression in SFN-treated cells, at least at the concentration 25µM. On the contrary, in cells treated with MGs, which displayed an increase in GRP78 expression, HMGB1 release was not observed. It could be possible that the observed HMGB1 release in SFN-treated cells is not linked to ER stress but to the activation of non-canonical PCD pathways, such as ferroptosis. However, having analysed only HMGB1 release, those results are too preliminary to conclude that SFN is capable or that MGs derivatives are not capable of inducing ICD. Other ICD markers should be analysed to further test their ability to trigger ICD.

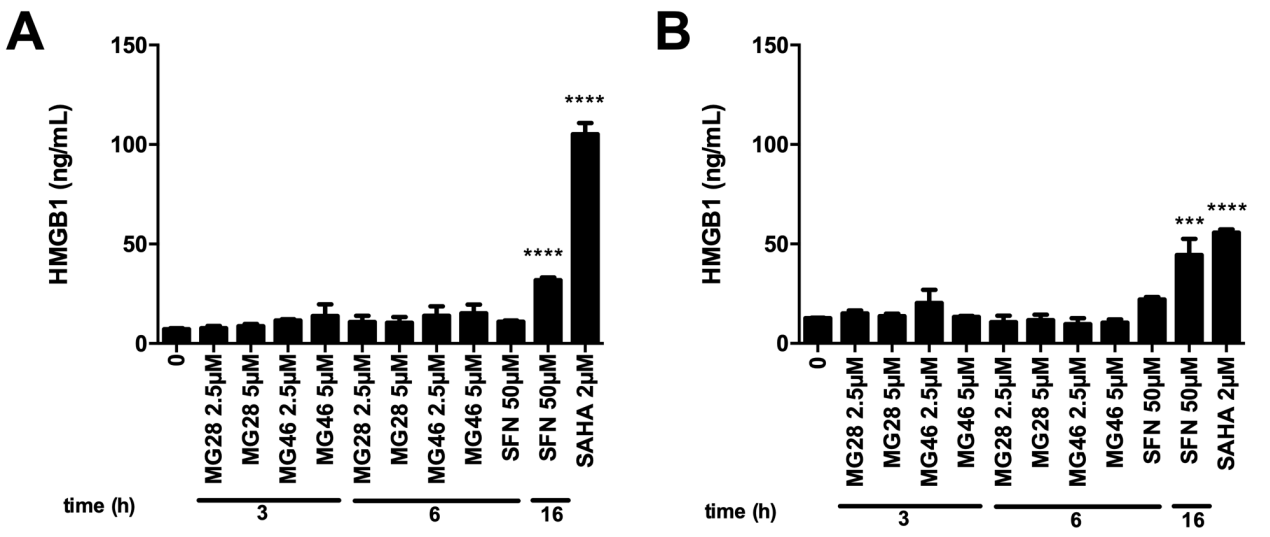

Figure 3.23 Amount of HMGB1 release (ng/mL) in U-937 (A) and MV4-11 (B) cells after treatment with MG28, MG46 or SFN at indicated times and concentrations. SAHA 2μM was used as positive control. *** $p < 0.001$; **** $p < 0.0001$ *versus* untreated cells.

MG28 and MG46 increase micronuclei frequency

Finally, to assess the toxicological profile of the two newly ITC derivatives, we tested their mutagenic potential by analysing the formation of micronuclei (MN). Micronucleus test allows to detect both clastogenic (*i.e.,* breakages of chromosomes) and aneuploidogen effects (*i.e.,* changes in chromosome number) [200]. MG28 and MG46 dose-dependently promoted MN formation. The increase in MN was statistically significant at the dose 4μM for both the ITC derivatives, while it was statistically significant already at 2μM only for MG46. In TK6 cells, at the higher tested dose 4μM, MG28 and MG46 induced 13.07±0.07 and 19.59±2.4 MN/1000 binucleated cells (Figure 3.24). The effect of both ITC derivatives was almost equal to that of mitomycin C and vinblastine, used as positive controls. Therefore, MG28 and MG46 possess mutagenic activity.

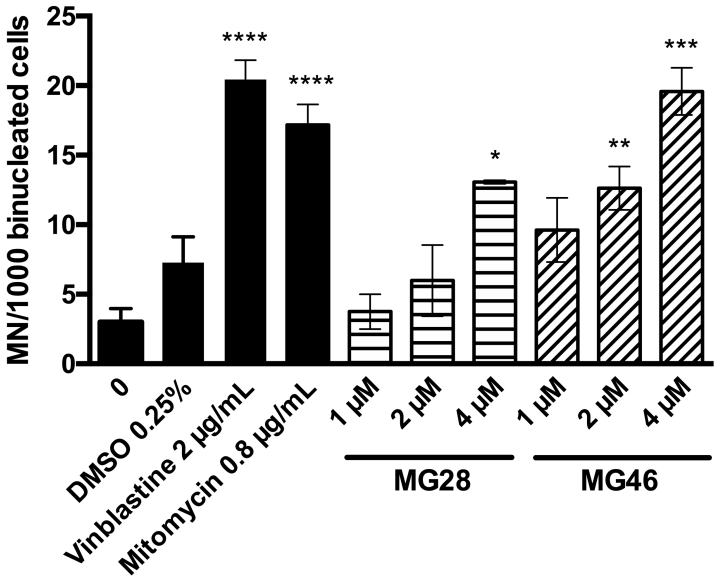

Fig. 3.24 Frequency of micronuclei (MN) in TK6 cells treated with MG28 and MG46 for 4h, and then grown in drug-free medium for 20h. Vinblastine 2µg/mL and mitomycin 0.8µg/mL were used as positive controls. * $p < 0.05$; ** $p < 0.01$; *** $p < 0.001$; *** $p < 0.001$; **** $p < 0.0001$ *versus* untreated cells.

3.4. Discussion

The ability to induce non-canonical cell death is now considered a promising strategy to efficiently treat cancer cells, and eventually to overcome cancer cells apoptosis resistance. In the first part of my PhD project, we investigated the anticancer activity of the isothiocyanate SFN and of two newly synthetized ITC derivatives, named MG28 and MG46, on different leukemia cell lines, with the specific goal to analyse their ability to induce non-canonical cell death. Among them, we found that only SFN triggered different cell death mechanisms, including non-canonical cell deaths, in a dose-dependent manner.

MG28 and MG46 are two newly developed ITC derivatives consisting of an ITC group condensed to a side chain obtained from rhodol, a fluorophore capable of targeting and delivering small molecules to subcellular organelles, as endoplasmic reticulum [186]. Our results demonstrated that MG compounds possess a strongly enhanced cytotoxic activity against different leukemia cell lines compared to the parental compound SFN. Indeed, comparing their IC_{50} with that of SFN, we observed a difference of about one order of magnitude in almost all tested cell lines. Moreover, we confirmed that the cytotoxic activity of MG28 and MG46 could be solely attributed to the presence of the ITC group, since rhodol failed to exhibit any cytotoxic effect on all tested cell lines.

It is interesting to note that the five tested leukemia cell lines exhibited a different sensitivity against MG28 and MG46. Indeed, MOLM-13 and MV4-11 cells were the most sensitive, whereas Jurkat, U-937 and OCI-AML3 cells shown to be less responsive. In order to further characterize the different sensitivity of MV4-11 and U-937 cells, next experiments were conducted on those two cell lines. MG28 and MG46 induced a rapid and dose-dependent increase in apoptotic cell death in these two cell lines. In U-937 cells, MGs treatment increased the percentage of apoptotic cells starting from 3h of treatment, achieving the maximum after 9h, and remaining constant, or even decreasing, after 24h of treatment. In MV4-11 cells, MGs showed a similar trend, even if they reached the maximum pro-apoptotic activity already after 3h of treatment, when apoptotic fraction was almost similar to that observed at longer treatment time. In MV4-11 cells, the apoptotic cell death onset triggered by the two ITC derivatives was more rapid than in U-937.

For SFN, only U-937 cells were found to be much more resistant to its cytotoxic activity while MV4-11, MOLM-13 and OCI-AML3 cells exhibited equal sensitivity. We therefore hypothesized that MOLM-13 and MV4-11 could possess some genetic mutations that make them more susceptible to the activity of the two ITC derivatives.

FMS-like tyrosine kinase 3 (FLT3) is a membrane receptor tyrosine kinase (RTK) belonging to type III receptor tyrosine kinase (RTK) family. FLT3 is expressed in multipotential hematopoietic stem cells and progenitors, in more mature cells of monocytic origin, and also in blast cells of most patients with AML and in AML-derived cell lines [201]. In AML, two different types of FLT3 mutations have been recorded: internal tandem duplication (ITD) of the juxtamembrane domain (FLT3-ITD, and missense mutations in the activation loop domain of the tyrosine kinase domain of the FLT3 receptor (FLT3-TKD) [201]. FTL3 mutations occur in about 30% of all AML cases, with the FLT3-ITD being the most prevalent form of FLT3 mutation, roughly 25% of all AML cases, while FLT3-TKD point mutations in approximately 7-10% of AML cases [202]. Many studies support that FLT3-ITD mutation is associated with an increased risk of relapse and a worse overall survival, thus being considered an unfavorable prognostic indicator [201]. On the contrary, the prognostic effects of FLT3-TKD mutation are not so well known. Many different studies, for example, have found slight associations between clinical outcomes and FLT3-TKD mutation occurrence, whereas at least one large study found no correlation with event-free survival or overall survival [202]. FLT3-ITD mutation allows the FLT3 receptor to become constitutive activated. Mice harboring an ITD in the region of FLT3 developed a myeloproliferative disease characterized by an increased amount of granulocyte-monocytic progenitors and mature myeloid cells [201]. Besides, also FLT3 high transcript levels without the presence of FLT3-ITD has been linked to an increased risk of relapse and a worse overall survival in AML patients [203,204].

Regarding the incidence of FLT3 mutations in AML cell lines, Quentmeier and colleagues performed a screening of FLT3 mutations in 69 AML cell lines [205]. They found that 4 AML cell lines carried a FLT3-ITD mutation: two of these (MUTZ-11 and MV4-11) expressed only the mutated allele, while the other two (PL-21, MOLM-13 and sister cell line MOLM-14) expressed the mutated and the wild-type allele. Additionally, it was found that only FLT3 mutant cell lines clearly express the phosphorylated receptor protein FTL3 [205]. Regarding FLT3-TKD point mutation, none of the 69 tested AML cell lines carried this type of FLT3 mutation [205].

Hence, the different sensitivity to MG derivatives exhibited by the AML cells tested in our experimental setting could be explained by the fact the most responsive cells (MV4-11 and MOLM-13) possess FLT3-ITD mutation, unlike the other tested cell lines. Bearing in mind that this mutation occurs in about 25% of all AML cases and, above all, AML harboring FLT3-ITD mutation is one of the forms of AML with high risk of relapse and a worse overall survival, our results suggest that MG28 and MG46 could represent two potentially highly effective anticancer agents in the treatment of this aggressive AML form.

A similar trend has been observed also with cabozantinib, a multikinase inhibitor that possesses anticancer activity in different cancer types [206]. Cabozantinib displayed a significant cytotoxic effect in

MV4-11 and MOLM-13, carrying FLT3-ITD, while K562, OCI-AML3 and THP-1 cells, lacking FLT3-ITD, were resistant to cabozantinib. This means that cabozantinib is selectively cytotoxic in AML cells harboring FLT3-ITD mutation [206]. Also the natural compound petromurin C, a bis-indolyl benzenoid isolated from the marine sponge *Epipolasis* sp., showed a higher activity in the FLT3-mutated cell line MV4-11 compared to FLT3-wild type U937 cell line [207].

Apoptosis is a programmed cell death mechanism characterized by specific molecular events. Both intrinsic and extrinsic apoptotic pathways converge into the cleavage of caspase-3 and its substrate PARP-1 in order to orchestrate the final apoptotic cell outcome. Moreover, among all the PCD programs, apoptosis, together with pyroptosis, is the only cell death mechanism that involves caspase activity, whereas all the others (*i.e.,* necroptosis, ferroptosis, and parthanatos) are classified as caspase-independent cell death mechanisms [5]. To investigate the involvement of caspases in MGs-induced cell death, we pre-treated cells with a pan-caspase inhibitor before treatment with the ITC derivatives. Pre-treatment with the pan-caspase inhibitor Z-VAD-FMK almost abrogated the induction of apoptosis triggered by the two MG compounds. Additionally, in MV4-11 and U-937 cells, caspase-3 and PARP-1 were strongly cleaved after treatment with ITC derivatives, effects that have been totally prevented by Z-VAD-FMK pre-treatment. All these findings led us to conclude that MG28 and MG46 exclusively trigger caspase-dependent apoptotic cell death. However, pyroptosis is a caspase-dependent cell death as well, based, in particular, on caspase-1 activation [5]. Thus, having exclusively analysed the expression of apoptotic caspase-3, it might be possible that also pyroptosis was involved in MG28- and MG46-induced cell death.

The ability of ITC derivatives to induce apoptosis is widely documented. In recent years, a huge number of SFN derivatives or analogues have been synthetized and their ability to induce apoptosis has been established. The magnolol-sulforaphane (MAG-SFN) hybrid CT1-3, synthetized by Tao *et al*, showed a more cytotoxic activity than its lead compounds MAG and SFN in multiple cancer cells. Moreover, CT1-3 triggered mitochondria-mediated apoptosis in human cancer cells and reduced the migration and invasion capacity of tumor cells through the regulation of E-cadherin/Snail axis and the inhibition of epithelial mesenchymal transition (EMT) process [208]. In addition, Minarini and colleagues synthesized three newly compounds incorporating the ITC group in the naphtalene diimide (NDI) scaffold [209]. On human T lymphoblastoid cells (Jurkat), all the three newly ITC derivatives displayed a potent cytotoxic activity, which has been related to their ability to trigger both intrinsic and extrinsic apoptotic cell death and to block cell cycle in G1 phase [209]. Moreover, other several developed NDI analogues bearing an ITC group showed to inhibit melanoma cells growth by efficiently triggering apoptosis [210]. Lastly, Hu *et al* developed many different SFN derivatives by replacing the methyl group of SFN with several different alkyl and aryl groups, and by changing the chain length between the ITC and sulfoxide

groups [211]. Among all, a benzyl-group-substituted ITC derivative resulted the most active with a significant cytotoxic activity on different cancer cell lines and the induction of apoptosis in hepatocellular carcinoma cells (HepG2) [211].

In our experimental setting, SFN exhibited a different behavior, as it was able to induce different cell death mechanisms in a dose-dependent manner. In both U-937 and MV4-11 cells, SFN 25μM activated apoptotic cell death, as shown by Hoescht and PI staining and cleavage of both caspase-3 and PARP-1. Additionally, all these effects were totally abolished by pre-treating cells with the pan-caspase inhibitor Z-VAD-FMK. Pre-treatment with Z-VAD-FMK almost totally abrogated apoptosis induction triggered by SFN 25μM, but it did not have any effect at the highest tested concentration of SFN (50μM), hence suggesting the involvement of other forms of PCD. Kaminski and colleagues found that SFN-induced cell death probably shift from apoptosis to necrosis depending on both dose treatment and drug exposure time: in CaCo-2 colorectal cancer cells, they reported a shift from apoptotic to necrotic cell death after increasing concentrations and treatment time with SFN, alone or in combination with oxaliplatin [212]. However, the authors have not investigated if SFN-induced necrosis was a type of non-canonical programmed cell death.

The ability to activate multiple cell death pathways has been observed especially for numerous naturally occurring compounds. In particular, in some cases the same compound induced different PCD pathways depending on the concentration. For example, low dose of shikonin (1μM) activated caspase-dependent apoptosis, while at high dose (10μM) it triggered caspase-independent cell death (*i.e.,* necroptosis) in U-937 AML cells [136]. Moreover, low concentrations (up to 25μM) of columbianadin (CBN) induced apoptosis, while high concentration (50μM) induced necroptosis [117]. Taxol induced different forms of cell death in a dose-dependent manner: at low concentration (35nM) it induced apoptosis, whereas at higher concentration (70μM) it induced paraptosis-like cell death without any classic apoptotic features (*i.e.,* phosphatidylserine externalization, caspase-3 involvement or nuclear fragmentation) [213]. Lastly, the tetrahydrobenzimidazole derivative TMQ0153 triggered caspase-dependent apoptosis at low concentrations (up to 20μM), while at higher concentrations (over 30μM) it induced necroptotic cell death with the concomitant induction of protective autophagy [214].
In other cases, the same dose of natural compounds could activate different PCD pathways: arctigenin induced both apoptosis and necroptosis at the same tested dose (5μM) in nasal septum carcinoma RPMI-2650 cells [112]; berberine at 100μM, alone or in combination with cisplatin, triggered apoptosis and necroptosis in ovarian cancer cells [114]; neoalbaconol at 40mM simultaneously activated both apoptosis and necroptosis in nasopharyngeal carcinoma cell line C-6661 [123]; tanshinone IIA at 5 or 10μg/mL induced both apoptosis and necroptosis in human hepatocellular carcinoma HepG2 cells [147].

In other circumstances, the activation of one cell death pathway rather than another one is, instead, cell-type dependent. For example, eupomatenoid-5 induced caspase-dependent apoptotic cell death in breast cancer MCF-7 cells and necroptosis in kidney 786-0 tumor cells [215]. It is well known that induction of necroptosis is strictly related to the expression of its molecular mediators, which are cancer-type-dependent: decreased RIP1/RIP3/MLKL expression was found in breast, colorectal, gastric, and ovarian cancer, in AML, melanoma, head and neck squamous cell carcinoma, cervical squamous cell carcinoma; increased RIP1 expression was reported in glioblastoma, and lung and pancreatic cancer, together with increased RIP3 and MLKL expression [76]. Additionally, in the same cancer type, RIP1/RIP3 expression could vary depending on the different cell line. For example, shikonin-induced cell death differed among different human pancreatic cancer cell lines and this discrepancy seemed to be consistent with the expression of RIP3 among the tested cell lines: in AsPC-1 cells, expressing high levels of RIP3 without RIP1 expression, shikonin mainly induced necroptosis; in Panc-1 cells, expressing low levels of RIP3 together with RIP1 expression, shikonin triggered apoptotic cell death [131].

Regarding the ability of SFN, and in general ITCs, to induce non-canonical cell death in cancer cells, very few studies have been conducted and all of them reported the induction of mitotic catastrophe. Mitotic catastrophe is a regulated oncosuppressive mechanism that prevents cells from proliferating and/or surviving when they are no longer able to complete mitosis due to extensive DNA damage, mitotic machinery challenges, and/or mitotic checkpoints failure [5]. Mitotic catastrophe is morphologically characterized by specific nuclear alterations, such as multinucleation and micronucleation, two possible consequences of chromosomal misaggregation, possibly due to persistent lagging or acentric chromosomes [5]. Lung cancer cells (A549 and H1299) treated with phenethyl isothiocyanate displayed some features of mitotic catastrophe, like the formation of multipolar mitotic spindles, the appearance of multinucleated giant cells and the increase in the number of polyploid cells [216]. The authors hypothesized that phenethyl isothiocyanate could alter microtubule organizing centers and potentially impair the nucleation of the spindle microtubules. Thus, the resulting mitotic disorganization/arrest would result in all the observed effects [216].

In colorectal HT-29 cancer cells, allyl-isothiocyanate induced the cells to rapidly round up and detach without any appearance of apoptosis induction; instead, detached cells showed disrupted tubulin [217]. In another study, allyl-isothiocyanate caused mitotic catastrophe through the phosphorylation of Bcl-2, thus activating the mitochondrial apoptotic pathway. In particular, bladder cancer cells treated with allyl-isothiocyanate displayed multiple micronuclei, aberrant and multipolar mitotic spindle and lack of separation of sister chromosomes, all features of mitotic catastrophe [218].

Even for SFN, several studies report its ability to induce mitotic catastrophe. Jackson *et al* recorded that SFN induced mitotic catastrophe in MCF-7 cells, as observed by aberrant mitosis and micronucleation [219]. On F3II cells, a sarcomatoid mammary carcinoma cell line, SFN blocked cell proliferation in phase

G2/M of the cell cycle and promoted mitotic arrest with a premature cdc2 kinase activity [220]. Lastly, SFN inhibited angiogenesis by suppressing endothelial cell proliferation. This anti-proliferative activity was related to its ability to induce mitotic catastrophe, as demonstrated by extensive micronucleation, aberrant cell cycle progression with mitotic figures lacking complete and symmetrically bipolar mitotic spindle arrays, micronuclei, and diffuse cytoplasmic microtubule staining of SFN-treated cells [221].

We found that SFN, at high dose, could activate different non-canonical cell death pathways. In particular, we observed that ferrostatin-1, a pharmacological inhibitor of ferroptosis, induced an almost total conversion of SFN-induced necrotic cells into apoptotic ones. The inhibition of both ferroptosis and apoptosis almost totally rescued cell viability of SFN-treated cells.
Ferroptotic cell death is finely regulated. The role of Nrf2 in ferroptosis is still controversial. Since Nrf2 pathway activation endorses iron storage and limits cellular iron uptake and ROS production, Nrf2 is considered as a negative ferroptosis regulator [63]. Ferroptosis inducers capable of activating Nrf2 pathway promote cellular adaptation and survival as well as render cancer cells less sensitive to ferroptosis induction themselves. Thus, it could be though that they cannot be considered as good candidates for anticancer therapy. However, as mentioned before, activation of Nrf2 pathway could also promote ferroptotic cell death [41,222]. In this context, the ability of SFN to upregulate the Nrf2 pathway and HMOX1 levels is widely documented and reviewed [172,223–225]. Hence, it may be possible that SFN could promote ferroptosis by increasing HMOX-1 levels in AML cells, even if it has to be confirmed. HMOX-1 is responsible for heme catabolism, which produces iron, carbon monoxide, and biliverdin: it is plausible assuming that the antioxidant properties of HMOX-1 are not enough to face the great iron production which unbalances cells and leads them to ferroptosis [222]. Accordingly, Kwon *et al* demonstrated that hemin, the most prevalent HMOX1-produced heme metabolite, induced lipid peroxidation probably as a consequence of iron increase [222].

Regarding the induction of necroptosis by high dose of SFN, our results were controversial. Necrostatin-1 is a pharmacological inhibitor able to prevent the activity of RIP1 kinase, a protein involved in the first stage of necroptosis and whose phosphorylation is essential in the formation of the complex called necrosome [76]. Necrosulfonamide, instead, targets MLKL and blocks necrosome formation [226]. Pre-treatment of cells with necrostatin-1 induced a switch of necrotic cells into apoptotic cells, and an almost total recovery of cell viability after pre-treatment with necrostatin-1 and Z-VAD-FMK. These effects resulted much less marked after pre-treatment of cells with necrosulfonamide. Moreover, our analysis of protein expression of MLKL and its phosphorylated (p-MLKL) form showed that even if MLKL was expressed in both tested AML cell lines, SFN treatment did not increase protein expression of p-MLKL at any tested treatment times. To date, the mechanism by which necroptosis is executed is still a matter of debate, but what is certain is that phosphorylation of MLKL is an essential step in necroptosis

execution allowing MLKL membrane translocation [75]. Hence, as we observed neither the expression of p-MLKL nor a total conversion of necrotic cells into apoptotic ones following pre-treatment with necrosulfonamide, it could be assumed that SFN could induce the phosphorylation of RIP1 or RIP3, but it is not able to fully activate the necroptotic process. However, it would be appropriate to evaluate the expression of other proteins involved in necroptosis such as RIP-1 and RIP-3, and their phosphorylated forms, to completely disentangle the necroptotic pathway of SFN.

Notably, some chemotherapeutic treatments can stimulate the immune response and induce an effect comparable to that of an anti-cancer vaccine. Such type of cell death is called ICD [8]. ICD is capable of warning the immune cells of a state of danger through the extracellular release, or surface exposure, of immunostimulatory factors or damage-associated molecular patterns (DAMPs) including CRT, ATP and HMGB1, which act as "eat me", "find me" and danger signals, respectively. Heat-shock protein 70 (HSP70) and HSP90 are additional DAMPs that stimulate immune response [8]. ICD is intimately associated with ER stress: induction of ICD resides in the ability of a compound to trigger ER stress concertedly to the generation of ROS. However, in some PCD pathways, as necroptosis, ROS-mediated ER stress could be not necessary for triggering ICD and the consequent *in vivo* immune responses [227]. In particular, necroptotic ICD was triggered without evident/detectable ER stress or PERK activation, unlike hypericin-PDT (photodynamic therapy) and anthracycline-induced ICD [228], showing that there may be additional engaging pathways in the induction of danger signals, and further supporting that ICD induction may be stimuli- and context-dependent [228]. This evidence is in line with our results. Indeed, MG28 and MG46 slightly enhanced GRP78 protein expression but they did not induce the release of HMGB1; on the contrary, SFN (50μM) treatment strongly enhanced HMGB1 release without increasing GRP78 protein expression, at least at the concentration 25μM. Hence, the possible induction of ICD by high dose of SFN may be triggered by other activating pathways. For instance, the observed release of HMGB1 in SFN-treated cells could be related to the activation of non-canonical PCD pathways, such as ferroptosis. This hypothesis is supported by the observed release of HMGB1 by ferroptotic dying cells treated with ferroptosis inducers erastin, sorafenib, RSL3, and FIN56 [229]. However, having analysed only HMGB1 release, it cannot be concluded that SFN is capable or that MGs derivatives are not capable of inducing ICD. Further experiments would be necessary to analyze other ICD markers and understand the potential ability to trigger ICD by our compounds.

Finally, to screen the toxicological profile of the two ITC derivatives, we analysed their ability to cause DNA damage. Indeed, the capacity of a compound to cause DNA damage is a crucial factor in determining its toxicological profile, as DNA mutations are involved in the pathogenesis of several degenerative disorders, as cancer [230]. Both ITC derivatives were mutagenic, as observed by the increased frequency of MN formation. As regards the genotoxic activity of the parental compound SFN,

various studies are available in the scientific literature. Some of them reported that SFN (10, 20, 30 and 50μM) caused DNA double-strand breaks in human leukemia [231] and cervical cancer cells [232] as well as the phosphorylation of H2A.X (P-H2A.X) in colon cancer cells [233]. However, at concentrations equal or below 10μM (0.3, 1, 3 and 10μM), SFN did not promote MN formation, suggesting the lack of a mutagenic effect, but even reduced the mutagenic activity of some known mutagens (*i.e.,* methyl methanesulfonate, vincristine, H_2O_2, and mitomycin) [234,235]. To note, SFN (10μM) slightly caused DNA double-strand breaks but it did not promote MN formation. This finding leads to suppose that DNA lesions may have been repaired by the intracellular DNA damage repair systems, thus without inducing stable mutations. The only exception is the study by Ferreira de Oliveira and colleagues [236], who reported the ability of SFN 5μM to promote the formation of MN [236]. However, this latter finding is not convincing. Indeed, they analysed only one concentration of SFN, thus being out of the recommendations of *OECD* guidelines for the testing of chemicals, which recommends that at least three concentrations should be evaluated for the *in vitro* cytogenetic assays, as the micronucleus test [188].
Overall, it could be plausible that the two ITC derivatives share with their parental compound SFN the ability to promote DNA damage. However, the nature of DNA damage seems to be different. SFN causes DNA lesions but, at concentrations equal or below 10μM, it did not induce a permanent damage. MG28 and MG46, instead, promote the formation of MN at concentrations below 10 μM (*i.e.,* 2 and 4μM), hence being classified as mutagens.

Chapter 4
INDOLES AND THEIR DERIVATIVES

4.1 Introduction

Indoles are aromatic heterocyclic compounds with a heterobicyclic structure composed by a six-membered ring fused to a five-membered pyrrole ring (Figure 4.1). The indole term comprises all the compounds possessing an indole ring system [237].

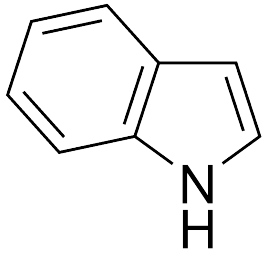

Figure 4.1. Chemical structure of indoles.

Indoles are widely present in nature, produced by plants and bacteria, where they act as signal molecules in both plants and animals [160]. Additionally, many natural compounds, such as alkaloids (*i.e.,* ergot alkaloids, and β-carboline alkaloids) and indigoids, originate from the bio-oxidation of indoles [160].
Besides their role in plants and animals, indoles play a pivotal role in cell physiology and are likely intermediary for several biological reactions [160]. Moreover, a plethora of indoles derivatives displayed many different biological effects, including anticancer activity, which has been widely reviewed [160,165,238–240].

4.1.1 Biosynthesis of indole alkaloids and derivatives

Indole alkaloids are widely present in nature, produced as secondary metabolites by plants, bacteria, fungi, and marine organism. Ergoline, prenylated, bis- and tris-indoles, and β-carboline are just some of the naturally occurring subclasses of indole alkaloids. Despite belonging to different subgroups, and especially being produced by diverse kingdom species, all indole alkaloids are bio-synthetized from the amino acid tryptophan [160,241]. Briefly, tryptophan, after its decarboxylation, produces tryptamine, which could be methylated leading to dimethyltryptamine. Indole alkaloids psilocin and psilobycin, for example, derive from the oxidation and eventually phosphorylation of dimethyltryptamine; β-carboline alkaloids originate from tryptamine after different chemical reactions, as Mannich reaction and/or oxidation [160].

Focusing on the marine ecosystem, an uncountable number of indoles derivatives were isolated from algae, sponges and other marine organisms. Granulatamides A and B are two cytotoxic simple indole alkaloids derived from tryptamine, isolated from the soft coral *Eunicella granulata* [241]. Caulerpin and caulersin are two bis-indole alkaloids isolated from different green and red algae; fragilamide, martensine, martefragines, and denticines belong to a group of bis-indoles alkaloids derived from the red alga *Martensia fragilis* [242]. Instead, the indole alkaloids meridianins F and G, and the two dibrominated indole enamides tanjungides A and B, were isolated from the tunicates *Aplidium meridianum* and *Diazona cf. formosa*, respectively [241]. The β-carboline alkaloids 3-bromofascaplysin, 10-bromofascaplysin, 3,10-dibromofascaplysin, 14-bromoreticulatine, 14-bromoreticulatate, and homofascaplysate A, instead, are just some of the isolated compounds from diverse tunicates of *Didemnum* sp. [241].
However, among all marine organisms, sponges are certainly the richest source of indole derivatives. Indeed, a plethora of indole alkaloids were isolated from marine sponges, as bis-indole alkaloids nortopsentins A–D extracted from *Spongosorites ruetzleri* spongethe and tris-indole alkaloids gelliusines A and B isolated from the deep water New Caledonian sponge *Gellius* or *Orina* sp [160]. Sponges belonging to *Hyrtios* sp are a rich source of indole derivatives as, among all, hyrtiocarboline, hyrioreticulins A-B, hainanerectamine C, hirtinadine A, hyrtioerectine A, dendridine A [160,243].

Moving to the terrestrial ecosystem, monoterpenoid indole alkaloids is another group of indole alkaloids widely present in plant kingdom, especially in some plant families as *Apocynaceae*, *Loganiaceae*, and *Rubiaceae* [244]. Several bioactive compounds belong to this class, including the antineoplastic agents camptothecin from *Camptotheca acuminata* and vinblastine and vincristine from *Catharanthus roseus* [244]. Monoterpenoid indole alkaloids are biosynthetized from the precursor strictosidine, which is the product of the condensation reaction of tryptamine and secologanin, an iridoid monoterpene [244].
Indoles could be broadly found also in cruciferous vegetables, belonging to *Brassicaceae* family. In cruciferous vegetables, as for ITCs, indoles are naturally biosynthesized from glucosinolates. Over the 115 naturally occurring glucosinolates found in crucifers, the indolyl glucosinolates glucobrassicin and neoglucobrassicin have been identified as indoles precursors [165]. Glucobrassicin, besides in vegetables of *Brassica* genus, is also present in woad (*Isatis tinctoria*, also known as German Indigo) [239]. As for isothiocyanates, myrosinase catalyzes the hydrolysis of the glucosinolate glucobrassicin, thus producing the breakdown products indoles. At neutral pH, the hydrolysis of glucobrassicin by mirosinase leads to the formation of indole-3-methyl isothiocyanate, an unstable ITC intermediate, which rapidly degrades into a thiocyanate ion and into indole-3-carbinol (I3C) (Figure 4.2) [165]. Instead, if the hydrolysis of glucobrassicin by mirosinase occurs at acidic pH, indole-3-acetonitrile, hydrogen sulfide, and elemental sulfur are produced [165].

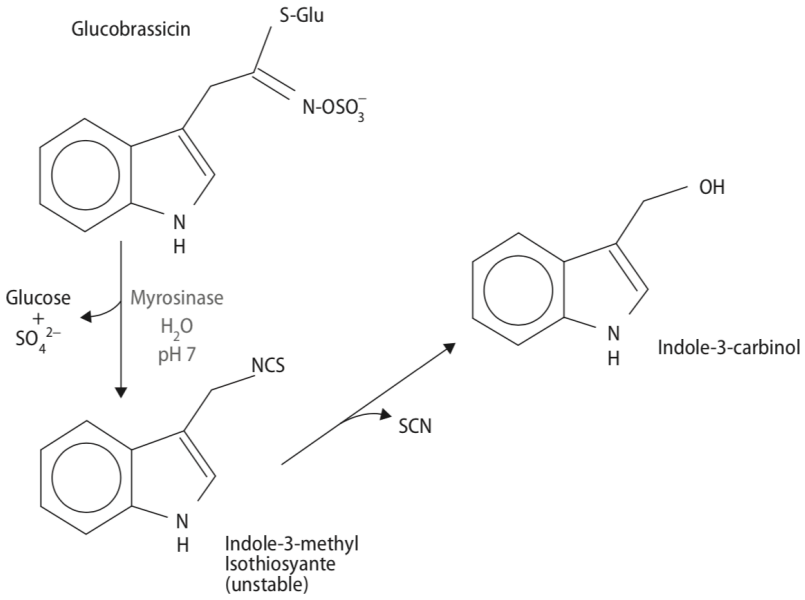

Figure 4.2 Biosynthesis of indole-3-carbinol from the hydrolysis of glucobrassicin by mirosinase [165]

When ingested, in particular when I3C is in stomach, which is characterized by an acidic pH, I3C condenses to form a variety of compounds, including 3,3'-diindolylmethane (DIM), and indolo (3,2-b) carbazole (Figure 3.3), both of which possess different pharmacological effects, including antitumor activity [165]. Moreover, I3C could also combine with ascorbic acid to generate ascorbigen (ASG) (Figure 4.3) [165].

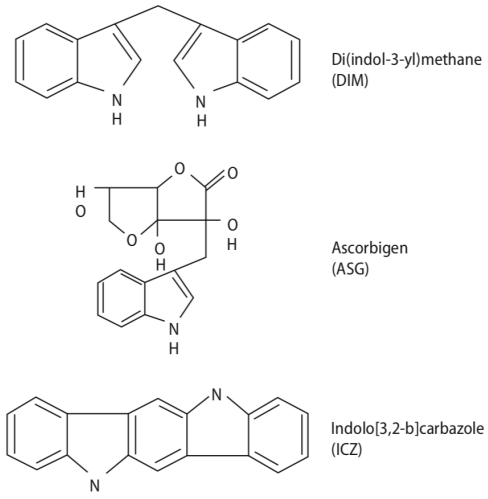

Figure 4.3 Chemical structure of 3,3'- diindolylmethane (DIM), ascorbigen (ASG), and indolo (3,2-b) carbazole, derived from I3C [165]

4.1.2 Anticancer potential of indoles I3C and DIM

The anticancer potential of I3C and its condensation product DIM has been reported in several studies. As for all the other natural compounds, the anticancer activity of indoles and their derivatives relies upon their ability to modulates many different steps involved in the carcinogenesis process. This ability is due to their intrinsic nature. Indeed, the intrinsic complex chemical composition of natural compounds makes them able to interact with multiple molecular targets and to modulate many different biological pathways involved in tumor development [245].

In addition to their ability to induce apoptotic cell death and the arrest of cell-cycle progression, I3C and DIM have been found to inhibit angiogenesis, to modulate estrogen and androgen receptors, to modulate the transcription of multiple transcription factor involved in carcinogenesis [*i.e.*, NF-kB, Nrf2, STAT3 (Signal transducer and activator of transcription 3)], and to possess immunomodulatory effects [238].

Antiproliferative and pro-apoptotic activity

The antiproliferative activity of I3C and DIM has been associated to their ability to induce apoptosis through multiple mechanisms, including downregulation of Bcl-2 and Bcl-xL, downregulation of CIAPs and XIAPs, upregulation of Bax, release of cytochrome c, caspases activation, and inhibition of NF-kB pathway [160,237]. In MCF-7 and MDA-MB-231 breast cancer cells, DIM induced apoptosis, as shown by phosphatidylserine externalization, chromatin condensation, and DNA fragmentation observed after DIM treatment [246].

Interestingly, I3C triggered apoptosis in breast cancer cells, but not in non-tumorigenic breast epithelial cells. In particular, in the tumorigenic counterpart, I3C increased Bax/Bcl-2 ratio, reduced Bcl-xL expression, and induced Bax translocation into mitochondria, leading to the loss of mitochondrial potential, the release of cytochrome c, and cell death [247]. The selective pro-apoptotic effect of I3C for cancer cells was also observed on MDA-MB-468 breast cancer cell line but not on the non-tumorigenic HBL100cell line [248].

Cytostatic activity

I3C and its condensation product DIM were able to inhibit cell-cycle progression in different cancer models. In human breast MCF-7cancer cells, I3C blocked cells in the G1 phase, through the inhibition of cyclin-dependent kinase (CDK) 2 and CDK6 [165]. In MCF-10A cells, containing wild-type p53, DIM prevented the CDK2-mediated transition from phase G1 to phase S of cell cycle through the activation of the ATM signaling pathway, the increase in p53 protein levels, and the induction of p21 expression [165]. In prostate cancer cells, I3C induced a G1 cell-cycle arrest upregulating $p21^{WAF1}$ and $p27^{Kip1}$ CDK

inhibitors in a p53-independent manner, together with the downregulation of both protein levels and activity of CDK6 and the inhibition of Rb protein hyperphosphorylation [165]. In ovarian cancer cells DIM induced a G2/M cell-cycle arrest activating the checkpoint kinase 2 (Chk2), which has been associated with DIM-induced DNA damage [249].

However, the observed cytostatic activity may in part be attributed to the condensed product DIM rather than I3C itself, since it has been reported that I3C rapidly and spontaneously condenses into DIM in culture conditions [250].

Inhibition of angiogenesis

Different *in vitro* and *in vivo* studies demonstrated that both I3C and DIM could modulate tumor progression through the inhibition of angiogenesis. A study conducted by Wu *et al* showed that I3C inhibits cell proliferation and angiogenesis in phorbol myristate acetate (PMA)-stimulated endothelial EA hy926 cells [251]. The inhibitory activity of I3C towards angiogenesis has been related to its ability to block vascular tube formation, which represents a key stage during the angiogenetic process [251]. Moreover, I3C decreased VEGF expression and matrix metalloproteinase-2 (MMP-2) and MMP-9 secretion [251]. Both VEGF and MMPs are *in vitro* angiogenesis markers. Indeed, deregulation of MMPs expression, which degrades different components present in the extracellular matrix (*i.e.,* collagens, fibronectin, glycoproteins, and others), contributes to invasion, metastasis formation, and angiogenesis [182]. VEGF, instead, after its release and binding to the VEGF receptor (VEGFR), triggers a cascade of signals responsible for new vessel formation[182].

Chang and colleagues demonstrated that also DIM inhibits angiogenesis, both *in vitro* and *in vivo*. In cultured human umbilical vein endothelial cells (HUVECs), together with cell proliferation inhibition, DIM decreased migration, invasion, and vessel tube formation [252]. Furthermore, DIM administration to female C57BL/6 mice strongly inhibited neovascularization [252]. Additionally, at the same dose able to block neovascularization, DIM inhibited tumor growth of MCF-7 xenografted female athymic (nu/nu) mice [252].

Chemosensitization of cancer cells

Resistance to chemotherapeutic drugs represents the major cause of chemotherapy failure. It is widely known that cancer cells could develop the ability of being insensitive to chemotherapeutic drugs. This phenomenon is called multiple drug resistance (MDR) [253]. The adenosine triphosphate-binding cassette (ABC) transporter superfamily is one of the membrane transporter proteins classes involved in the development of MDR in cancer cells [253]. Among all the 49 proteins belonging to ABC superfamily, P-glycoprotein (P-gp; MDR1/ABCB1), MDR-associated protein (MRP1; ABCC1), and breast cancer resistance protein (BCRP; ABCG2) are well known to be involved in MDR [253].

P-gp normally acts as a pump to remove chloride outside cells [253]. However, P-gp is also responsible for drugs extracellular transport through two hydrolyses of ATP, provoking a conformational change of P-gp, and the consequent release of drugs into the extracellular space [254]. Among chemotherapeutic drugs, P-pg could bind vinblastine, vincristine, doxorubicin, daunorubicin, actinomycin D, etoposide, and paclitaxel, thus contributing to the development of MDR against these anticancer drugs [254].
In this scenario, naturally occurring compounds able of targeting P-gp could represent a compelling strategy to overcome MDR. In vinblastine-resistant K-562 human chronic myeloid leukemia cells, I3C reduced P-gp protein expression and enhanced the sensitivity of tumor cells towards vinblastine cytotoxic activity [255,256]. In LNCap human prostate cancer cells, pre-treatment with I3C increased both mRNA and protein levels of TRAIL death receptor DR4 and DR5 and enhanced the pro-apoptotic activity of TRAIL [257].

4.2 Materials and methods

Cell cultures

Human T-lymphoblastic cells (Jurkat), human colorectal adenocarcinoma cells (DLD1), human breast adenocarcinoma cells (MCF-7), human neuroblastoma cells (SH-SY5Y) were provided from LGC (LGC Group, Middlesex, UK). Jurkat and DLD-1 cells were cultured in RPMI 1640 medium supplemented with 10% heat-inactivated bovine serum, 1% penicillin/streptomycin solution, and 1% l-glutamine solution (all obtained from Sigma Aldrich). MCF-7 were cultured in Eagle's Minimum Essential Medium (EMEM) supplemented with 10% heat-inactivated bovine serum, 1% penicillin/streptomycin solution, and 1% l-glutamine solution (all obtained from Sigma Aldrich). SH-SY5Y were cultured in Dulbecco's Modified Eagle Medium (DMEM) supplemented with 10% heat-inactivated bovine serum, 1% penicillin/streptomycin solution, and 1% l-glutamine solution (all obtained from Sigma).
Cells were maintained at 37°C and 5% CO_2 in a humidified atmosphere, without never exceeding the maximum cell density.

Chemicals and treatments

AD05 (Figure 4.4) was synthesized by Prof. Subhas S. Karki of KLE University (Belgaum, India).

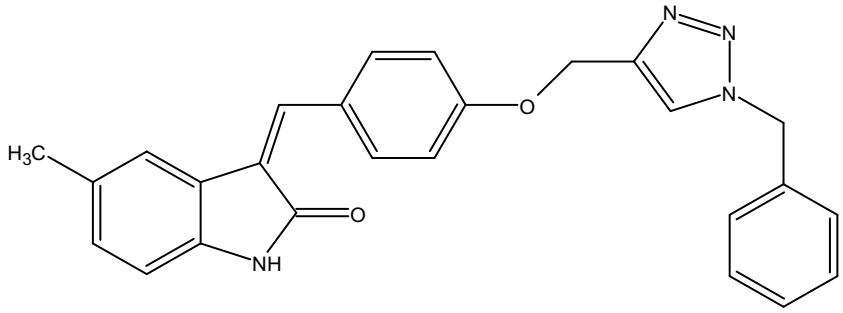

Figure 4.4 Chemical structure of AD05.

AD05 was dissolved in DMSO at the concentration of 37.035mM. 7-Cl-O-Nec-1 or necrostatin-1s (Nec-1s; Sigma Aldrich), ferrostatin-1 (Ferr-1; Sigma Aldrich), and olaparib (Ola; Selleckem, Houston, TX, USA) were dissolved in DMSO at the concentration of 200mM; N-benzyloxycarbonyl-Val-Ala-Asp (O-Me) fluoromethyl ketone (Z-VAD-FMK; BioVision, CA, USA) and deferoxamine mesylate (DFO, Across Organics, Thermofisher Scientific, MA, USA) were dissolved in DMSO at the concentration of 50mM; vitamin E (Vit E, Sigma Aldrich) was dissolved in ethanol at the concentration of 220mM.

Cells were treated with increasing concentration (0-64μM) of AD05 for 1, 3, 6, 24 or 48h depending on experimental conditions. Etoposide (10μg/mL) (Sigma Aldrich), camptothecin (2μM) (Sigma Aldrich), and H_2O_2 (0.5 and 1mM) (Sigma Aldrich) were used as positive controls.

To evaluate the induction of non-canonical cell death pathways, cells were pre-treated for 1h with different chemical inhibitors and then treated with AD05 8μM for 24 or 48h. For this purpose, the following blockers were used: the pan-caspase inhibitor Z-VAD-FMK, 75μM; the PARP-1/-2 inhibitor olaparib, 5μM; the RIP1 inhibitor II necrostatin-1s, 75μM; the inhibitor of ROS generation and lipid peroxidation ferrostatin-1, 1μM; the iron chelator deferoxamine mesylate, 10μM, and the peroxyl radical scavenger vitamin E, 100μM, in order to inhibit apoptosis, parthanatos, necroptosis and ferroptosis, respectively.

Analysis of cell viability

Determination of Jurkat cells viability was performed using Guava ViaCount Reagent (Merck Millipore, Burlington, MA, USA) according to manufacturer's instructions. Briefly, cells were diluted with the reagent containing 7-amino-actinomycin D (7-AAD) and after incubation at room temperature in the dark for 5 minutes cells were detected with flow cytometer.

A second dye (eosin B) exclusion test was used to analyse Jurkat cells viability. As 7-AAD, eosin B (Sigma Aldrich), due to its chemical-physical properties, remains excluded from live cells with intact membrane, hence penetrating, instead, in dead cells, whose membrane is damaged. Briefly, each sample was prepared by mixing the cell suspension with 0.2 % eosin solution, according to an appropriate dilution factor.

Determination of cell viability of DLD-1, MCF-7 and SH-SY5Y cells was performed using the 4-methylumbelliferyl heptanoate (MUH) assay [258]. The MUH assay is based on the production of the highly fluorescent 4-methylumbelliferone, which can be measured in a microplate fluorimeter, as result of MUH hydrolysis by intracellular esterases of viable cells [258]. Briefly, after treatment of 24h with AD05, cells were washed twice in PBS (Phosphate buffered saline) 1X; then, 100 μL of MUH 0.1 mg/mL was added to each well. After incubation of 30 minutes at 37°C in the dark, fluorescence of 4-methylumbelliferone was measured using the microplate reader Victor X3 (Perkin Elmer) equipped with 355 nm excitation and 460 nm emission filters.

Analysis of cell death mechanisms

To discriminate between apoptotic and necrotic events, Guava Nexin Reagent (Merck Millipore) was used. This reagent, containing 7-AAD and annexin V-phycoerythrin (PE) is able to discriminate apoptotic and necrotic events. After incubation of 20 minutes at room temperature in the dark cells were analysed by flow cytometry. Three cell populations can be detected: live cells (annexin− / 7-AAD−), early apoptotic cells (annexin+ / 7-AAD−), and late apoptotic or necrotic cells (annexin+ / 7-AAD+).

Evaluation of non-apoptotic cell death pathways was performed analysing cell viability with SYTOX™ Green Nucleic Acid Stain (Thermo Fisher Scientific), according to manufacturer's protocol. SYTOX™ Green Nucleic Acid Stain is a fluorescent dye that does not cross intact cell membranes but easily

penetrates compromised membranes of dead cells where it binds DNA, thus exhibiting an increase of its fluorescence. Briefly, after pre-treatment of 1h with the different chemical inhibitors and treatment of 24 and 48h with AD05, cells were supplemented with SYTOX™ Green Nucleic Acid Stain 10nM and after incubation of 20 minutes at room temperature in the dark, cells were analysed by flow cytometry.

Measurement of mitochondrial potential

Mitochondrial membrane potential was assessed using MitoProbeTM DilC1(5) Assay kit (Molecular Probes, Thermo Fisher Scientific), according to manufacturer' instructions. DilC1(5) (1,1,3,3',3',3'-hexamethylindo dicarbo-cyanine iodide) accumulates in mitochondria with active membrane potential, and the dye stain intensity decreases when cells are treated with agents that disrupt mitochondrial potential. Briefly, after 24h of treatment with AD05, 10^6 cells were washed and supplemented with 50nM DilC1(5) for 20 minutes at 37°C, 5% CO_2. Cells were then washed with PBS 1X and suspended again in PBS 1X for flow cytometric analysis. CCCP (carbonyl cyanide 3-chlorophenylhydrazone) 50µM was used as positive control. Results were expressed as % of cells with decreased mitochondrial potential compared to untreated cells.

Evaluation of caspase-8 and caspase-3 activity

Caspase activity was assessed using Caspase 8 Colorimetric Protease Assay Kit or Caspase 3 Colorimetric Protease Assay Kit, respectively (both purchased by Thermo Fisher Scientific), according to manufacturer's instructions. Briefly, after 24h treatment, cells were washed in PBS 1X and suspended in Cell Lysis Buffer on ice for 10 minutes. Cellular lysates were centrifuged, collected, and normalized in terms of protein concentration, according to Bradford assay [259]. Cellular lysates were then incubated for 2 h at 37°C in the dark with 2X Reaction Buffer, containing DTT 10mM and 200µM of caspase 8 or caspase 3 substrate. Both substrates consist of a synthetic tetrapeptide, IETD (Ile-Glu-Thr-Asp) specific for caspase-8, and DEVD (Asp-Glu-Val-Asp) specific for caspase-3, conjugated with the chromophore p-nitroanilide (pNA). In presence of caspases' activity, the specific substrate is cleaved from the chromophore and free pNA is used as a reporter, whose absorbance is measured at 405 nm, using the microplate reader Victor X3 (Perkin Elmer). Caspase activity was expressed as the fold increase of treated cells compared to untreated cells.

Measurement of ROS generation

Intracellular ROS generation was determined using the probe 2',7'-dichlorodihydrofluorescein diacetate (H_2DCFDA) (Sigma Aldrich). H_2DCFDA is a non-fluorescent and cell-permeable probe which diffuses in viable cells where it is hydrolyzed by intracellular esterases into 2',7'-dichlorodihydrofluorescein (H_2DCF). H_2DCF is in turn oxidized, in presence of ROS, into 2',7'-dichlorofluorescein (DCF), which is highly fluorescent. Briefly, 20 minutes before the different time end points (1, 3, or 6h of treatment with

AD05), 10 μM H_2DCFDA was added in each well, and cells were incubated for 20 minutes at 37 °C and 5% CO_2. After incubation, 1×10^6 cells were centrifuged, resuspended in PBS 1x and, finally, analysed by flow cytometry for oxidation of H_2DCF. Intracellular ROS levels were expressed as fold increase of treated cells compared to untreated cells.

Cell-cycle analysis

The percentages of cells in G0/G1, S, and G2/M phases were quantified by the analysis of DNA content using Guava Cell Cycle Reagent (Merck Millipore). After treatment with AD05 for 6 and 24h, cells were fixed with 70% ice-cold ethanol; after washing, cells were suspended in 200 μL Guava Cell Cycle Reagent, containing propidium iodide, and incubated 30 minutes at room temperature in the dark before analysis by flow cytometry.

Analysis of cyclin A, cyclin B1, and CDK1 expression

After treatment with AD05 for 24h, for each condition 1×10^6 cells were fixed by 70% cold ethanol and permeabilized using 0.25% cold Triton X-100 in Wash Buffer (WB; PBS 1X + 1% BSA). Samples were then washed and incubated with the corresponding primary antibody anti-cyclin A (1:50, Invitrogen, Thermo Fisher Scientific), anti-cyclin B1 (1:50, Invitrogen, Thermo Fisher Scientific), and anti-CDK1 (1:200, Invitrogen, Thermo Fisher Scientific) for 30 minutes. Next, cells were washed in WB and stained with the respective secondary antibody (anti-mouse 1:200; anti-rabbit 1:200; Invitrogen) for other 30 minutes. Cells were washed and then analysed by flow cytometry, recording the mean fluorescence intensity (MFI) values. Cyclin A, Cyclin B1, and CDK1 expressions were indicated as fold increase of treated cells compared to untreated cells.

Analysis of DNA damage

In order to assess the genotoxic potential of AD05, phosphorylation of histone γ-H2A.X was evaluated as marker of DNA double-strand breaks. In brief, after 5h treatment with increasing concentrations of AD05, cells were fixed, permeabilized, and incubated for 30 minutes in the dark at room temperature with an anti γ-H2A.X-Alexa Fluor® (Merck Millipore, Darmstadt, Germany). Etoposide 10μg/mL was used as positive control. Samples were analysed via flow cytometry.

Flow cytometry

All flow cytometric analyses were performed using an EasyCyte 5HT flow cytometer (Guava Technologies-Millipore, Hayward, CA, USA).

Statistical analysis

All experiments are expressed as the mean ± SEM of at least three independent experiments. IC_{50} (concentration of drug responsible for the inhibition of 50% of cell viability) value of drug against cellular

viability was determined by non-linear regression fitting curve using GraphPad InStat 6.0 version (GraphPad Prism, San Diego, CA, USA). Statistical analyses were performed by Repeated Measures ANOVA. Tukey or Dunnett or Bonferroni were used as a post-test, using the statistical software GraphPad InStat 6.0 version. *p*-values below 0.05 were considered as significant and represented as $* p < 0.05$, $** p < 0.01$, $*** p < 0.001$, and $**** p < 0.0001$.

4.3 Results

AD05 exhibits cytotoxic activity on Jurkat cells

First, to evaluate the potential anticancer activity of AD05, the cytotoxicity of AD05 was analysed on Jurkat cells. AD05 induced a dose-dependent decrease of cell viability following 24h (data not shown) and 48h treatment. After 48h of treatment, AD05 induced a dose-dependent decrease of cell viability starting from the concentration of 2μM (76.3% *versus* 89.6% of untreated cells). At 4μM cell viability was about 47.4%, reaching a 29% at 8 μM (Figure 4.5). Therefore, AD05 is a compound with a strong cytotoxic potential with a calculated IC_{50} of 3.75μM.

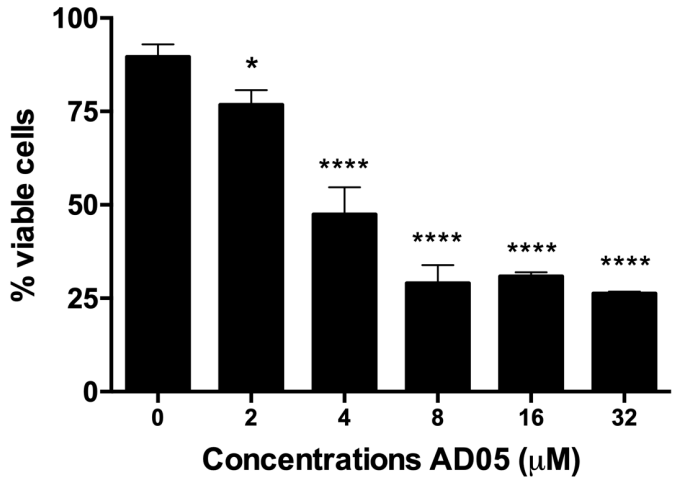

Figure 4.5 Percentage (%) of viable cells after 48h treatment of Jurkat cells with increasing concentrations of AD05. *p< 0.05; ****p< 0.0001 *versus* untreated cells.

Next, we tested AD05 on DLD1 human colorectal adenocarcinoma cells, MCF-7 human breast adenocarcinoma cells, and on SH-SY5Y human neuroblastoma cells in order to characterize the cytotoxic activity of AD05 on different solid tumors. However, on these cell lines cytotoxicity of AD05 was significantly lower than that induced on Jurkat cells (data not shown), which were therefore selected for further investigations.

AD05 exclusively induces caspase-dependent apoptosis in Jurkat cells and activates both intrinsic and extrinsic apoptotic pathways

In order to investigate the mechanism responsible for the cytotoxic effect of AD05, we used the annexin V/7-AAD assay. Phosphatidylserine (PS) exposure represents a crucial stage during the apoptotic process. The use of annexin V binding to PS plus 7-AAD allows detecting apoptotic cells (annexin V^+/7-AAD^- cells) and necrotic cells (annexin V^+/7-AAD^+ cells) due to its ability to permeate only cells with cell membrane damaged [260].

After 24h of treatment, AD05 led to a significant and dose-dependent increase in the fraction of apoptotic cells. The percentage of apoptotic cells started to increase from the concentration 2μM (14% *versus* 3.9% in untreated cells), and further increased up to the highest tested concentration, where they reached about 27%. Alongside the increase in apoptotic cells, an increment in the fraction of necrotic cells has not been observed, since the percentage of necrotic cells remained constant between 3% and 7% at all tested concentrations (Figure 4.6).

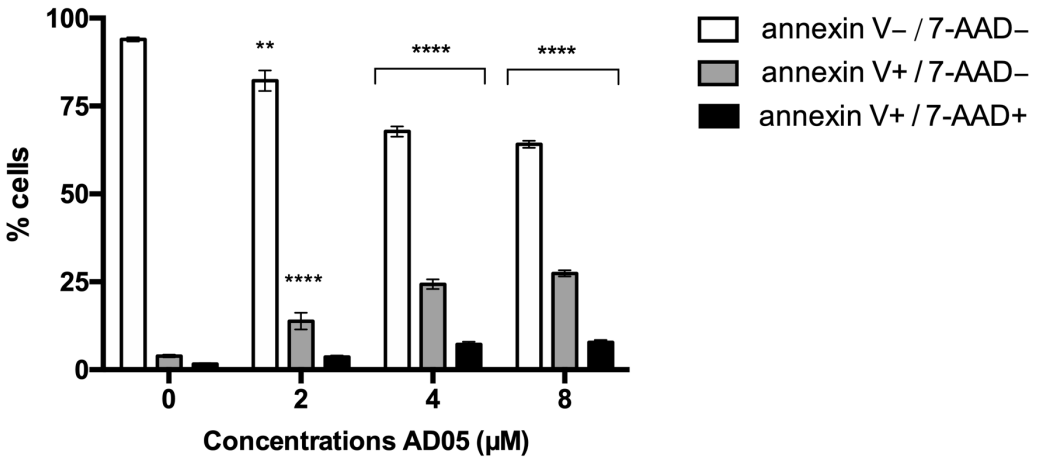

Figure 4.6 Percentage (%) of viable (annexin V^-/7-AAD^-), early apoptotic annexin (V^+/7-AAD^-), and late apoptotic or necrotic (annexin V^+/ 7-AAD^+) cells after 24h treatment of Jurkat cells with increasing concentrations of AD05. ** $p< 0.01$; **** $p< 0.0001$ *versus* untreated cells.

At this point, some of the molecular pathways modulated by AD05 have been explored. In particular, the activity of caspase-3 has been evaluated. Caspase-3 is an effector caspase activated from both the intrinsic and extrinsic apoptotic pathway [5]. Its activity was markedly increased after treatment with AD05, up to about 8 times at the concentrations of 4 and 8μM (Figure 4.7), confirming apoptosis induction by the indole derivative.

Next, to investigate the involvement of the extrinsic apoptotic pathway in the pro-apoptotic activity of AD05, we analysed the activity of caspase-8. Its activity increased up to about 4 times at the concentrations of 4 and 8μM after AD05 treatment (Figure 4.7).

To assess the involvement of the intrinsic apoptotic pathway, we measured the decrease in mitochondrial transmembrane potential. A significant increase in cells with reduced potential was recorded starting from the concentration of 4μM (35% of cells with decreased potential *versus* 7.4% in untreated cells) and the percentage further increased at about 46% at 8μM (Figure 4.7).

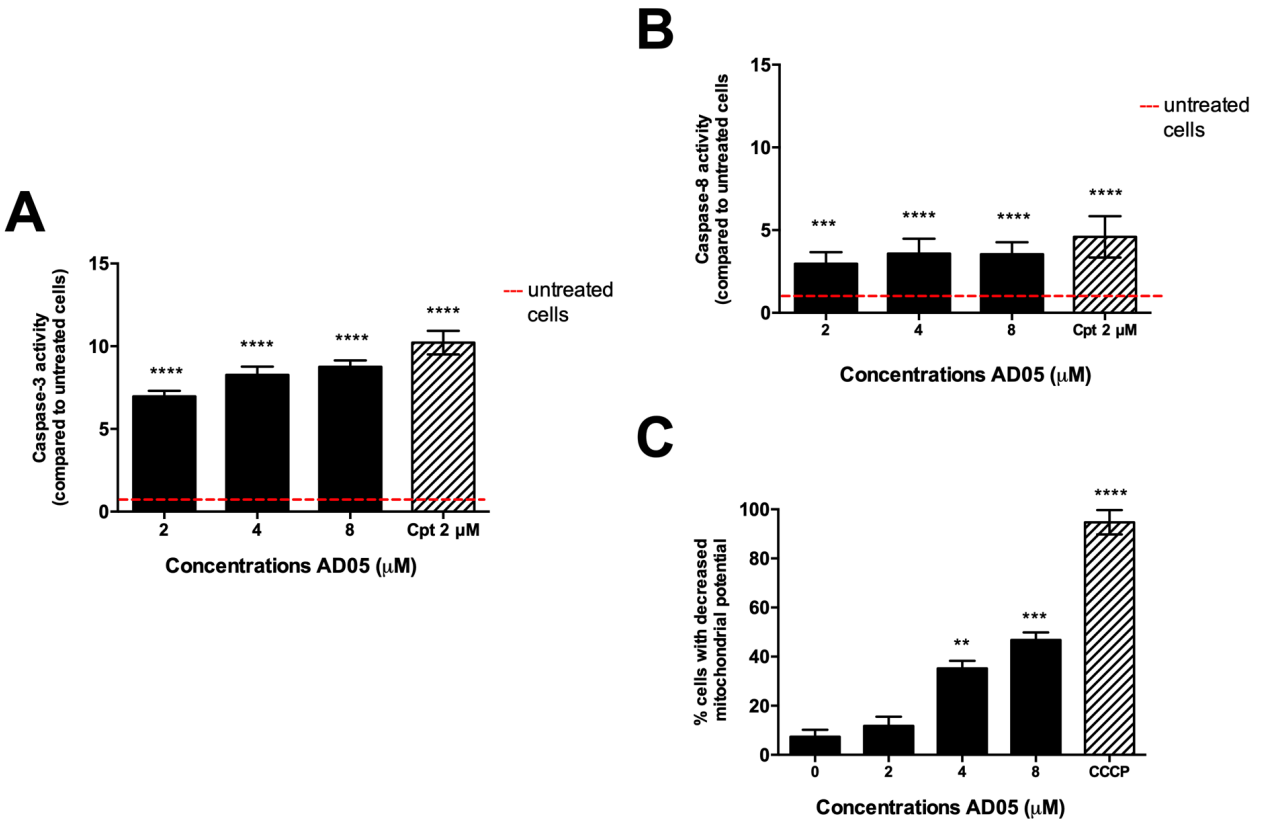

Figure 4.7 Activity of caspase-3 (A) and caspase-8 (B) and percentage (%) of cells with decreased mitochondrial potential (C) after 24h of treatment of Jurkat cells with increasing concentrations of AD05. Cpt (camptothecin) 2μM and CCCP (carbonyl cyanide 3-chlorophenylhydrazone) 50μM were used as positive controls. ***p*< 0.01; ****p*< 0.001; *****p*< 0.0001 *versus* untreated cells.

On the whole, our results indicate that AD05 is able of activating both apoptotic pathways.

To determine whether AD05 could activate non-canonical cell death programs, Jurkat cells were pre-treated for 1h with different chemical inhibitor (*i.e.,* Z-VAD-FMK, olaparib, necrostatin-1s, ferrostatin-1, DFO, and vitamin E) in order to inhibit apoptosis, parthanatos, necroptosis and ferroptosis, respectively. Then, after pre-treatment, cells were treated with AD05 8μM for 24h and 48h and cell viability was analysed by flow cytometry.

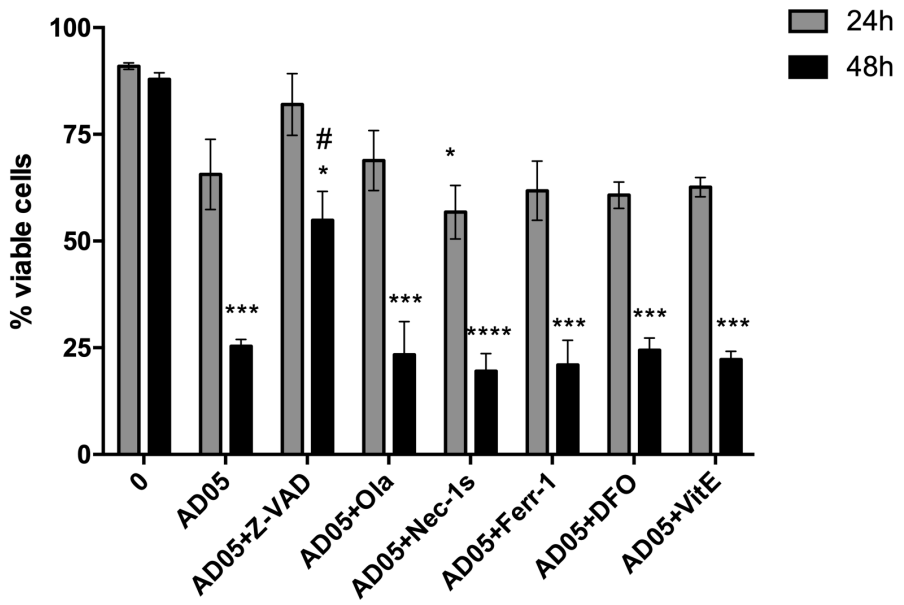

Figure 4.8 Percentage (%) of viable cells after pre-treatment for 1h with Z-VAD-FMK (Z-VAD), olaparib (Ola), necrostatin-1s (Nec-1s), ferrostatin-1 (Ferr-1), deferoxamine mesylate (DFO), or vitamin E (VitE) following 24h and 48h treatment with AD05 8μM. *p< 0.05; ***p< 0.001; ****p< 0.0001 *versus* untreated cells. # p< 0.05 *versus* AD05-treated cells.

Among all the pharmacological inhibitor, only the pan-caspases inhibitor Z-VAD-FMK increased Jurkat cells viability, just partially after 24h and significantly only after 48h (Figure 4.8). Recorded cell viability of Z-VAD-FMK pre-treated cells was 82% at 24h (*versus* 65% of AD05-treated cells) and 55% at 48h (*versus* 25% of AD05-treated cells). Our results indicate that AD05 does not induce non-canonical cell deaths as ferroptosis, necroptosis or parthanatos, but exclusively caspase-dependent apoptosis.

ROS are not involved in AD05 pro-apoptotic activity

ROS play a central role in cell signaling and represent one of many stimuli that leads to apoptotic cell death [5]. We measured intracellular ROS levels after different treatment times with AD05. AD05 did not induce any significant modulation of ROS levels (Figure 4.9). Hence, it seems that ROS generation is not involved in the orchestration of the cytotoxic response evoked by AD05. However, it is not possible to exclude the involvement of other radical species, such as the superoxide anion, which are not detectable through the probe used in this analysis.

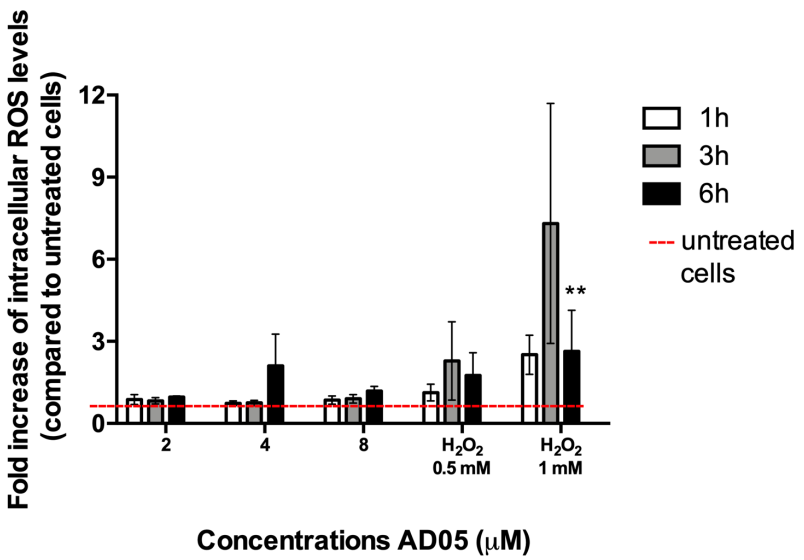

Figure 4.9 Intracellular ROS levels, expressed as fold increase *versus* untreated cells, of Jurkat cells treated with increasing concentrations of AD05 for different time points. H_2O_2 (0.5 and 1mM) was used as positive control. $^{**}p < 0.01$ *versus* untreated cells.

AD05 causes cell-cycle perturbations

In the following experiments, we demonstrated a cytostatic effect for AD05. The treatment with increasing concentrations of AD05 induced a significant accumulation of cells in the G2/M phase. Starting from the concentration of 4μM the accumulation of cells in the G2/M phase appeared to be statistically significant, with 57% *versus* 31% of untreated cells; at the highest tested concentration, the percentage further increased up to 64%. This observed increase was accompanied, at all tested concentrations, by a slight compensatory decrease in the G0/G1 phase, from 59% of untreated cells to 23% of cells treated with AD05 8μM (Figure 4.10).

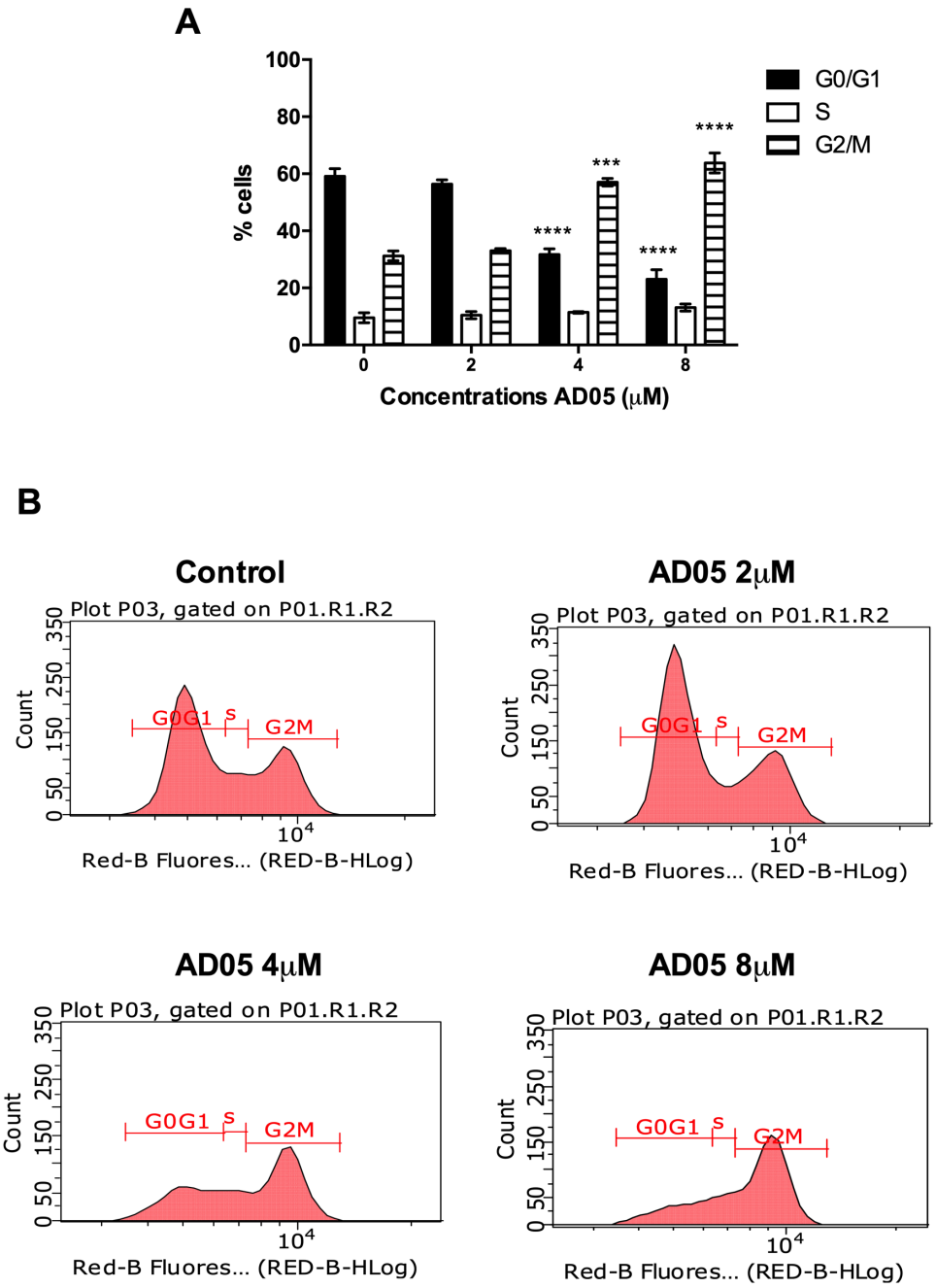

Figure 4.10 Histograms (A) and cytograms (B) of cell-cycle distribution after Jurkat cells treatment with AD05 for 24h. ***p< 0.001; ****p< 0.0001 *versus* untreated cells.

Cell cycle is tightly controlled by two classes of proteins, namely cyclin-dependent kinases (CDK) and cyclins. Cyclin A is synthesized starting from the S phase of cell cycle and reaches its maximal expression in the G2 phase until its degradation during the transition from G2 to M phase of cell cycle. Cyclin B, instead, starts to be expressed from the G2 phase and extensively accumulates prior to mitosis. Finally, CDK1 could be activated by both interphase cyclins (*i.e.,* cyclins D, E, and A) and mitotic cyclin B [261]. Hence, to determine whether AD05-treated cells accumulate in G2 or M phase, the expression of cyclin A and B1, and CDK1 was analysed. After 24h of treatment, AD05 did not modulate the expression of

cyclin B1 and CDK1; however, a slight downregulation of cyclin A was observed (Figure 4.11), meaning that probably AD05 leads to cells accumulation in the late G2 phase, just prior the entry into mitosis.

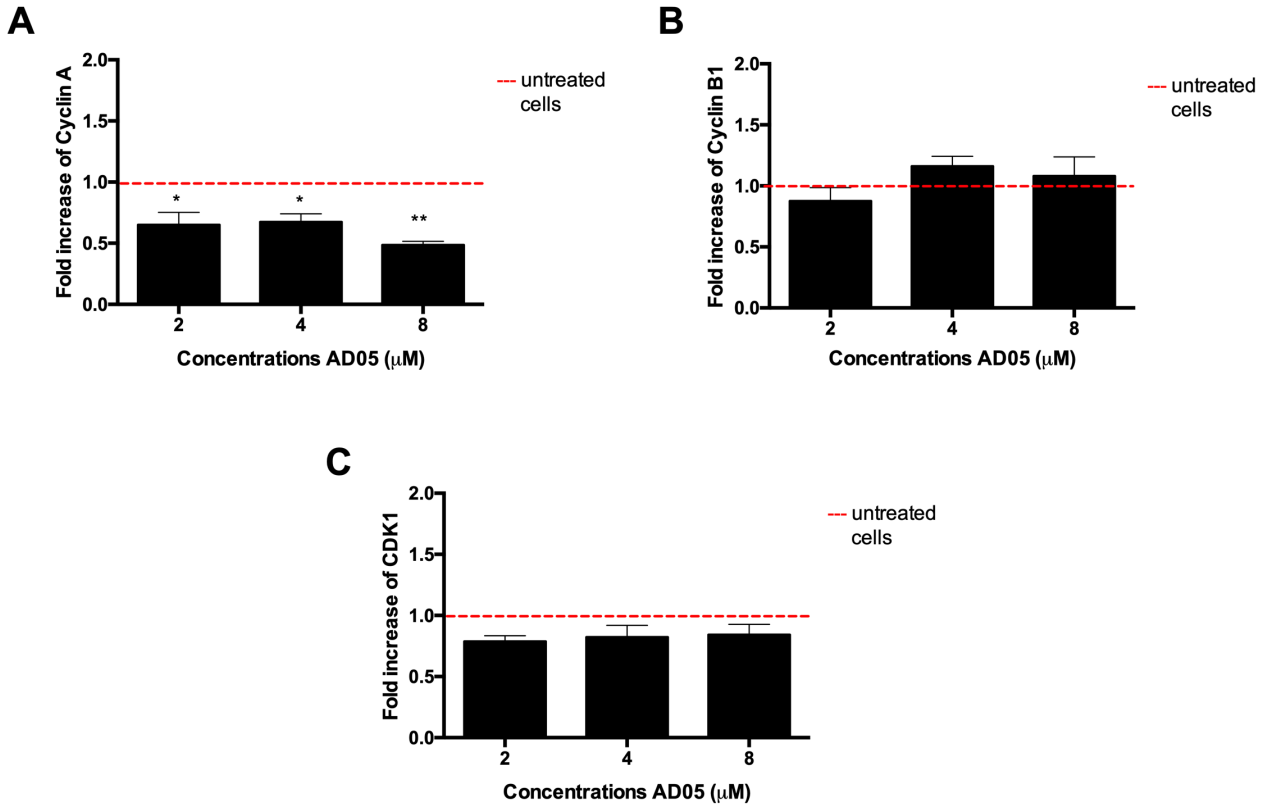

Figure 4.11 Expression of cyclin A (A), cyclin B1 (B), and CDK1 (C), indicated as fold increase *versus* untreated cells, following 24h treatment of Jurkat cells with increasing concentration of AD05. *p< 0.05; **p< 0.01 *versus* untreated cells.

The pro-apoptotic activity of AD05 is linked to its cytostatic activity

Next, the pro-apoptotic and cytostatic activity of AD05 were analysed after 6h of treatment with AD05 to assess whether the two events were related or independent from each other. Since AD05 did not induce cell death, while a substantial block of cell cycle was already evident at 6h of treatment (Figure 4.12), it has been hypothesized that AD05-induced apoptosis could be a secondary effect, related to its cytostatic activity rather than an independent event.

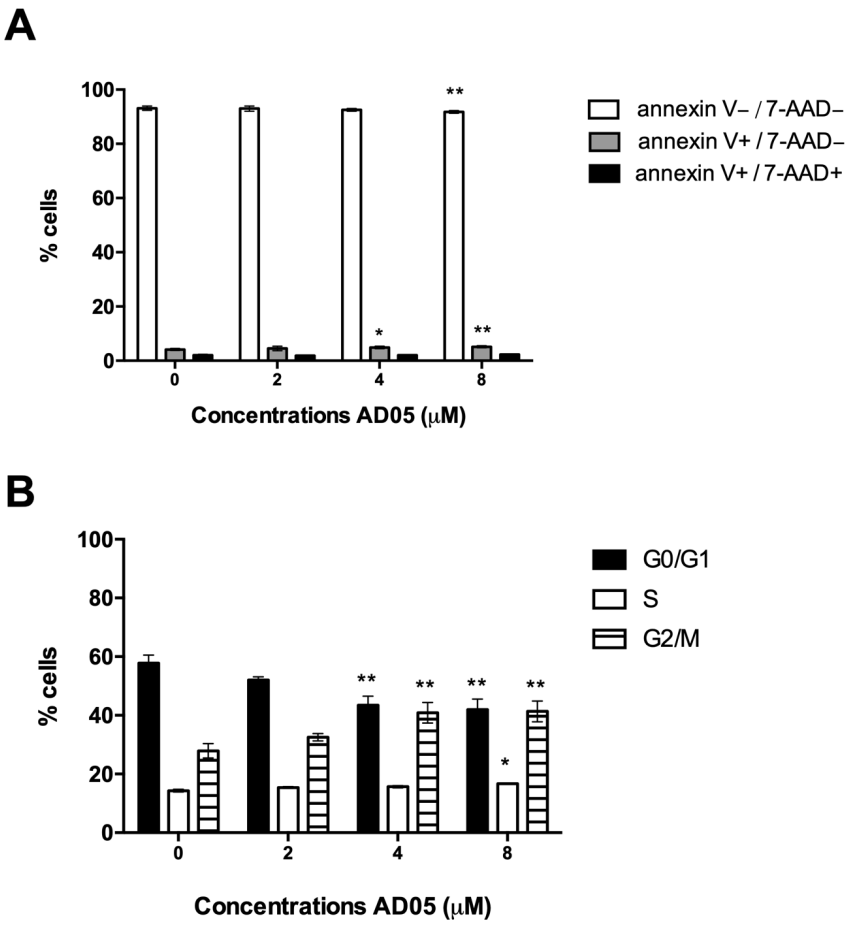

Figure 4.12 Percentage (%) of viable (annexin V$^-$/7-AAD$^-$), early apoptotic annexin (V$^+$/7-AAD$^-$), and late apoptotic or necrotic (annexin V$^+$/7-AAD$^+$) cells (A) and cell-cycle distribution (B) following 6h treatment of Jurkat cells with increasing concentrations of AD05. *p< 0-05; **p< 0.01 *versus* untreated cells.

AD05 is not genotoxic

Given the interesting anticancer activity showed by AD05, a preliminary assessment of its toxicological profile was performed by analysing its genotoxicity through the phosphorylation of H2A.X (P-H2A.X) at Serine 139. P-H2A.X is considered an early cellular response to DNA double-strand breaks. Therefore, the analysis of this event is useful to detect the ability of a compound to induce DNA damage [262]. Following 5h treatment of Jurkat cells with AD05, no significant increase in H2A.X phosphorylation was observed at any tested concentration (Figure 4.13), thus excluding any genotoxic activity of AD05.

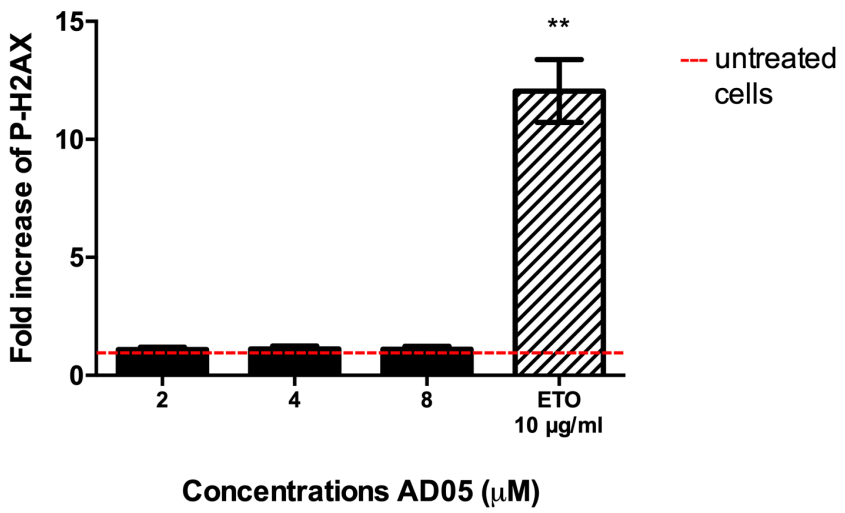

Figure 4.13 Relative expression of P-H2AX following 5h treatment of Jurkat cells with increasing concentrations of AD05. Etoposide (ETO) 10µg/mL was used as positive control. $^{**}p < 0.01$ *versus* untreated cells.

4.3 Discussion

Indoles are natural compounds broadly found in nature, in both terrestrial and marine ecosystems. Indole compounds are produced as secondary metabolites by plants, bacteria, fungi and marine organisms, where they act as signalling molecules [160]. Besides their role as protective secondary metabolites, indoles are involved in cell physiology and, as intermediary, in many different biological reactions. Moreover, indoles possess several biological effects, including a marked antitumor activity against diverse cancer diseases [160,241,263]. Among all the natural sources of indoles, a huge number of indoles and indole derivatives were isolated by aquatic organisms and many of them showed interesting chemopreventive and chemotherapeutic properties towards different cancer types [160,241]. Among all marine organisms, sponges, belonging to the *phylum Porifera*, represent a rich source of bioactive compounds. This fact should come as no surprise: sponges, in fact, are sessile invertebrates, do not have an innate immune system or defence structures and, therefore, they could preserve themselves only by producing secondary metabolites [264]. In addition, the enormous biodiversity of sponges results in a chemical variety of the molecules produced: so far have been discovered, as active compounds, nucleosides, sterols, alkaloids, peroxides, terpenes, fatty acids, amino acid derivatives and cyclic peptides [264]. Sponges, therefore, are an important source of secondary metabolites, many of which have shown interesting chemopreventive and chemotherapeutic properties towards cancer [160]. Among the various metabolites produced by sponges there are also several indole derivatives.

A critical point in the discovery of new active compounds by marine organisms, as sponges, algae and corals, is certainly the supply of raw materials, which requires specific equipment, properly trained staff and, moreover, is an extremely expensive process. Additionally, another limitation in the process of drug development from aquatic species is the sustained existence of sufficient amount of organisms and substances without damaging the marine ecosystem [264]. Hence, these supply problems are solved more and more often by recurring to process of marine biotechnology or to chemical synthesis/semi-synthesis/modification [264]. For all these reasons, in the second part of my PhD project we investigated the potential induction of non-canonical cell death by AD05, a newly synthesized indole derivative. We found that AD05 induces exclusively caspase-dependent apoptosis in lymphoblastic Jurkat cells; moreover, we hypothesized that its pro-apoptotic activity was mainly due to its ability to inhibit cell proliferation.

AD05 significantly increased the percentage of apoptotic cells after 24h of treatment. In order to investigate the potential mechanism involved in AD05-induced cell death, we found that AD05 activates both the intrinsic and extrinsic apoptotic pathway, as indicated by the significant increase in the caspase-8 activity, a marker of the extrinsic apoptotic pathway, and in the percentage of cells with reduced mitochondrial potential, a marker of the intrinsic pathway. Lastly, also the activity of caspase-3 was

enhanced by AD05, thus confirming its pro-apoptotic activity. The importance of the activation of both apoptotic pathways by AD05 is given by the fact that cancer cells are characterized by high genetic and genomic instability, which can lead to the mutation of some of the molecular actors involved in a specific apoptotic pathway. The result is the development of drug resistance and the lack of efficacy of anticancer therapy [16]. Just to give some examples, overexpression of Bcl-2 and associated anti-apoptotic proteins, impairment of the assembly of a functional apoptosome, inactivation of caspase-8, decreased expression of CD95 or mutations in the CD95 gene [16,17] are just some of the mechanisms involved in apoptosis resistance. As a result, the evidence that AD05 is able to modulate both apoptotic pathways could potentially increase its clinical potential.

The pro-apoptotic activity of AD05 is in line with the results reported in the scientific literature. Indeed, a huge plethora of marine indole derivatives exhibit their anticancer activity through the induction of apoptosis [160]. For example, the marine bis-indole alkaloid 2,2-bis(6-bromo-3-indolyl) ethylamine (BrBIn), isolated from the Californian tunicate *Didemnum candidumand* and the New Caledonian sponge *Orina*, induced caspase-dependent apoptosis in human myelomonocytic lymphoma U-937 cell line, as suggested by caspase-3/-8/-9 cleavage, PARP-1 cleavage, and increased Bax/Bcl2 *ratio* [265].

As mentioned before, the unique mechanism of cell death triggered by AD05 was caspase-dependent apoptosis. Indeed, among all the tested pharmacological inhibitor of apoptosis (*i.e.,* Z-VAD-FMK), parthanatos (*i.e.,* olaparib), necroptosis (*i.e.,* necrostatin-1s), and ferroptosis (*i.e.,* ferrostatin-1, deferoxamine mesylate, and vitamin E), only Z-VAD-FMK increased cell viability of AD05-treated cells, hence confirming the occurrence of only apoptosis in cancer cells after AD05 treatment. Regarding the ability of indoles and indole derivatives, no evidence has been found about their ability to trigger non-canonical cell death. A study conducted by Behnisch-Cornwell and colleagues, for example, investigated ferroptosis induction in human cervical cancer SISO cells by a series of newly synthesized indole-based pentathiepins, heterocyclic compounds found in different ascidians belonging to the genus *Lissoclinum*, establishing that these new derivatives induce apoptosis rather than ferroptosis [266].

Cell cycle is a sequence of closely coordinated molecular processes that control DNA replication and chromosome division, ultimately leading to cell division and transfer of genetic material. Cell cycle resides into four distinct phases: G1 (gap), S (synthesis), G2 (gap) and M (mitosis), all strictly controlled by cyclins and CDKs [261]. Briefly, in the G1 phase, activation of cyclin D-CDK4/6 complex leads to the phosphorylation of RB1 protein, thus promoting the expression of different genes that regulate cell-cycle progression. Then, when cells progress into the S phase, cyclin A replaces cyclin D and, thanks to its association with CDK2, DNA replication starts; during the end of the S phase, the cyclin A-CDK1 complex together with the cyclin A-CDK2 complex promotes the transition into the mitotic phase. Cyclin A reaches its maximal expression in the G2 phase, and then it starts to be degraded when cells

start the mitosis. During the mitosis cyclin B accumulates, resulting in cyclin B-CDK1 complex activation and mitosis progression [261]. Since the G1/S and G2/M checkpoints finely control cell proliferation, cell-cycle arrest is considered one of the most common events triggering the inhibition of cell proliferation. Hence, to explore the cytostatic potential of AD05 we analysed cell-cycle progression of AD05-treated cells together with the expression of cyclins and CDKs. AD05 induced a significant and dose-dependent accumulation of cells in the G2/M phase, accompanied by a slight compensatory decrease in the G0/G1 phase. We then analysed the expression of cyclin A, cyclin B1, and CDK1, which regulate the progression of G2/M phase of the cell cycle: no modulation of neither cyclin B1 nor CDK1 expression by AD05 has been observed. AD05 caused only a slight downregulation of cyclin A expression. As we noticed a decrease in cyclin A expression, but not a modulation of cyclin B and CDK1, we could speculate that AD05 may block cell-cycle progression during the transition from the G2 to the M phase, where cyclin A starts to be degraded prior to the entry of cells in mitosis. Moreover, this hypothesis could explain why we did not observe any modulation of cyclin B1 and CDK1 expression.

The pro-apoptotic and cytostatic activity of AD05 was also explored after 6h of treatment to assess whether the two events were related or independent from each other. At 6h of treatment, AD05 did not induce apoptosis, while it was already evident a substantial block of the cell cycle. This means that AD05-induced apoptosis could be linked to its cytostatic activity rather to be an independent event.

To conclude, in order to preliminarily assess the toxicological profile of AD05, we analysed the phosphorylation of H2A.X, a sensitive molecular marker of DNA damage occurrence [262]. Following treatment of Jurkat cells with AD05 (2, 4 and 8 μM), we did not observe an increase in P-H2A.X. This suggests, at least for now, that AD05 possesses a favourable toxicological profile. On the contrary, other indole derivatives, as an indole hydrazide [267] and two bis-indolinone derivatives [268], induced DNA damage in breast adenocarcinoma cells (MCF-7) and in human transformed fibroblasts (BJ-EHLT), respectively, as shown by a significant increase in H2A.X phosphorylation [267,268]. In particular, the two bis-indolinone derivatives were tested as human telomeric G-quadruplexes (G4) ligands thanks to their similarity to other known G4 ligands [268]. These compounds, stabilizing the G-quadruplexes, lead to DNA damage and consequently to apoptotic cell death [268]. Therefore, the finding that they promoted H2A.X phosphorylation should not be surprising.

Overall, the reason for these discrepant data could be due to two main factors. First, the longer treatment times used to test the two bis-indolinone derivatives (0.5-5μM for 24h) as well as the indole hydrazide (3.01μM for 48h) compared to that used for AD05 (2-8μM for 5h). Second, since these indole derivatives are all structurally different, the distinct substituents present on the indole ring could influence their ability to bind and damage DNA.

Conclusions

On the whole, our results indicate that, on our experimental models, only sulforaphane triggers non-canonical cell death, while the two isothiocyanate derivates MG28 and MG46 and the indole derivative AD05 induce caspase-dependent apoptotic cell death. Anyway, even if they were not able to trigger non-canonical cell death, they exhibited a strong anticancer potential.

MG28 and MG46 induced a striking cytotoxic activity compared to their parental compound sulforaphane. In addition, particular attention must be paid to the fact that the cells that most markedly succumbed to MG28 and MG46 cytotoxicity were MV4-11 AML cells, known to bear FLT3-ITD mutated form, wherein apoptosis onset occurred very rapidly. These observations suggest that the two isothiocyanate derivatives could be effective to treat AML forms bearing FLT3-ITD mutations, which are extremely common, and most importantly are related to a worst prognosis [202]. To date, different FLT3 inhibitors are under investigation as effective anticancer drugs to treat patients with FLT3-mutated AML. First generation FLT3 inhibitor midostaurin, for example, has been approved by FDA in 2017 for the treatment of adult patients with newly diagnosed FLT3-mutated AML, in combination with standard chemotherapy. Indeed, if used alone, midostaurin had limited and transient antileukemic activity [202]. In addition, the use of both first and next generation of FLT3 inhibitors is severely limited by the appearance of primary and secondary acquired resistance, which represents the rationale behind the numerous studies that are investigating the efficacy of the association of combined treatment regimens with FLT3 inhibitor plus approved antileukemic therapies or investigational agents [202].

Hence, taking into account the higher sensitivity exhibited by FLT3-mutated cells towards MG28 and MG46, it could be supposed, albeit prematurely, that after obviously further investigations these two isothiocyanate derivates could be useful in combination treatment with FLT3 inhibitors. In particular, further studies should demonstrate that the higher sensitivity of MV4-11 cells could be attributed without any doubt to their specific genetic pattern.

Shifting the focus on the indole derivative AD05, this compound showed to be highly cytotoxic on the tested leukemia cell line, being able to block cell cycle and consequently to induce caspase-dependent apoptotic cell death. In particular, it is important to emphasize that AD05 was able to activate both the intrinsic and the extrinsic apoptotic pathway. Bearing in mind that resistance to pro-apoptotic drugs is related to mutations of the different molecular actors participating in the orchestration of the apoptotic process, AD05 could be considered, thanks to its pleiotropic activity, as a promising anticancer agent for which surely it is worth conducting further investigations to disentangle its anticancer effects.

Lastly, moving to sulforaphane, it was the only compound among those investigated that was able to induce non-canonical cell death together with apoptosis in a dose-dependent manner. This should come as no surprise. Indeed, many natural compounds induce non-canonical death, as reported in Table 2 and

Table 3, but very few of them selectively activate non-canonical cell programs demise. All PCDs modalities, thus including apoptosis, necroptosis, and ferroptosis, are strictly connected in both molecular and functional terms. Focusing on necroptosis, for example, this cell death process occurs when the apoptotic cell death is impaired by caspase-8 inhibition [5], and is strictly related to the expression of its molecular mediators, which are cancer-type-dependent [76]. Even ferroptosis occurs in a cancer type-dependent manner. Indeed, the analysis of sensitivity of a panel of 860 cancer cells towards four ferroptosis inducers (erastin, RSL3, ML210 and ML162) indicates that cancer cell lines derived by non-epithelial tissues were more sensitive to ferroptosis inducers compared to those of epithelial origin [269]. Hence, all these pieces of evidence may lead us to think that there is a coexistence of all these cell death pathways, imaging them as many musicians who take part of the same orchestra, and who could start to play as "reserves", being conducted by two notably selective orchestra directors: cancer type and cancer cells mutations.

Since non-canonical cell death mechanisms were discovered quite recently, further investigations are needed to better characterize the molecular pathways behind these cell demise programs, and to deeper disentangle the existing crosstalk among them. New findings, indeed, could be surely useful to establish the role of natural compounds as non-canonical cell death inducers.

Concluding, from a toxicological point of view, the three new semi-synthetic derivatives exhibited a different nature. If AD05 lacked any genotoxic activity, MG28 and MG46 were found to be mutagenic. Since multiple anticancer drugs exert their activity by interacting and damaging DNA, the mutagenicity of the two newly ITC derivatives does not necessarily imply that they cannot be used as anticancer drugs, but that a deeper investigation of their toxicological profiles is indispensable to ensure a favourable risk/benefit assessment.

References

1 WHO | World Health Organization. . [Online]. Available: https://www.who.int/. [Accessed: 01-Dec-2020]

2 Oliveira, P.A. *et al.* (2007) Chemical carcinogenesis. *An. Acad. Bras. Cienc.* 79, 593–616

3 Hanahan, D. and Weinberg, R.A. (2000) The hallmarks of cancer. *Cell* 100, 57–70

4 Hanahan, D. and Weinberg, R.A. (2011) Hallmarks of cancer:the next generation. *Cell* 144, 646–674

5 Galluzzi, L. *et al.* (2018) Molecular mechanisms of cell death: recommendations of the Nomenclature Committee on Cell Death 2018. *Cell Death Differ.* 25, 486–541

6 Park, S.-Y. and Kim, I.-S. (2017) Engulfment signals and the phagocytic machinery for apoptotic cell clearance. *Exp. Mol. Med.* 49, e331

7 Gardai, S.J. *et al.* (2006) Recognition ligands on apoptotic cells: a perspective. *J. Leukoc. Biol.* 79, 896–903

8 Krysko, D.V. *et al.* (2012) Immunogenic cell death and DAMPs in cancer therapy. *Nat. Rev. Cancer* 12, 860–875

9 Obeid, M. *et al.* (2007) Calreticulin exposure dictates the immunogenicity of cancer cell death. *Nat. Med.* 13, 54–61

10 Pop, C. and Salvesen, G.S. (2009) Human caspases: activation, specificity, and regulation. *J. Biol. Chem.* 284, 21777–21781

11 Guicciardi, M.E. and Gores, G.J. (2009) Life and death by death receptors. *FASEB J.* 23, 1625–1637

12 Shamas-Din, A. *et al.* (2013) Mechanisms of action of Bcl-2 family proteins. *Cold Spring Harb. Perspect. Biol.* 5, a008714–a008714

13 D'Arcy, M.S. (2019) Cell death: a review of the major forms of apoptosis, necrosis and autophagy. *Cell Biol. Int.* 43, 582–592

14 Kitazumi, I. and Tsukahara, M. (2011) Regulation of DNA fragmentation: the role of caspases and phosphorylation: phosphorylation and caspases in DNA fragmentation. *FEBS J.* 278, 427–441

15 D'Amours, D. *et al.* (2001) Gain-of-function of poly(ADP-ribose) polymerase-1 upon cleavage by apoptotic proteases: implications for apoptosis. *J. Cell Sci.* 114, 3771–3778

16 Mohammad, R.M. *et al.* (2015) Broad targeting of resistance to apoptosis in cancer. *Semin. Cancer Biol.* 35 Suppl, S78–S103

17 Fulda, S. (2009) Tumor resistance to apoptosis. *Int. J. Cancer* 124, 511–515

18 Jung, J. *et al.* (2014) Interaction of translationally controlled tumor protein with Apaf-1 is involved in the development of chemoresistance in HeLa cells. *BMC Cancer* 14, 165

19 Budhidarmo, R. and Day, C.L. (2015) IAPs: modular regulators of cell signalling. *Semin. Cell Dev. Biol.* 39, 80–90

20 Pan, S.-T. *et al.* (2016) Molecular mechanisms for tumour resistance to chemotherapy. *Clin. Exp. Pharmacol. Physiol.* 43, 723–737

21 Guaman-Ortiz, L. *et al.* (2017) Natural compounds as modulators of non-apoptotic cell death in cancer cells. *Curr. Genomics* 18, 132–155

22 Dixon, S.J. *et al.* (2012) Ferroptosis: an iron-dependent form of nonapoptotic cell death. *Cell* 149, 1060–1072

23 Li, J. *et al.* (2020) Ferroptosis: past, present and future. *Cell Death Dis.* 11, 88

24 Yang, W.S. and Stockwell, B.R. (2008) Synthetic lethal screening identifies compounds activating iron-dependent, nonapoptotic cell death in oncogenic-RAS-harboring cancer cells. *Chem. Biol.* 15, 234–245

25 Friedmann Angeli, J.P. *et al.* (2014) Inactivation of the ferroptosis regulator Gpx4 triggers acute renal failure in mice. *Nat. Cell Biol.* 16, 1180–1191

26 Linkermann, A. *et al.* (2014) Synchronized renal tubular cell death involves ferroptosis. *Proc. Natl. Acad. Sci.* 111, 16836–16841

27 Alim, I. *et al.* (2019) Selenium drives a transcriptional adaptive program to block ferroptosis and treat stroke. *Cell* 177, 1262-1279.e25

28 Yu, H. *et al.* (2017) Ferroptosis, a new form of cell death, and its relationships with tumourous diseases. *J. Cell. Mol. Med.* 21, 648–657

29 Stockwell, B.R. *et al.* (2017) Ferroptosis: a regulated cell death nexus linking metabolism, redox biology, and disease. *Cell* 171, 273–285

30 Shen, Z. *et al.* (2018) Emerging strategies of cancer therapy based on ferroptosis. *Adv. Mater.* 30, 1704007

31 Nagpal, A. *et al.* (2019) Neoadjuvant neratinib promotes ferroptosis and inhibits brain metastasis in a novel syngeneic model of spontaneous HER2+ve breast cancer metastasis. *Breast Cancer Res.* 21, 94

32 Greco, G. *et al.* (2021) Natural products as inducers of non-canonical cell death: a weapon against cancer. *Cancers* 13, 304

33 Bridges, R.J. *et al.* (2012) System xc-cystine/glutamate antiporter: an update on molecular pharmacology and roles within the CNS: System xc-cystine/glutamate antiporter. *Br. J. Pharmacol.* 165, 20–34

34 Hassannia, B. *et al.* (2019) Targeting ferroptosis to iron out cancer. *Cancer Cell* 35, 830–849

35 Feng, H. and Stockwell, B.R. (2018) Unsolved mysteries: How does lipid peroxidation cause ferroptosis? *PLOS Biol.* 16, e2006203

36 Yang, W.S. *et al.* (2014) Regulation of ferroptotic cancer cell death by GPX4. *Cell* 156, 317–331

37 Weïwer, M. *et al.* (2012) Development of small-molecule probes that selectively kill cells induced to express mutant RAS. *Bioorg. Med. Chem. Lett.* 22, 1822–1826

38 Woo, J.H. *et al.* (2015) Elucidating compound mechanism of action by network perturbation analysis. *Cell* 162, 441–451
39 Bentinger, M. *et al.* (2007) The antioxidant role of coenzyme Q. *Mitochondrion* 7 Suppl, S41-50
40 Gaschler, M.M. *et al.* (2018) FINO2 initiates ferroptosis through GPX4 inactivation and iron oxidation. *Nat. Chem. Biol.* 14, 507–515
41 Hassannia, B. *et al.* (2018) Nano-targeted induction of dual ferroptotic mechanisms eradicates high-risk neuroblastoma. *J. Clin. Invest.* 128, 3341–3355
42 Andrews, N.C. and Schmidt, P.J. (2007) Iron homeostasis. *Annu. Rev. Physiol.* 69, 69–85
43 Sun, X. *et al.* (2015) HSPB1 as a novel regulator of ferroptotic cancer cell death. *Oncogene* 34, 5617–5625
44 Xie, Y. *et al.* (2016) Ferroptosis: process and function. *Cell Death Differ.* 23, 369–379
45 Dixon, S.J. and Stockwell, B.R. (2014) The role of iron and reactive oxygen species in cell death. *Nat. Chem. Biol.* 10, 9–17
46 Su, L.-J. *et al.* (2019) Reactive Oxygen Species-Induced Lipid Peroxidation in Apoptosis, Autophagy, and Ferroptosis. *Oxid. Med. Cell. Longev.* 2019, 5080843
47 Yang, W.S. *et al.* (2016) Peroxidation of polyunsaturated fatty acids by lipoxygenases drives ferroptosis. *Proc. Natl. Acad. Sci.* 113, E4966–E4975
48 Shah, R. *et al.* (2018) Resolving the role of lipoxygenases in the initiation and execution of ferroptosis. *ACS Cent. Sci.* 4, 387–396
49 Ayala, A. *et al.* (2014) Lipid peroxidation: production, metabolism, and signaling mechanisms of malondialdehyde and 4-hydroxy-2-nonenal. *Oxid. Med. Cell. Longev.* 2014, 360438
50 Zeng, C.-M. *et al.* (2017) Aldo-keto reductase AKR1C1-AKR1C4: functions, regulation, and intervention for anti-cancer therapy. *Front. Pharmacol.* 8, 119
51 Chen, Y. *et al.* (2018) Quantitative profiling of protein carbonylations in ferroptosis by an aniline-derived probe. *J. Am. Chem. Soc.* 140, 4712–4720
52 Agmon, E. *et al.* (2018) Modeling the effects of lipid peroxidation during ferroptosis on membrane properties. *Sci. Rep.* 8, 5155
53 Buccarelli, M. *et al.* (2018) Inhibition of autophagy increases susceptibility of glioblastoma stem cells to temozolomide by igniting ferroptosis. *Cell Death Dis.* 9, 841
54 Hou, W. *et al.* (2016) Autophagy promotes ferroptosis by degradation of ferritin. *Autophagy* 12, 1425–1428
55 Liu, J. *et al.* (2019) Autophagic degradation of the circadian clock regulator promotes ferroptosis. *Autophagy* 15, 2033–2035
56 Yang, M. *et al.* (2019) Clockophagy is a novel selective autophagy process favoring ferroptosis. *Sci. Adv.* 5, eaaw2238
57 Song, X. *et al.* (2018) AMPK-mediated BECN1 phosphorylation promotes ferroptosis by directly blocking system Xc– activity. *Curr. Biol.* 28, 2388-2399.e5
58 Hong, S.H. *et al.* (2017) Molecular crosstalk between ferroptosis and apoptosis: emerging role of ER stress-induced p53-independent PUMA expression. *Oncotarget* 8, 115164–115178
59 Liu, J. *et al.* (2020) The regulation of ferroptosis by tumor suppressor p53 and its pathway. *Int. J. Mol. Sci.* 21,
60 Kang, R. *et al.* (2019) The tumor suppressor protein p53 and the ferroptosis network. *Free Radic. Biol. Med.* 133, 162–168
61 Zheng, D.-W. *et al.* (2017) Switching apoptosis to ferroptosis: metal–organic network for high-efficiency anticancer therapy. *Nano Lett.* 17, 284–291
62 Dodson, M. *et al.* (2019) NRF2 plays a critical role in mitigating lipid peroxidation and ferroptosis. *Redox Biol.* 23, 101107
63 Xu, T. *et al.* (2019) Molecular mechanisms of ferroptosis and its role in cancer therapy. *J. Cell. Mol. Med.* 23, 4900–4912
64 Sun, X. *et al.* (2016) Activation of the p62-Keap1-NRF2 pathway protects against ferroptosis in hepatocellular carcinoma cells: Hepatobiliary Malignancies. *Hepatology* 63, 173–184
65 Roh, J.-L. *et al.* (2017) Nrf2 inhibition reverses the resistance of cisplatin-resistant head and neck cancer cells to artesunate-induced ferroptosis. *Redox Biol.* 11, 254–262
66 Eling, N. *et al.* (2015) Identification of artesunate as a specific activator of ferroptosis in pancreatic cancer cells. *Oncoscience* 2, 517–532
67 Bebber, C.M. *et al.* (2020) Ferroptosis in cancer cell biology. *Cancers* 12, 164
68 Maurel, M. *et al.* (2015) Controlling the unfolded protein response-mediated life and death decisions in cancer. *Semin. Cancer Biol.* 33, 57–66
69 Zhu, S. *et al.* (2017) HSPA5 regulates ferroptotic cell death in cancer cells. *Cancer Res.* 77, 2064–2077
70 Laster, S.M. *et al.* (1988) Tumor necrosis factor can induce both apoptic and necrotic forms of cell lysis. *J. Immunol. Baltim. Md 1950* 141, 2629–2634
71 Vercammen, D. *et al.* (1998) Inhibition of caspases increases the sensitivity of L929 cells to necrosis mediated by tumor necrosis factor. *J. Exp. Med.* 187, 1477–1485
72 Holler, N. *et al.* (2000) Fas triggers an alternative, caspase-8-independent cell death pathway using the kinase RIP as effector molecule. *Nat. Immunol.* 1, 489–495
73 Degterev, A. *et al.* (2005) Chemical inhibitor of nonapoptotic cell death with therapeutic potential for ischemic brain injury. *Nat. Chem. Biol.* 1, 112–119
74 Qin, X. *et al.* (2019) The role of necroptosis in cancer: a double-edged sword? *Biochim. Biophys. Acta Rev. Cancer* 1871, 259–266
75 Chen, J. *et al.* (2019) Molecular Insights into the mechanism of necroptosis: the necrosome as a potential therapeutic target. *Cells* 8, 1486
76 Gong, Y. *et al.* (2019) The role of necroptosis

in cancer biology and therapy. *Mol. Cancer* 18, 100
77 Pasparakis, M. and Vandenabeele, P. (2015) Necroptosis and its role in inflammation. *Nature* 517, 311–320
78 Cai, Z. *et al.* (2014) Plasma membrane translocation of trimerized MLKL protein is required for TNF-induced necroptosis. *Nat. Cell Biol.* 16, 55–65
79 Chen, W. *et al.* (2013) Diverse sequence determinants control human and mouse receptor interacting protein 3 (RIP3) and mixed lineage kinase domain-like (MLKL) interaction in necroptotic signaling. *J. Biol. Chem.* 288, 16247–16261
80 Dias, D.A. *et al.* (2012) A historical overview of natural products in drug discovery. *Metabolites* 2, 303–336
81 Newman, D.J. and Cragg, G.M. (2020) Natural products as sources of new drugs over the nearly four Decades from 01/1981 to 09/2019. *J. Nat. Prod.* 83, 770–803
82 Wei, G. *et al.* (2019) Natural product albiziabioside A conjugated with pyruvate dehydrogenase kinase inhibitor dichloroacetate to induceaApoptosis-ferroptosis-M2-TAMs polarization for combined cancer therapy. *J. Med. Chem.* 62, 8760–8772
83 Mbaveng, A.T. *et al.* (2018) A naturally occuring triterpene saponin ardisiacrispin B displayed cytotoxic effects in multi-factorial drug resistant cancer cells via ferroptotic and apoptotic cell death. *Phytomedicine* 43, 78–85
84 Chen, Y. *et al.* (2020) Amentoflavone suppresses cell proliferation and induces cell death through triggering autophagy-dependent ferroptosis in human glioma. *Life Sci.* 247, 117425
85 Wang, N. *et al.* (2019) Artesunate activates the ATF4-CHOP-CHAC1 pathway and affects ferroptosis in Burkitt's Lymphoma. *Biochem. Biophys. Res. Commun.* 519, 533–539
86 Ishikawa, C. *et al.* (2020) Evaluation of artesunate for the treatment of adult T-cell leukemia/lymphoma. *Eur. J. Pharmacol.* 872, 172953
87 Wang, K. *et al.* (2019) Role of GRP78 inhibiting artesunate-induced ferroptosis in KRAS mutant pancreatic cancer cells. *Drug Des. Devel. Ther.* Volume 13, 2135–2144
88 Greenshields, A.L. *et al.* (2017) Contribution of reactive oxygen species to ovarian cancer cell growth arrest and killing by the anti-malarial drug artesunate: impact of artesunate on ovarian cancer. *Mol. Carcinog.* 56, 75–93
89 Malfa, G.A. *et al.* (2019) Betula etnensis Raf. (Betulaceae) extract induced HO-1 expression and ferroptosis cell death in human colon cancer cells. *Int J Mol Sci* 20, 2723
90 Du, J. *et al.* (2019) DHA inhibits proliferation and induces ferroptosis of leukemia cells through autophagy dependent degradation of ferritin. *Free Radic. Biol. Med.* 131, 356–369
91 Chen, Y. *et al.* (2019) Dihydroartemisinin-induced unfolded protein response feedback attenuates ferroptosis via PERK/ATF4/HSPA5 pathway in glioma cells. *J. Exp. Clin. Cancer Res.* 38, 402
92 Chen, G.-Q. *et al.* (2020) Artemisinin compounds sensitize cancer cells to ferroptosis by regulating iron homeostasis. *Cell Death Differ.* 27, 242–254
93 Lin, Y.-S. *et al.* (2019) Danshen improves survival of patients with breast cancer and dihydroisotanshinone I induces ferroptosis and apoptosis of breast cancer cells. *Front. Pharmacol.* 10, 1226
94 Mbaveng, A.T. *et al.* (2018) Cytotoxicity of epunctanone and four other phytochemicals isolated from the medicinal plants Garcinia epunctata and Ptycholobium contortum towards multi-factorial drug resistant cancer cells. *Phytomedicine* 48, 112–119
95 Llabani, E. *et al.* (2019) Diverse compounds from pleuromutilin lead to a thioredoxin inhibitor and inducer of ferroptosis. *Nat. Chem.* 11, 521–532
96 Khorsandi, K. *et al.* (2020) Anti-cancer effect of gallic acid in presence of low level laser irradiation: ROS production and induction of apoptosis and ferroptosis. *Cancer Cell Int.* 20, 18
97 Niu, Y. *et al.* (2019) Physcion 8-O-β-glucopyranoside induced ferroptosis via regulating miR-103a-3p/GLS2 axis in gastric cancer. *Life Sci.* 237, 116893
98 Yamaguchi, Y. *et al.* (2018) Piperlongumine rapidly induces the death of human pancreatic cancer cells mainly through the induction of ferroptosis. *Int. J. Oncol.* DOI: 10.3892/ijo.2018.4259
99 Song, Z. *et al.* (2019) Ruscogenin induces ferroptosis in pancreatic cancer cells. *Oncol. Rep.* DOI: 10.3892/or.2019.7425
100 Zhu, H.-Y. *et al.* (2019) Typhaneoside prevents acute myeloid leukemia (AML) through suppressing proliferation and inducing ferroptosis associated with autophagy. *Biochem. Biophys. Res. Commun.* 516, 1265–1271
101 Mbaveng, A.T. *et al.* (2019) Cytotoxicity of ungeremine towards multi-factorial drug resistant cancer cells and induction of apoptosis, ferroptosis, necroptosis and autophagy. *Phytomedicine* 60, 152832
102 Yu, S. *et al.* (2017) A review on the phytochemistry, pharmacology, and pharmacokinetics of amentoflavone, a naturally-occurring biflavonoid. *Molecules* 22, 299
103 Dixon, S.J. *et al.* (2014) Pharmacological inhibition of cystine–glutamate exchange induces endoplasmic reticulum stress and ferroptosis. *eLife* 3, e02523
104 Crawford, R.R. *et al.* (2015) Human CHAC1 protein degrades glutathione, and mRNA induction is regulated by the transcription factors ATF4 and ATF3 and a bipartite ATF/CRE regulatory element. *J. Biol. Chem.* 290, 15878–15891
105 Hassannia, B. *et al.* (2020) Withaferin A: From ayurvedic folk medicine to preclinical anti-cancer drug. *Biochem. Pharmacol.* 173, 113602
106 Sun, W. *et al.* (2016) 2-Methoxy-6-acetyl-7-methyljuglone (MAM), a natural naphthoquinone, induces NO-dependent apoptosis and necroptosis by H

2 O 2 -dependent JNK activation in cancer cells. *Free Radic. Biol. Med.* 92, 61–77
107 Sun, W. *et al.* (2019) Inhibition of lung cancer by 2-methoxy-6-acetyl-7-methyljuglone through induction of necroptosis by targeting receptor-interacting protein 1. *Antioxid. Redox Signal.* 31, 93–108
108 Yu, J. *et al.* (2020) 2-Methoxy-6-acetyl-7-methyljuglone (MAM) induced programmed necrosis in glioblastoma by targeting NAD(P)H: Quinone oxidoreductase 1 (NQO1). *Free Radic. Biol. Med.* 152, 336–347
109 Ge, D. *et al.* (2020) 11-Methoxytabersonine induces necroptosis with autophagy through AMPK/mTOR and JNK pathways in human lung cancer cells. *Chem. Pharm. Bull. (Tokyo)* 68, 244–250
110 Balhamar, S.O.M.S. *et al.* (2019) Differential cytotoxic potential of acridocarpus orientalis leaf and stem extracts with the ability to induce multiple cell death pathways. *Molecules* 24, 3976
111 Lee, Y.-J. *et al.* (2020) Arctigenin induces necroptosis through mitochondrial dysfunction with CCN1 upregulation in prostate cancer cells under lactic acidosis. *Mol. Cell. Biochem.* 467, 45–56
112 Lee, Y.-J. *et al.* (2020) Apoptosis and necroptosis-inducing effects of arctigenin on nasal septum carcinoma RPMI-2650 cells in 2D and 3D culture. *Mol. Cell. Toxicol.* 16, 1–11
113 Mbaveng, A.T. *et al.* (2020) N-acetylglycoside of oleanolic acid (aridanin) displays promising cytotoxicity towards human and animal cancer cells, inducing apoptotic, ferroptotic and necroptotic cell death. *Phytomedicine* 76, 153261
114 Liu, L. *et al.* (2019) Berberine in combination with cisplatin induces necroptosis and apoptosis in ovarian cancer cells. *Biol. Res.* 52, 37
115 Xiong, J. *et al.* (2017) MYC is a positive regulator of choline metabolism and impedes mitophagy-dependent necroptosis in diffuse large B-cell lymphoma. *Blood Cancer J.* 7, e582–e582
116 Guo, D. *et al.* (2019) Celastrol induces necroptosis and ameliorates inflammation via targeting biglycan in human gastric carcinoma. *Int. J. Mol. Sci.* 20, 5716
117 Kang, J.I. *et al.* (2016) Columbianadin inhibits cell proliferation by inducing apoptosis and necroptosis in HCT116 colon cancer cells. *Biomol. Ther.* 24, 320–327
118 Wu, M. *et al.* (2013) Deoxypodophyllotoxin triggers necroptosis in human non-small cell lung cancer NCI-H460 cells. *Biomed. Pharmacother.* 67, 701–706
119 Zhou, J. *et al.* (2020) Emodin induced necroptosis in the glioma cell line U251 via the TNF-α/RIP1/RIP3 pathway. *Invest. New Drugs* 38, 50–59
120 Jung, S. *et al.* (2018) Anticancer activity of gomisin J from Schisandra chinensis fruit. *Oncol. Rep.* 41, 711–717
121 Jia, M.-M. *et al.* (2020) Jujuboside B promotes the death of acute leukemia cell in a RIPK1/RIPK3/MLKL pathway-dependent manner. *Eur. J. Pharmacol.* 876, 173041
122 Xu, B. *et al.* (2017) Matrine induces RIP3-dependent necroptosis in cholangiocarcinoma cells. *Cell Death Discov.* 3, 16096
123 Deng, Q. *et al.* (2013) Neoalbaconol induces energy depletion and multiple cell death in cancer cells by targeting PDK1-PI3-K/Akt signaling pathway. *Cell Death Dis.* 4, e804–e804
124 Lu, Z. *et al.* (2019) Ophiopogonin D' induces RIPK1-dependent necroptosis in androgen-dependent LNCaP prostate cancer cells. *Int. J. Oncol.* 56, 439–447
125 Zhao, H. *et al.* (2016) Pristimerin triggers AIF-dependent programmed necrosis in glioma cells via activation of JNK. *Cancer Lett.* 374, 136–148
126 Mbaveng, A.T. *et al.* (2020) Cytotoxicity of a naturally occuring spirostanol saponin, progenin III, towards a broad range of cancer cell lines by induction of apoptosis, autophagy and necroptosis. *Chem. Biol. Interact.* 326, 109141
127 Khorsandi, L. *et al.* (2017) Quercetin induces apoptosis and necroptosis in MCF-7 breast cancer cells. *Bratisl. Med. J.* 118, 123–128
128 Han, Q. *et al.* (2018) Resibufogenin suppresses colorectal cancer growth and metastasis through RIP3-mediated necroptosis. *J. Transl. Med.* 16, 201
129 Hammerová, J. *et al.* (2012) Necroptosis modulated by autophagy is a predominant form of melanoma cell death induced by sanguilutine. *Biol. Chem.* 393, 647–658
130 Shahsavari, Z. *et al.* (2015) Shikonin induced necroptosis via reactive oxygen species in the T-47D breast cancer cell linev. *Asian Pac. J. Cancer Prev.* 16, 7261–7266
131 Chen, C. *et al.* (2017) Shikonin induces apoptosis and necroptosis in pancreatic cancer via regulating the expression of RIP1/RIP3 and synergizes the activity of gemcitabine. *Am. J. Transl. Res.* 9, 5507–5517
132 Zhang, Z. *et al.* (2017) Shikonin induces necroptosis by reactive oxygen species activation in nasopharyngeal carcinoma cell line CNE-2Z. *J. Bioenerg. Biomembr.* 49, 265–272
133 Kim, H.-J. *et al.* (2017) Shikonin-induced necroptosis is enhanced by the inhibition of autophagy in non-small cell lung cancer cells. *J. Transl. Med.* 15, 123
134 Wada, N. *et al.* (2015) Shikonin, dually functions as a proteasome inhibitor and a necroptosis inducer in multiple myeloma cells. *Int. J. Oncol.* 46, 963–972
135 Fu, Z. *et al.* (2013) The anti-tumor effect of shikonin on osteosarcoma by inducing RIP1 and RIP3 dependent necroptosis. *BMC Cancer* 13, 580
136 Piao, J.-L. *et al.* (2013) The molecular mechanisms and gene expression profiling for shikonin-induced apoptotic and necroptotic cell death in U937 cells. *Chem. Biol. Interact.* 205, 119–127
137 Huang, C. *et al.* (2013) Shikonin kills glioma cells through necroptosis mediated by RIP-1. *PLoS ONE* 8, e66326
138 Lu, B. *et al.* (2017) Shikonin induces glioma cell necroptosis in vitro by ROS overproduction and

promoting RIP1/RIP3 necrosome formation. *Acta Pharmacol. Sin.* 38, 1543–1553
139 Zhou, Z. *et al.* (2017) RIP1 and RIP3 contribute to shikonin-induced DNA double-strand breaks in glioma cells via increase of intracellular reactive oxygen species. *Cancer Lett.* 390, 77–90
140 Ding, Y. *et al.* (2019) MLKL contributes to shikonin-induced glioma cell necroptosis via promotion of chromatinolysis. *Cancer Lett.* 467, 58–71
141 Liu, T. *et al.* (2019) Shikonin-induced necroptosis in nasopharyngeal carcinoma cells via ROS overproduction and upregulation of RIPK1/RIPK3/MLKL expression. *OncoTargets Ther.* 12, 2605–2614
142 Lee, M.-J. *et al.* (2014) Shikonin time-dependently induced necrosis or apoptosis in gastric cancer cells via generation of reactive oxygen species. *Chem. Biol. Interact.* 211, 44–53
143 Park, S. *et al.* (2013) Shikonin induces programmed necrosis-like cell death through the formation of receptor interacting protein 1 and 3 complex. *Food Chem. Toxicol.* 55, 36–41
144 Shahsavari, Z. *et al.* (2018) Targeting cell necroptosis and apoptosis induced by shikonin via receptor interacting protein kinases in estrogen receptor positive breast cancer cell line, MCF-7. *Anticancer Agents Med. Chem.* 18, 245–254
145 Shahsavari, Z. *et al.* (2016) RIP1K and RIP3K provoked by shikonin induce cell cycle arrest in the triple negative breast cancer cell line, MDA-MB-468: necroptosis as a desperate programmed suicide pathway. *Tumor Biol.* 37, 4479–4491
146 Liu, X. *et al.* (2020) Induction of an MLKL mediated non-canonical necroptosis through reactive oxygen species by tanshinol A in lung cancer cells. *Biochem. Pharmacol.* 171, 113684
147 Lin, C.-Y. *et al.* (2016) Simultaneous induction of apoptosis and necroptosis by Tanshinone IIA in human hepatocellular carcinoma HepG2 cells. *Cell Death Discov.* 2, 16065
148 Wang, Y. *et al.* (2020) The anti-cancer mechanisms of berberine: a review. *Cancer Manag. Res.* Volume 12, 695–702
149 Haider, A. *et al.* (2018) PCYT1A regulates phosphatidylcholine homeostasis from the inner nuclear membrane in response to membrane stored curvature elastic stress. *Dev Cell* 45, 481-495.e8
150 Lwin, T. *et al.* (2013) A microenvironment-mediated c-Myc/miR-548m/HDAC6 amplification loop in non-Hodgkin B cell lymphomas. *J. Clin. Invest.* 123, 4612–4626
151 Feng, S. *et al.* (2007) Cleavage of RIP3 inactivates its caspase-independent apoptosis pathway by removal of kinase domain. *Cell. Signal.* 19, 2056–2067
152 Feoktistova, M. *et al.* (2011) cIAPs block ripoptosome formation, a RIP1/Caspase-8 containing intracellular cell death complex differentially regulated by cFLIP isoforms. *Mol. Cell* 43, 449–463
153 Tenev, T. *et al.* (2011) The ripoptosome, a signaling platform that assembles in response to genotoxic stress and loss of IAPs. *Mol. Cell* 43, 432–448
154 Zhang, D.-W. *et al.* (2009) RIP3, an energy metabolism regulator that switches TNF-induced cell death from apoptosis to necrosis. *Science* 325, 332–336
155 Wang, H. *et al.* (2014) Mixed lineage kinase domain-like protein MLKL causes necrotic membrane disruption upon phosphorylation by RIP3. *Mol. Cell* 54, 133–146
156 Moriwaki, K. *et al.* (2015) Differential roles of RIPK1 and RIPK3 in TNF-induced necroptosis and chemotherapeutic agent-induced cell death. *Cell Death Dis.* 6, e1636–e1636
157 Tait, S.W.G. and Green, D.R. (2013) Mitochondrial regulation of cell death. *Cold Spring Harb. Perspect. Biol.* 5, a008706–a008706
158 Strilic, B. *et al.* (2016) Tumour-cell-induced endothelial cell necroptosis via death receptor 6 promotes metastasis. *Nature* 536, 215–218
159 Palliyaguru, D.L. *et al.* (2018) Isothiocyanates: translating the power of plants to people. *Mol. Nutr. Food Res.* 62, 1700965
160 El-sayed, M.T. *et al.* (2015) Indoles as anticancer agents. *Adv. Mod. Oncol. Res.* 1, 20
161 Fimognari, C. and Hrelia, P. (2007) Sulforaphane as a promising molecule for fighting cancer. *Mutat. Res.* 635, 90–104
162 Sestili, P. and Fimognari, C. (2015) Cytotoxic and antitumor activity of sulforaphane: the role of reactive oxygen species. *BioMed Res. Int.* 2015, 402386
163 Lafarga, T. *et al.* (2018) Effects of thermal and non-thermal processing of cruciferous vegetables on glucosinolates and its derived forms. *J. Food Sci. Technol.* 55, 1973–1981
164 Rask, L. *et al.* (2000) Myrosinase: gene family evolution and herbivore defense in Brassicaceae. *Plant Mol. Biol.* 42, 93–113
165 Hayes, J.D. *et al.* (2008) The cancer chemopreventive actions of phytochemicals derived from glucosinolates. *Eur. J. Nutr.* 47 Suppl 2, 73–88
166 Mitsiogianni *et al.* (2019) The role of isothiocyanates as cancer chemo-preventive, chemo-therapeutic and anti-melanoma agents. *Antioxidants* 8, 106
167 Guengerich, F.P. (2008) Cytochrome p450 and chemical toxicology. *Chem. Res. Toxicol.* 21, 70–83
168 Kamal, M.M. *et al.* (2020) Sulforaphane as an anticancer molecule: mechanisms of action, synergistic effects, enhancement of drug safety, and delivery systems. *Arch. Pharm. Res.* 43, 371–384
169 Abdull Razis, A.F. *et al.* (2018) Isothiocyanates and xenobiotic detoxification. *Mol. Nutr. Food Res.* 62, 1700916
170 Briones-Herrera, A. *et al.* (2018) New highlights on the health-improving effects of sulforaphane. *Food Funct.* 9, 2589–2606
171 Arumugam, A. and Abdull Razis, A.F. (2018) Apoptosis as a mechanism of the cancer chemopreventive activity of glucosinolates: a review. *Asian Pac. J. Cancer Prev. APJCP* 19, 1439–1448
172 Jiang, X. *et al.* (2018) Chemopreventive activity of sulforaphane. *Drug Des. Devel. Ther.* 12,

2905–2913
173 Sasaki, K. and Yoshida, H. (2015) Organelle autoregulation-stress responses in the ER, Golgi, mitochondria and lysosome. *J. Biochem. (Tokyo)* 157, 185–195
174 Jo, C. *et al.* (2014) Sulforaphane induces autophagy through ERK activation in neuronal cells. *FEBS Lett.* 588, 3081–3088
175 Zou, X. *et al.* (2017) Endoplasmic reticulum stress mediates sulforaphane-induced apoptosis of HepG2 human hepatocellular carcinoma cells. *Mol. Med. Rep.* 15, 331–338
176 Herman-Antosiewicz, A. *et al.* (2006) Sulforaphane causes autophagy to inhibit release of cytochrome C and apoptosis in human prostate cancer cells. *Cancer Res.* 66, 5828–5835
177 Kanematsu, S. *et al.* (2010) Autophagy inhibition enhances sulforaphane-induced apoptosis in human breast cancer cells. *Anticancer Res.* 30, 3381–3390
178 Singh, S.V. *et al.* (2004) Sulforaphane-induced G2/M phase cell cycle arrest involves checkpoint kinase 2-mediated phosphorylation of cell division cycle 25C. *J. Biol. Chem.* 279, 25813–25822
179 Myzak, M.C. *et al.* (2006) Sulforaphane inhibits histone deacetylase activity in BPH-1, LnCaP and PC-3 prostate epithelial cells. *Carcinogenesis* 27, 811–819
180 Parnaud, G. *et al.* (2004) Mechanism of sulforaphane-induced cell cycle arrest and apoptosis in human colon cancer cells. *Nutr. Cancer* 48, 198–206
181 Suppipat, K. *et al.* (2012) Sulforaphane induces cell cycle arrest and apoptosis in acute lymphoblastic leukemia cells. *PloS One* 7, e51251
182 Arvelo, F. *et al.* (2016) Tumour progression and metastasis. *Ecancermedicalscience* 10, 617
183 Asakage, M. *et al.* (2006) Sulforaphane induces inhibition of human umbilical vein endothelial cells proliferation by apoptosis. *Angiogenesis* 9, 83–91
184 Bertl, E. *et al.* (2006) Inhibition of angiogenesis and endothelial cell functions are novel sulforaphane-mediated mechanisms in chemoprevention. *Mol. Cancer Ther.* 5, 575–585
185 Thejass, P. and Kuttan, G. (2006) Antimetastatic activity of Sulforaphane. *Life Sci.* 78, 3043–3050
186 Meinig, J.M. *et al.* (2015) Synthesis of fuorophores that target small molecules to the endoplasmic reticulum of living mammalian cells. *Angew. Chem. Int. Ed.* 54, 9696–9699
187 Strober, W. (2015) Trypan blue exclusion test of cell viability. *Curr. Protoc. Immunol.* 111,
188 Organisation for Economic Co-operation and Development (2016) *In vitro mammalian cell micronucleus test. 487 487*, OECD Publishing.
189 Atale, N. *et al.* (2014) Cell-death assessment by fluorescent and nonfluorescent cytosolic and nuclear staining techniques. *J. Microsc.* 255, 7–19
190 Galluzzi, L. *et al.* (2007) Cell death modalities: classification and pathophysiological implications. *Cell Death Differ.* 14, 1237–1243
191 Angeli, J.P.F. *et al.* (2017) Ferroptosis inhibition: mechanisms and opportunities. *Trends Pharmacol. Sci.* 38, 489–498
192 Han, C. *et al.* (2020) Ferroptosis and its potential role in human diseases. *Front. Pharmacol.* 11, 239
193 Conrad, M. and Pratt, D.A. (2019) The chemical basis of ferroptosis. *Nat. Chem. Biol.* 15, 1137–1147
194 Zong, W.-X. (2006) Necrotic death as a cell fate. *Genes Dev.* 20, 1–15
195 Kinnally, K.W. *et al.* (2011) Is mPTP the gatekeeper for necrosis, apoptosis, or both? *Biochim. Biophys. Acta BBA - Mol. Cell Res.* 1813, 616–622
196 Nakagawa, T. *et al.* (2005) Cyclophilin D-dependent mitochondrial permeability transition regulates some necrotic but not apoptotic cell death. *Nature* 434, 652–658
197 Galluzzi, L. *et al.* (2016) Mitochondrial regulation of cell death: a phylogenetically conserved control. *Microb. Cell* 3, 101–108
198 Fatokun, A. (2018) Parthanatos: poly ADP ribose polymerase (PARP)-mediated cell death. In *Apoptosis and Beyond* pp. 535–558, John Wiley & Sons, Ltd
199 Izzo, V. *et al.* (2016) Mitochondrial permeability transition: new findings and persisting uncertainties. *Trends Cell Biol.* 26, 655–667
200 Araldi, R.P. *et al.* (2015) Using the comet and micronucleus assays for genotoxicity studies: A review. *Biomed. Pharmacother.* 72, 74–82
201 Kiyoi, H. *et al.* (2020) FLT3 mutations in acute myeloid leukemia: therapeutic paradigm beyond inhibitor development. *Cancer Sci.* 111, 312–322
202 Daver, N. *et al.* (2019) Targeting FLT3 mutations in AML: review of current knowledge and evidence. *Leukemia* 33, 299–312
203 Ozeki, K. *et al.* (2004) Biologic and clinical significance of the FLT3 transcript level in acute myeloid leukemia. *Blood* 103, 1901–1908
204 Kang, H.J. *et al.* (2010) High transcript level of FLT3 associated with high risk of relapse in pediatric acute myeloid leukemia. *J. Korean Med. Sci.* 25, 841–845
205 Quentmeier, H. *et al.* (2003) FLT3 mutations in acute myeloid leukemia cell lines. *Leukemia* 17, 120–124
206 Lu, J.-W. *et al.* (2016) Cabozantinib is selectively cytotoxic in acute myeloid leukemia cells with FLT3-internal tandem duplication (FLT3-ITD). *Cancer Lett.* 376, 218–225
207 Ha, Y.N. *et al.* (2020) Petromurin C induces protective autophagy and apoptosis in FLT3-ITD-positive AML: synergy with gilteritinib. *Mar. Drugs* 18, 57
208 Tao, C. *et al.* (2020) CT1-3, a novel magnolol-sulforaphane hybrid suppresses tumorigenesis through inducing mitochondria-mediated apoptosis and inhibiting epithelial mesenchymal transition. *Eur. J. Med. Chem.* 199, 112441
209 Tumiatti, V. *et al.* (2009) Design, synthesis,

and biological evaluation of substituted naphthalene imides and diimides as anticancer agent. *J. Med. Chem.* 52, 7873–7877
210 Sk, U.H. *et al.* (2011) Development of novel naphthalimide derivatives and their evaluation as potential melanoma therapeutics. *Eur. J. Med. Chem.* 46, 3331–3338
211 Hu, K. *et al.* (2013) Synthesis and biological evaluation of sulforaphane derivatives as potential antitumor agents. *Eur. J. Med. Chem.* 64, 529–539
212 Kaminski, B.M. *et al.* (2011) Sulforaphane potentiates oxaliplatin-induced cell growth inhibition in colorectal cancer cells via induction of different modes of cell death. *Cancer Chemother. Pharmacol.* 67, 1167–1178
213 Guo, W.-J. *et al.* (2010) Taxol induces concentration-dependent apoptotic and paraptosis-like cell death in human lung adenocarcinoma (ASTC-a-1) cells. *J. X-Ray Sci. Technol.* 18, 293–308
214 Song, S. *et al.* (2020) Tetrahydrobenzimidazole TMQ0153 triggers apoptosis, autophagy and necroptosis crosstalk in chronic myeloid leukemia. *Cell Death Dis.* 11, 109
215 Longato, G.B. *et al.* (2015) Different cell death responses induced by eupomatenoid-5 in MCF-7 and 786-0 tumor cell lines. *Toxicol. Vitro Int. J. Publ. Assoc. BIBRA* 29, 1026–1033
216 Pawlik, A. *et al.* (2012) Phenethyl isothiocyanate-induced cytoskeletal changes and cell death in lung cancer cells. *Food Chem. Toxicol.* 50, 3577–3594
217 Smith, T.K. (2004) Allyl-isothiocyanate causes mitotic block, loss of cell adhesion and disrupted cytoskeletal structure in HT29 cells. *Carcinogenesis* 25, 1409–1415
218 Geng, F. *et al.* (2011) Allyl isothiocyanate arrests cancer cells in mitosis, and mitotic arrest in turn leads to apoptosis via Bcl-2 protein phosphorylation. *J. Biol. Chem.* 286, 32259–32267
219 Jackson, S.J.T. and Singletary, K.W. (2004) Sulforaphane inhibits human MCF-7 mammary cancer cell mitotic progression and tubulin polymerization. *J. Nutr.* 134, 2229–2236
220 Jackson, S.J.T. and Singletary, K.W. (2004) Sulforaphane: a naturally occurring mammary carcinoma mitotic inhibitor, which disrupts tubulin polymerization. *Carcinogenesis* 25, 219–227
221 Jackson, S.J.T. *et al.* (2007) Sulforaphane suppresses angiogenesis and disrupts endothelial mitotic progression and microtubule polymerization. *Vascul. Pharmacol.* 46, 77–84
222 Kwon, M.-Y. *et al.* (2015) Heme oxygenase-1 accelerates erastin-induced ferroptotic cell death. *Oncotarget* 6, 24393–24403
223 Russo, M. *et al.* (2018) Nrf2 targeting by sulforaphane: a potential therapy for cancer treatment. *Crit. Rev. Food Sci. Nutr.* 58, 1391–1405
224 Houghton, C.A. *et al.* (2016) Sulforaphane and other nutrigenomic Nrf2 activators: can the clinician's expectation be matched by the reality? *Oxid. Med. Cell. Longev.* 2016, 1–17
225 Yang, L. *et al.* (2016) Frugal chemoprevention: targeting Nrf2 with foods rich in sulforaphane. *Semin. Oncol.* 43, 146–153
226 Sun, L. *et al.* (2012) Mixed lineage kinase domain-like protein mediates necrosis signaling downstream of RIP3 kinase. *Cell* 148, 213–227
227 Aaes, T.L. *et al.* (2016) Vaccination with necroptotic cancer cells induces efficient anti-tumor immunity. *Cell Rep.* 15, 274–287
228 Serrano-del Valle, A. *et al.* (2019) Immunogenic cell death and immunotherapy of multiple myeloma. *Front. Cell Dev. Biol.* 7, 50
229 Wen, Q. *et al.* (2019) The release and activity of HMGB1 in ferroptosis. *Biochem. Biophys. Res. Commun.* 510, 278–283
230 Nohmi, T. (2018) Thresholds of Genotoxic and Non-Genotoxic Carcinogens. *Toxicol. Res.* 34, 281–290
231 Sestili, P. *et al.* (2010) Sulforaphane induces DNA single strand breaks in cultured human cells. *Mutat. Res. Mol. Mech. Mutagen.* 689, 65–73
232 Sekine-Suzuki, E. *et al.* (2008) Sulforaphane induces DNA double strand breaks predominantly repaired by homologous recombination pathway in human cancer cells. *Biochem. Biophys. Res. Commun.* 377, 341–345
233 Rudolf, E. and Červinka, M. (2011) Sulforaphane induces cytotoxicity and lysosome- and mitochondria-dependent cell death in colon cancer cells with deleted p53. *Toxicol. In Vitro* 25, 1302–1309
234 Fimognari, C. *et al.* (2005) Micronucleus formation and induction of apoptosis by different isothiocyanates and a mixture of isothiocyanates in human lymphocyte cultures. *Mutat. Res. Toxicol. Environ. Mutagen.* 582, 1–10
235 Fimognari, C. *et al.* (2005) Effect of sulforaphane on micronucleus induction in cultured human lymphocytes by four different mutagens. *Environ. Mol. Mutagen.* 46, 260–267
236 Ferreira de Oliveira, J.M.P. *et al.* (2014) Sulforaphane Induces DNA Damage and Mitotic Abnormalities in Human Osteosarcoma MG-63 Cells: Correlation with Cell Cycle Arrest and Apoptosis. *Nutr. Cancer* 66, 325–334
237 Ahmad, A. *et al.* (2011) Mechanisms and therapeutic implications of cell death induction by indole compounds. *Cancers* 3, 2955–2974
238 Aggarwal, B.B. and Ichikawa, H. (2005) Molecular targets and anticancer potential of indole-3-carbinol and its derivatives. *Cell Cycle Georget. Tex* 4, 1201–1215
239 Biersack, B. and Schobert, R. (2012) Indole compounds against breast cancer: recent developments. *Curr. Drug Targets* 13, 1705–1719
240 Royston, K.J. and Tollefsbol, T.O. (2015) The epigenetic impact of cruciferous vegetables on cancer prevention. *Curr. Pharmacol. Rep.* 1, 46–51
241 Netz, N. and Opatz, T. (2015) Marine indole alkaloids. *Mar. Drugs* 13, 4814–4914
242 Güven, K.C. *et al.* (2010) Alkaloids in marine algae. *Mar. Drugs* 8, 269–284
243 Sawadogo, W. *et al.* (2015) A survey of marine

natural compounds and their derivatives with anti-cancer activity reported in 2012. *Molecules* 20, 7097–7142
244 Pan, Q. *et al.* (2016) Monoterpenoid indole alkaloids biosynthesis and its regulation in Catharanthus roseus: a literature review from genes to metabolites. *Phytochem. Rev.* 15, 221–250
245 Catanzaro, E. *et al.* (2018) Natural products to fight cancer: a focus on Juglans regia. *Toxins* 10,
246 Hong, C. *et al.* (2002) 3,3'-Diindolylmethane (DIM) induces a G(1) cell cycle arrest in human breast cancer cells that is accompanied by Sp1-mediated activation of p21(WAF1/CIP1) expression. *Carcinogenesis* 23, 1297–1305
247 Rahman, K.M.W. *et al.* (2003) Indole-3-carbinol (I3C) induces apoptosis in tumorigenic but not in nontumorigenic breast epithelial cells. *Nutr. Cancer* 45, 101–112
248 Howells, L.M. *et al.* (2002) Indole-3-carbinol inhibits protein kinase B/Akt and induces apoptosis in the human breast tumor cell line MDA MB468 but not in the nontumorigenic HBL100 line. *Mol. Cancer Ther.* 1, 1161–1172
249 Kandala, P.K. and Srivastava, S.K. (2010) Activation of checkpoint kinase 2 by 3,3'-diindolylmethane is required for causing G2/M cell cycle arrest in human ovarian cancer cells. *Mol. Pharmacol.* 78, 297–309
250 Staub, R.E. *et al.* (2002) Fate of indole-3-carbinol in cultured human breast tumor cells. *Chem. Res. Toxicol.* 15, 101–109
251 Wu, H.-T. *et al.* (2005) Inhibition of cell proliferation and in vitro markers of angiogenesis by indole-3-carbinol, a major indole metabolite present in cruciferous vegetables. *J. Agric. Food Chem.* 53, 5164–5169
252 Chang, X. *et al.* (2005) 3,3'-Diindolylmethane inhibits angiogenesis and the growth of transplantable human breast carcinoma in athymic mice. *Carcinogenesis* 26, 771–778
253 Mansoori, B. *et al.* (2017) The different mechanisms of cancer drug resistance: a brief review. *Adv. Pharm. Bull.* 7, 339–348
254 Liu, F.-S. (2009) Mechanisms of chemotherapeutic drug resistance in cancer therapy—a quick review. *Taiwan. J. Obstet. Gynecol.* 48, 239–244
255 Arora, A. and Shukla, Y. (2003) Modulation of vinca-alkaloid induced P-glycoprotein expression by indole-3-carbinol. *Cancer Lett.* 189, 167–173
256 Arora, A. *et al.* (2005) Modulation of P-glycoprotein-mediated multidrug resistance in K562 leukemic cells by indole-3-carbinol. *Toxicol. Appl. Pharmacol.* 202, 237–243
257 Jeon, K.-I. *et al.* (2003) Pretreatment of indole-3-carbinol augments TRAIL-induced apoptosis in a prostate cancer cell line, LNCaP. *FEBS Lett.* 544, 246–251
258 Virág, L. *et al.* (1995) A simple, rapid and sensitive fluorimetric assay for the measurement of cell-mediated cytotoxicity. *J. Immunol. Methods* 185, 199–208
259 Bradford, M.M. (1976) A rapid and sensitive method for the quantitation of microgram quantities of protein utilizing the principle of protein-dye binding. *Anal. Biochem.* 72, 248–254
260 Zimmermann, M. and Meyer, N. (2011) Annexin V/7-AAD staining in keratinocytes. *Methods Mol. Biol. Clifton NJ* 740, 57–63
261 Hochegger, H. *et al.* (2008) Cyclin-dependent kinases and cell-cycle transitions: does one fit all? *Nat. Rev. Mol. Cell Biol.* 9, 910–916
262 Mah, L.-J. *et al.* (2010) γH2AX: a sensitive molecular marker of DNA damage and repair. *Leukemia* 24, 679–686
263 Singh, T.P. and Singh, O.M. (2018) Recent progress in biological activities of indole and indole alkaloids. *Mini Rev. Med. Chem.* 18, 9–25
264 Lindequist, U. (2016) Marine-derived pharmaceuticals - challenges and opportunities. *Biomol. Ther.* 24, 561–571
265 Salucci, S. *et al.* (2018) Marine bisindole alkaloid: Aapotential apoptotic inducer in human cancer cells. *Eur. J. Histochem. EJH* 62, 2881
266 Behnisch-Cornwell, S. *et al.* (2020) Pentathiepins: a novel class of glutathione peroxidase 1 inhibitors that induce oxidative stress, loss of mitochondrial membrane potential and apoptosis in human cancer cells. *ChemMedChem* DOI: 10.1002/cmdc.202000160
267 Kilic-Kurt, Z. *et al.* (2020) Novel indole hydrazide derivatives: synthesis and their antiproliferative activities through inducing apoptosis and DNA damage. *Arch. Pharm. (Weinheim)* 353, 2000059
268 Amato, J. *et al.* (2014) Bis-indole derivatives with antitumor activity turn out to be specific ligands of human telomeric G-quadruplex. *Front. Chem.* 2,
269 Viswanathan, V. (2015) , Cellular features predicting susceptibility to ferroptosis: insights from cancer cell-line profiling. , Columbia University